SOLID STATE SPEED CONTROL OF INDUCTION MOTORS

A Thesis Submitted
In Partial Fulfilment of the Requirements
for the Degree of
DOCTOR OF PHILOSOPHY

By
M. ARUNACHALAM

to the
DEPARTMENT OF ELECTRICAL ENGINEERING
INDIAN INSTITUTE OF TECHNOLOGY, KANPUR
NOVEMBER, 1977

DEDICATED TO

MY BELOVED

PARENTS

EE-1977-D-ARU-SOL

I.I.T. KANPUR
CENTRAL LIBRARY
Acc. No. A 55482.
17 OCT 1978

30.11.77

CERTIFICATE

It is certified that this work, 'Solid State Speed Control of Induction Motors' by M. Arunachalam, has been carried out under my supervision and that this work has not been submitted elsewhere for a degree.

Ramamoorty

(M. Ramamoorty)
Professor,
Department of Electrical Engg.
Indian Institute of Technolo
Kanpur, India.

ACKNOWLEDGEMENTS

It is with very great pleasure I express my profound gratitude to Dr. M. Ramamoorty who suggested the research problems discussed in this thesis and provided me with excellent guidance and inspiration all along.

I am thankful to Dr. S.R. Doradla, Mr. N.S. Wani, Mr. A. Krishnan, Mr. K. Gopalan, Mr. K.S. Rama Rao, Mr. S.R. Nigam, Mr. K.K. Ray, Mr. S.V. Tambe and all other friends wh helped me on various occasions at various stages of my work. My thanks are also due to Mr. D.V.S.S.N. Murthy and Mr. S. Bhatnagar for their help during experiments.

I wish to acknowledge the research facilities provided by the authorities of I.I.T. Kanpur and the patient and ski typing of Mr. C.M. Abraham.

I.I.T. Kanpur,
November 1977.

M. Arunachalam

TABLE OF CONTENTS

Page

LIST OF FIGURES ix

LIST OF PRINCIPAL SYMBOLS xiii

SYNOPSIS xv

CHAPTER 1 : INTRODUCTION

1.1 General Discussion 1

1.2 Stator Voltage Control 2

1.3 Stator Voltage and Frequency Control 4

1.4 Rotor Power Control 7

1.5 Rotor Impedance Control 8

1.6 Outline of the thesis 10

CHAPTER 2 : PHASE CONTROLLED SINGLE PHASE MACHINE

2.1 Introduction 16

2.2 Mathematical Model 17

2.3 Harmonic Analysis Method 21

2.4 Algorithm for the Suggested Procedure 25

2.5 Comparison of Results 27

2.6 Conclusion 31

CHAPTER 3 : PHASE CONTROLLED THREE PHASE INDUCTION MOTOR

3.1 Introduction 32

3.2 Various Modes of Operation 34

3.3 State Space Analysis 38

3.3.1 Solution for 3/2 mode 44

3.3.2 Solution for 2/0 mode 47

3.4 Method of Harmonic Analysis 49

3.5 Experimental Observations and Comparison of Results 55

3.6 Conclusion 55

CHAPTER 4 : FREQUENCY DEPENDENCY OF MACHINE PARAMETERS

4.1 Introduction 57

4.2 Variation of Stator and Rotor Resistances with Frequency 59

4.3 Effects of Harmonics on Machine Inductances 61

4.4 Harmonic Equivalent Circuits and Harmonic Torques 61

4.5 Three Thyristors-Three Diodes Systems 64

4.6 Six Thyristor Configuration 67

4.7 Conclusion 67

CHAPTER 5 : ITERATIVE METHOD APPLIED TO INVERTER DRIVEN SYSTEMS

5.1 Introduction 69

5.2 Voltage Source Driven System 71

    5.2.1 System description 71

    5.2.2 Prediction of dc link current waveform 73

    5.2.3 Iterative procedure to solve for the sixth harmonic voltage 76

    5.2.4 Sixth harmonic torque 79

5.3 Current Source Driven System 80

    5.3.1 System description 80

    5.3.2 Prediction of dc link voltage waveform 84

    5.3.3 Iterative procedure for the estimation of sixth harmonic dc link current 87

5.4 Conclusion 90

CHAPTER 6 : SPEED CONTROL USING PHASE CONTROLLED RESISTANCE IN THE ROTOR

6.1 Introduction 91

6.2 System Representation 94

6.3 Operation of the Converter System-Review 96

6.4 State Space Analysis 98

  6.4.1 Modes of operation 98
  6.4.2 Three thyristor conduction 100
  6.4.3 Two thyristor conduction 103
  6.4.4 State space solution 106
  6.4.5 Speed-torque characteristic 111

6.5 Simplified ac Equivalent Circuit 116

6.6 Comparision With Chopper Controlled Scheme 123

6.7 Conclusion 123

CHAPTER 7 : SPEED CONTROL USING DELTA CONNECTED PHASE CONTROLLED SCRs IN THE ROTOR

7.1 Introduction 125

7.2 System Representation 126

7.3 Various Modes of Operation 128

7.4 Solution for 1/0 Mode 132

7.5 State Space Solution for 2/1 Mode of Operation 134

7.6 Harmonic Method of Solution for 2/1 Mode 144

7.7 Application to Steady State Analysis of Induction Motor 150

7.8 Conclusion 153

CHAPTER 8 : FIRING SCHEME AND FEED BACK CONTROL FOR ROTOR PHASE CONTROL SYSTEM WITH DELTA CONNECTED SCRs

8.1 Introduction 155

8.2 Review of Triggering Schemes Used for Rotor Phase Control 156

8.3 Proposed Firing Scheme 158

8.4 Performance of Closed Loop System with Delta Connected SCRs in the Rotor 162

  8.4.1 System description 162
  8.4.2 Transfer function of the functional blocks 163

8.4.2.1 Tachogenerator and filter 165
8.4.2.2 Controller 165
8.4.2.3 Firing circuit 167
8.4.2.4 Induction motor 168
8.4.3 System performance 173
8.5 Conclusion 181

CHAPTER 9 : CONCLUSION

9.1 General 182
9.2 Review of the Work Done 182
9.3 Scope for Future Research Work 187

LIST OF REFERENCES 189

APPENDIX A : TO OBTAIN THE INITIAL GUESS FOR β THE CONDUCTION ANGLE USED IN THE HARMONIC ANALYSIS METHOD OF SINGLE PHASE MACHINE 193

APPENDIX B : HARMONIC ANALYSIS ON THE VOLTAGE WAVEFORM APPLIED TO THE STATOR OF THE SINGLE PHASE INDUCTION MACHINE 195

APPENDIX C : HARMONIC ANALYSIS ON MACHINE VOLTAGE WAVEFORM 197

APPENDIX D : HARMONIC ANALYSIS ON MACHINE CURRENT WAVEFORM 198

APPENDIX E : THE VARIOUS GAINS AND TIME CONSTANTS USED FOR THE PERTURBATION STUDY 199

CURRICULUM VITAE 200

LIST OF FIGURES

Figure No.	Figure Caption	Page
1.1	Motor characteristic with stator voltage control	3
1.2	Motor characteristics with stator frequency control	6
1.3	Motor characteristics with rotor impedance control	9
2.1	Schematic diagram	18
2.2	Equivalent circuit of single phase machine	18
2.3	Voltage and current waveform of single phase machine	22
2.4	Nth harmonic equivalent circuit of single phase machine	22
2.5	Speed-torque characteristic of single phase machine	28
2.6	Voltage and current waveform of single phase machine (Analytical result)	29
2.7	Oscillogram of voltage and current waveform	30
3.1	Various circuit configurations	33
3.2	Current waveforms when the system is in 3/2 mode	36
3.3	Current waveforms when the system is in 2/0 mode	37
3.4	Speed-torque characteristic for 3 thyristors 3 diodes case	48
3.5	nth harmonic equivalent circuit	52
3.6	Oscillograms demonstrating different modes of operation	53
3.7	Current waveforms	54
4.1	Variation of machine resistance with frequency	60
4.2	Fundamental frequency equivalent circuit	62
4.3	nth harmonic equivalent circuit	62
4.4	Speed-torque characteristic for 3 thyristors 3 diodes case	65

Figure No.	Figure Caption	Page
4.5	Speed-torque characteristic for 6 thyristor case	66
5.1	System representation	72
5.2	Steady state equivalent circuit	72
5.3	Voltage and current waveforms	74
5.4	Voltage waveform	77
5.5	Variation of sixth harmonic torque with average torque developed	81
5.6	System representation	83
5.7	System current waveforms	83
5.8	Line a-b voltage waveforms	89
5.9	Voltage waveform at dc link	89
6.1	Schematic diagram	95
6.2	Equivalent circuit with parameters referred to secondary	95
6.3	Rotor induced voltage waveforms	97
6.4	The equivalent circuit when T1, T3 and T5 conduct	97
6.5	The equivalent circuit when T1 and T5 conduct	104
6.6	Rotor current waveform	112
6.7	Speed-torque characteristic	115
6.8	Per-phase ac current waveform when the ac current is ripple free and commutation interval neglected	118
6.9	ac equivalent circuit	118
6.10	ac equivalent circuit with parameters rearranged	118
6.11	Variation of torque with firing angle	122
7.1	Schematic diagram	127
7.2	Equivalent circuit when parameters referred to secondary	127
7.3	System waveforms	129
7.4	Equivalent circuit when T3 and T1 are ON	135

Figure No.	Figure Caption	Page
7.5	Equivalent circuit when T1 alone conducts	138
7.6	Current waveform for passive load	145
7.7	nth harmonic equivalent circuit	149
7.8	Speed-torque characteristic	151
7.9	Oscillograms of current waveforms	152
8.1	The proposed firing scheme	159
8.2	Block diagram of the feedback system	164
8.3	Tachogenerator and associated filter	164
8.4	Functional blocks of the closed loop system	166
8.5	Circuit configuration of the controllers	166
8.6	Variation of torque with α	170
8.7	δ V_s α graph	172
8.8	Torque V_s speed graph	172
8.9	Response curve for load perturbation with P controller (N_o = 1050 rpm)	176
8.10	Response curve for reference speed perturbation with P controller (N_o = 750 rpm)	176
8.11	Response curve for load perturbation with PI controller (N_o = 1050 rpm)	176
8.12	Response curve for speed perturbation with PI controller (N_o = 1050 rpm)	177
8.13	Response curve for load perturbation with PI controller (N_o = 750 rpm)	177
8.14	Response curve for speed perturbation with PI controller (N_o = 750 rpm)	177
8.15	Response to load perturbation (N_o = 1050 rpm, P controller)	178
8.16	Response to reference speed perturbation (N_o = 750 rpm, P controller)	178
8.17	Response to load perturbation (N_o = 1050 rpm, PI controller)	179

Figure No.	Figure Caption	Page
8.18	Response to reference speed perturbation (N_o = 1050 rpm, PI controller)	179
8.19	Response to load perturbation (N_o = 750 rpm, PI controller)	180
8.20	Response to reference speed perturbation (N_o = 750 rpm, PI controller)	180

LIST OF PRINCIPAL SYMBOLS

R_1	per phase stator resistance
R'_1	per phase stator resistance referred to secondary
R_2	per phase rotor resistance
R'_2	per phase rotor resistance referred to primary
X_1	per phase stator leakage reactance
X'_1	per phase stator leakage reactance referred to secondary
X_2	per phase rotor leakage reactance
X'_2	per phase rotor leakage reactance referred to primary
X_m	magnetising reactance referred to primary
r_s	stator resistance in P.U.
r'_r	rotor resistance referred to stator in P.U.
x_m	magnetising reactance in P.U.
x'_r	rotor self reactance referred to stator in P.U.
T_d	average torque developed by the machine
T_L	load torque
α	firing angle
μ	commutation angle
f	stator supply frequency of the machine
s	slip of the rotor
T_6	amplitude of sixth harmonic torque
E_6	sixth harmonic voltage in the dc link
L	inductance of the filter choke
V_c	output voltage of the controller

V_R	reference voltage representing reference set speed
K_1	combined gain of tachogenerator and the associated filte
T_1	effective time constant of the filter
K_2	gain of the controller
T_2	time constant of the controller
K_3	gain of the firing circuit
T_3	time constant of the firing circuit
$_o$	speed of the machine in rad/sec at the operating point
N_o	speed of the machine in rpm at the operating point
ΔN	change in speed in rpm
	change in speed in rad/sec
ΔT_d	change in developed torque
$\Delta\alpha$	change in firing angle
K_G	gain of the rotating system
T_G	time constant of the rotating system
J	moment of inertia of the rotating system
F	frictional constant of the rotating system
Rex	per phase external resistance in the rotor
R	external resistance connected in the dc side of the converter
X_s	source reactance in P.U.

SYNOPSIS

M. ARUNACHALAM
Ph.D.
Department of Electrical Engineering
Indian Institute of Technology, Kanpur
July, 1977

SOLID STATE SPEED CONTROL OF INDUCTION MOTORS

The solid state variable speed a.c. drives find wide spread applications in to-day's industries. The development of power semiconductor devices and solid state integrated circuits are responsible for the opening up of this new field in industrial drives. The solid state drives can claim many advantages, such as reliability, fast acting, long life, less maintenance, high efficiency and low cost, over the older schemes which use motor-generator sets, magnetic controllers and gas discharge valves. The induction motor, which is the best choice among a.c. machines for many industrial applications, is simple, cheap and robust. It is basically a constant speed motor. Many industrial applications demand a variable speed-torque characteristic. The well-known techniques of speed control are : (i) stator voltage control, (ii) stator voltage and frequency control, (iii) rotor power control, and (iv) rotor impedance control. Of all these techniques, first and last ones are simple and economical. The last method gives wide speed variation and high starting torque. These two methods are however less efficient particularly at low speeds. Therefore, they are usually employed for small motors

and where economy and not efficiency is the prime consideration. The phase controlled SCRs connected in various configurations have been used for the stator voltage control of squirrel cage and wound rotor induction machines. Recently, attempts have also been made to make use of the phase controlled SCR circuits in the rotor of the slip ring induction machines to have wide-range speed control. The main advantage of the phase control circuit is that it employs line or natural commutation and there is no need for additional commutating elements. However, the analysis of phase control circuits is quite complicated because the instant at which the conducting SCR goes off in the case of motor loads is unknown and it is difficult to predict the voltage that may come across the open circuited phase. Two well known methods have been in use for solving the thyristor controlled machine problems. They are : (i) state space method and (ii) harmonic analysis method.

In the present thesis the above two methods of analysis are applied to some of the economical a.c. machine speed control schemes using phase controlled SCRs either in the stator or rotor of the induction machine. The results obtained are compared with experimentalvalues.

The harmonic analysis method is applied to a single phase a.c. machine which uses phase controlled SCRs in the stator. The suggested procedure iterates on the conduction period alone and avoides iterating on the induced e.m.f. The results obtained by this procedure are compared with state space results and experimental values. A three diodes - three thyristors stator voltage control scheme for a three phase induction machine is discussed. The various possible modes of operation are explained. The firing angle and speed decide the particular mode of operation. A state space procedure which is already available in the literature is extended to this system. A modified harmonic analysis method is also developed. An attempt has been made to consider the frequency dependency of the machine parameters using the modified harmonic analysis method. The analytical results are compared with experimental values.

The applicability of harmonic equivalent circuits for the steady state performance calculations of inverter driven systems are also explained. Both voltage and current source driven systems are considered. A simple and fast iterative procedure is presented for the estimation of the steady state behaviour of the inverter driven systems including the input filter characteristics. The iterative procedure explains how the effect of the sixth harmonic ripples, which are present in the input side of the inverter can be taken into account for calculating the performance characteristics.

The rotor impedance control using phase controlled SCRs in the rotor circuits in two different configurations has also been investigated in this thesis. A phase controlled resistance method of speed control using a controlled bridge and external resistance in the rotor is explained. The chopper controlled external resistance method of speed control has been already discussed in the literature. In this method, a diode bridge and a chopper is used in the rotor circuit of the machine. The power is fed to the chopper controlled resistance through the diode bridge. The effective rotor impedance is varied by controlling the chopper on-off frequency. In the present scheme, a fully controlled bridge is used to feed the external resistance. The effective rotor impedance is continuously controllable by advancing or retarding the firing angle of the controlled rectifier. A smoothing reactor is used in the d.c. side to make the current continuous. The different modes of operation of this system are explained. A state space procedure is developed to obtain the rotor current and hence the performance characteristics of the system. The state space procedure does not involve iterations and the variables used are the actual rotor variables of the machine.

One of the important problems facing the investigators in obtaining the steady state performance of the thyristor controlled machine is the imposition of the open circuit condition for the thyristors in the mathematical model. Ref Lipo and Krause have suggested a procedure where the current zero is imposed by applying a voltage equal to the induced e.m.f. across the open circuited phase of the machine. In the present work, an alternative concept is employed. When one of the phases of the machine with isolated neutral gets open circuited, the other two phase currents and their derivatives are equal and opposite to each other. Therefore, one more differential equation is available and is used in the mathematical model. A simplified a.c. equivalent circuit is also developed for obtaining the performance characteristic of the scheme. The results obtained by the analytical procedures are compared with the experimental values which were already available.

The effective rotor impedance can also be continuously varied by using delta-connected phase controlled SCRs in the rotor circuit. This scheme is also discussed in detail in the present thesis. The schemes uses equal external resistance in the rotor phases and the phase controlled SCRs are placed at the open star point of the rotor circuit. The speed of the machine is controlled by varying the firing angle of the phase controlled thyristors. There are two different modes of operation depending upon the firing angle and speed. One is 2/1 mode where two thyristor and one thyristor conduction occur alternatively and the other one is 1/0 mode where one thyristor conduction is followed by an off period. When the machine is in 1/0 mode the rotor current is easily obtainable considering the rotor induced voltage and the equivalent machine parameters. A state space procedure similar to that described for the phase controlled resistance scheme is used to obtain rotor current waveform for 2/1 mode of operation. A harmonic analysis method suitable for this problem is also discussed. Here an iterative procedure is used to obtain the current zero instant. The iterations are carried out until the r.m.s. value of the phase current during the off period is reasonably low. The analytical results obtained by these methods are compared with experimental observations. A simple and reliable firing circuit suitable for the rotor phase control schemes is also presented.

A feed-back control scheme for variable speed operation using delta connected SCRs in the rotor is studied in this thesis. A voltage proportional to the speed of the machine is compared with a reference voltage and the error signal is amplified and given to a controller. The output of the controller adjusts the firing angle to the required value. For the present study, both P and PI controllers are used. The behaviour of the closed loop system for the perturbations in load torque and reference voltage are obtained analytically and the results are compared with experimental observations.

CHAPTER 1

INTRODUCTION

1.1 General Discussion :

The advent of Silicon Controlled Rectifiers (SCRs) has revolutionized the field of speed control of electrical machines. Today SCRs of reasonably large voltage and current ratings are available and efforts are being made by the researchers to develop devices of still larger ratings. The solid state speed control system has many advantages over the older schemes which use motor-generator sets, magnetic controllers and gas discharge valves such as, (i) reliability, (ii) fast acting, (iii) long life, (iv) less maintenance, (v) high efficiency, and (vi) low cost.

AC and dc machines are the competitors in the industrial drive field. It is easy to control the speed of dc machines and the control module is inexpensive, but the dc machines cost more than that of ac machines of same capacity. In addition, dc machines need careful maintenance and are not suitable when the environment contains inflammable gases. Though the control module of ac drive involves complicated circuitry and costs comparatively higher, often the economy is realized through the inexpensive ac machines. Also the ac machines are the best alternatives when the environment demands ruggedness and flameproof construction. The induction machine, often the best choice for many drive applications, is basically a constant speed machine. The attractions towards ac machines are due to its simplicity, ruggedness and low cost. However, to control its speed is not an easy task and investigations are being made to develop simple control schemes. The various techniques of speed control of induction motors are (i) stator voltage control, (ii) stator voltage and frequency control, (iii) rotor power control, and (iv) rotor impedance control. They are discussed in the following sections.

1.2 Stator Voltage Control

This is the simplest and most straight forward method of controlling the speed of induction motors. Since the torque developed by the motor at a given speed is directly proportional to the square of the r.m.s. value of the air gap voltage of the machine, the developed torque at different speeds of the machine can be adjusted by varying the stator voltage. Therefore, a variable speed-torque characteristic is possible with stator voltage control. If the driven load is having parabolic speed-torque characteristic like that of pumps and fans, then the speed-torque curve of the load can intersect the machine characteristic curves at various points giving wide speed range. If it is a constant torque load, then the speed range is limited. Fig. 1.1

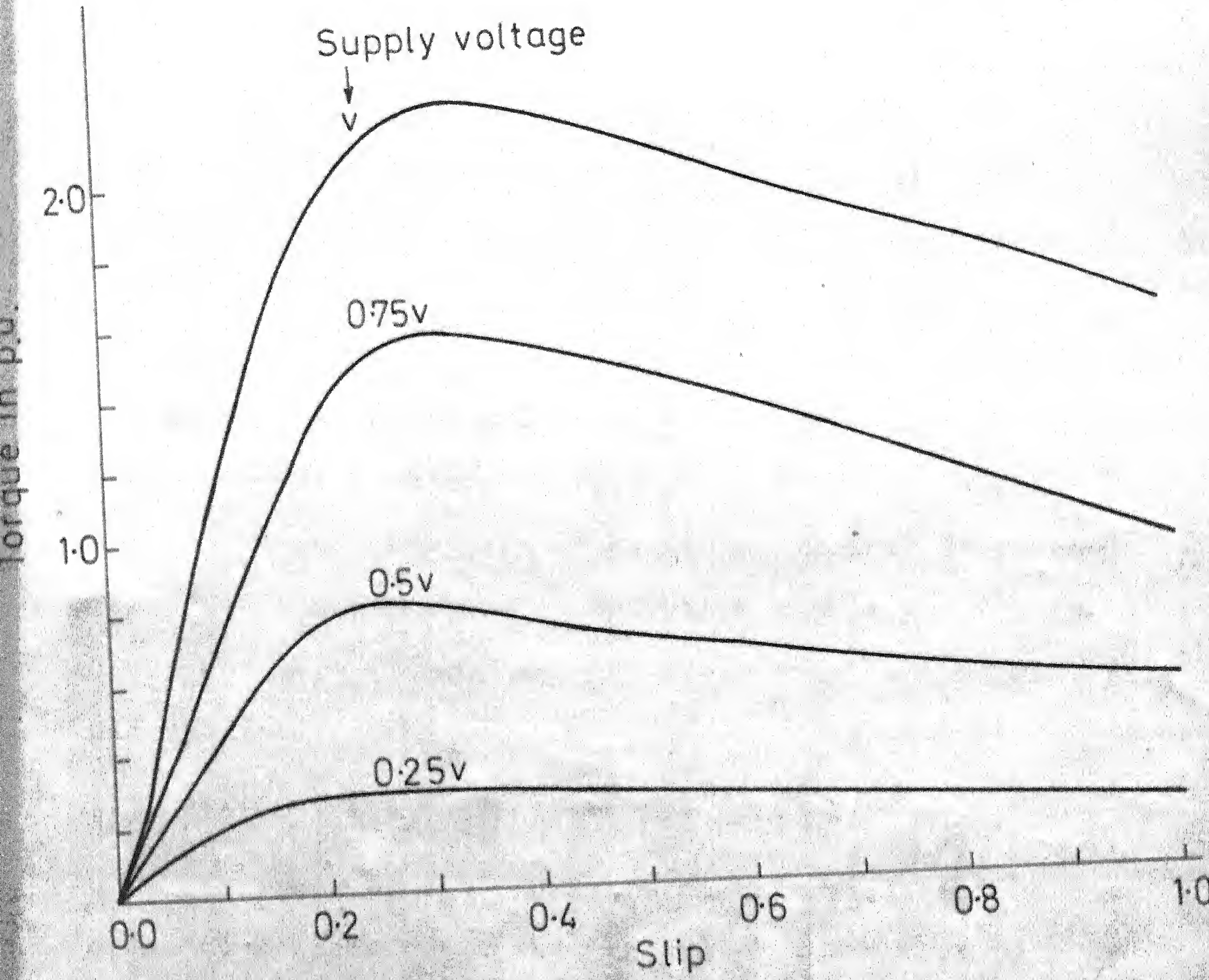

FIG.1·1 MOTOR CHARACTERISTICS WITH STATOR VOLTAGE CONTROL shows the motor characteristics with stator voltage control.

The stator voltage was obtained using tap changers or series reactors before the introduction of thyristors. This system is expensive and sluggish. Now-a-days triacs or thyristors in various configurations are used in the stator circuit of the machine to control the stator voltage. This method of control is suitable to both squirrel cage and slipring machines. The main advantages of these control schemes are that they use phase controlled SCRs and the type of commutation used is the natural commutation. These schemes are efficient at low speeds because slip times the air gap power goes as heat loss in the rotor circuit. Further the pullout torque decreases as the input voltage is reduced. Therefore these methods of control are employed for small machines where economy and not efficiency is the prime considerations.

1.3 Stator Voltage and Frequency Control

The rotor of the induction machine will tend to run close to synchronous speed decided by the number of poles for which the machine is wound and the stator supply frequency. Therefore, the speed of the machine can be varied by controlling the stator supply frequency. For economical considerations, the magnetic circuit of the machine is designed such that the operating point is near the knee of the magnetization curve of the machine. When the frequency of the stator excitation is varied, the r.m.s. value of the stator voltage must also be adjusted to keep the air gap flux of the machine constant. In other words, V/f must be kept constant for the entire range of operation which ensures constant air gap flux.

This method of control is quite expensive and is suitable for large machines. Previously, motor-generator sets were used to get variable voltage variable frequency supply. Now, thyristors are used for this purpose due to cost considerations. From fixed frequency fixed voltage supply, a variable dc voltage is obtained using controlled rectifiers and the dc supply is fed to an inverter which applies a variable frequency supply to the machine. The stator excitation (V/f) is controlled by adjusting the firing angle of the controlled rectifier and the frequency of the inverter. With the help of suitable feed-back to control the rotor slip and stator excitation, it is possible to have constant torque or constant horse power operation. The characteristics are shown in Fig. 1.2. Instead of controlled voltage source, controlled current source can also be used to feed the inverter. The current source inverters have the advantages of reliability, regenerative capability and case of protection. The developed torque of the machine is controlled by adjusting the dc link current. When the induction machine is current fed, it tends to operate in the negative slope region of the torque - slip characteristic. Hence suitable feed back must be employed for stable operation

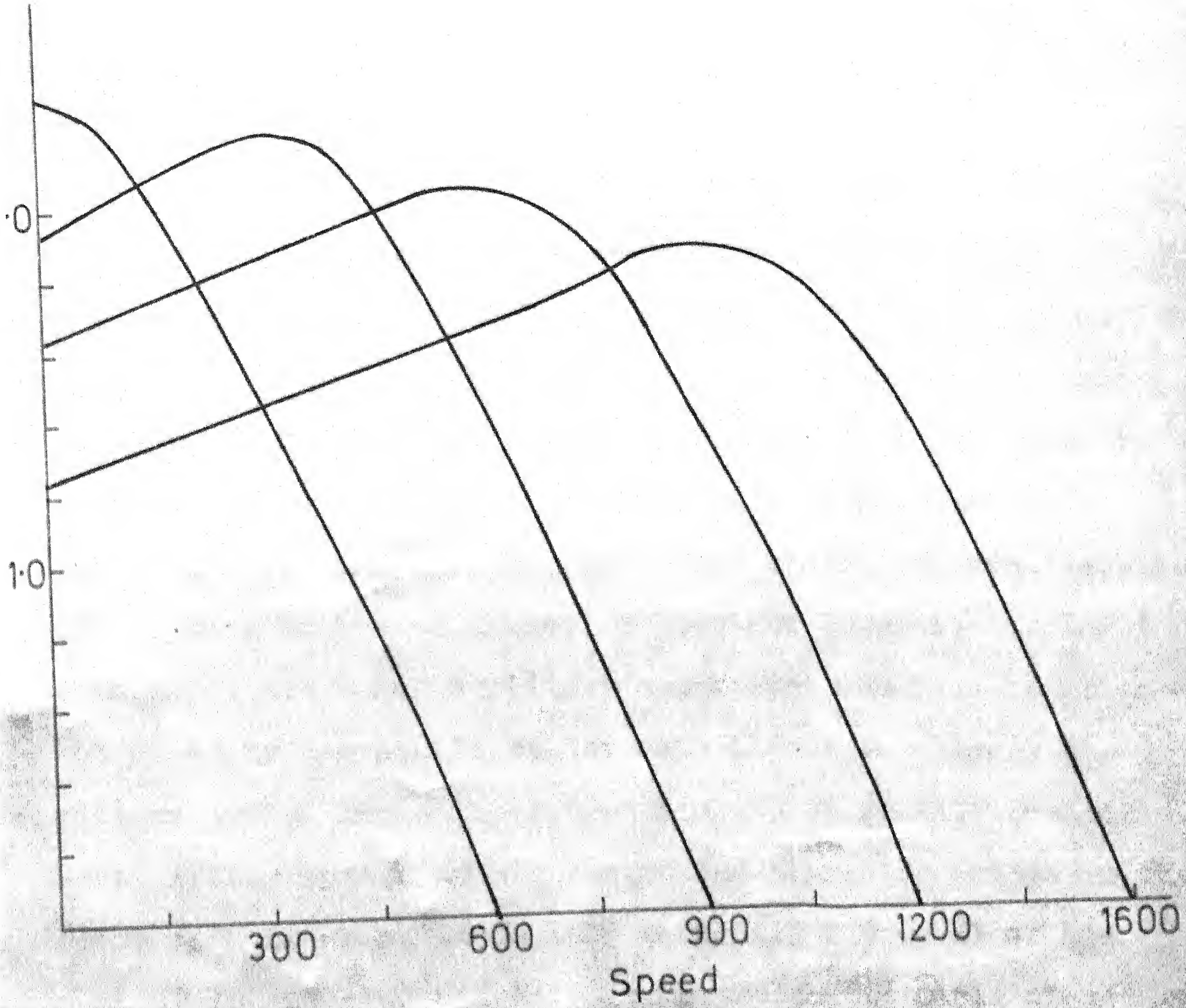

FIG·1·2 MOTOR CHARACTERISTICS WITH STATOR FREQUENCY CONTROL and to avoid magnetic saturation in the machine.

1.4 Rotor Power Control

Speed - torque characteristics of the induction machine can be changed to suit for variable speed drive applications by controlling the rotor power. Both sub-synchronous and super-synchronous operations are possible by extracting out or injecting in electrical power in the rotor circuit. When the machine is running at less than one - half synchronous speed, more than one - half of the air gap power is transferred to the rotor circuit. A large portion of this slip power can be extracted out and used to drive some other electrical equipment or fed back to the ac mains. Kramer and Scherbius employed this principle using auxiliary commutator machines of size and capacity comparable to the main induction motor. These systems occupy large floor area and are sluggish. The solid state Kramer system uses a controlled thyristor bridge in the rotor circuit which feeds a dc machine. The speed of the machine is adjusted by controlling the firing angle of the controlled bridge. Here only sub-synchronous speed alone are possible. In solid state Scherbius system, two controlled thyristor bridges separated by a dc link are used in the rotor circuit to have both sub-synchronous and super-synchronous operation. For sub-synchronous operation, the bridge connected to the slipring is operated in the converting mode to rectify the slip power. The output of this bridge is fed to the second bridge, which is operated as inverter, through the dc link. The second bridge output is connected to the ac mains to feed the power back to the supply. For super-synchronous operation, the first one operates as an inverter and the second bridge as a converter. Now power is injected into the rotor. The efficiency of the system is quite high and it requires large initial investment. This method of control is therefore suitable for large machines.

The rotor power can also be controlled by having cyclo-converters in the rotor circuit. Here also power can be made to flow both ways and so both sub-synchronous and super-synchronous operations are possible.

1.5 Rotor Impedance Control

The torque developed by the induction motor at a given slip can be varied by adjusting the effective rotor impedance. Therefore, variable speed-torque characteristics suitable for drive applications can be obtained by controlling the rotor impedance. External passive elements like resistors, saturable reactors and capacitors were used before introduction of SCRs to have high starting torque and wide range speed variations. These systems are sluggish, costly and are not suitable for closed loop operations. Recently, SCRs are introduced in the rotor circuit to control the effective rotor impedance and hence the speed of the machine. Both phase controlled and

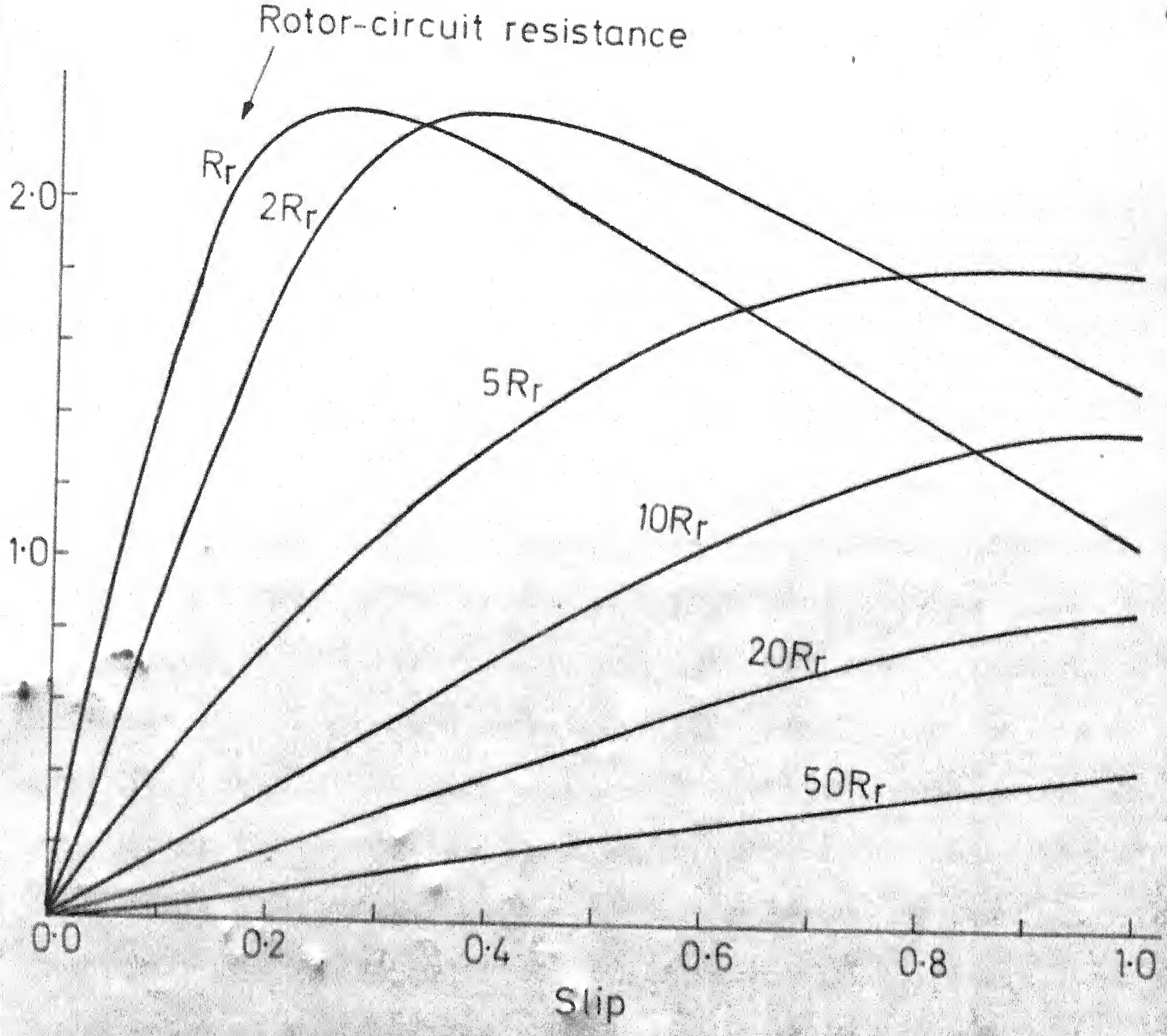

FIG.1·3 MOTOR CHARACTERISTICS WITH VARIABLE ROTOR IMPEDANCE chopper controlled circuits are used for the purpose. In the systems which use phase controlled circuits, the speed of the machine is varied by controlling the firing angle of the SCRs. The speed variation is obtained in the chopper controlled systems by varying the ON-OFF time of the chopper. These types of drive systems are simple and economical. However, the efficiency of the system is poor particularly at low speeds. Fig. 1.3 shows the motor characteristic with variable rotor impedance.

1.6 Outline of the Thesis

The review of the various methods of speed control of induction motors given in the previous sections has made it clear that the stator voltage and rotor impedance control methods are simple and economical for small machines. The present thesis deals with some of the control schemes which come under the above two categories. The scheme uses phase controlled SCRs either in the stator or rotor of the induction machine. The analysis of the phase controlled circuits are however complicated because of the following reasons : (i) In the case of motor loads, the instant at which the conducting SCR goes off is unknown, and (ii) it is not easy to predict the voltage that may come across the open circuited machine phase.

Two methods of analysis, (i) state space method, and (ii) harmonic analysis method are used to obtain the performance characteristics of the various systems discussed in the present thesis.

In Chapter 2, a harmonic analysis method suitable for a single phase ac machine whose stator voltage is controlled using a pair of thyristors connected in antiparallel in series with the stator winding is discussed. The procedure discussed in [1] iterates on conduction period and the induced e.m.f. The procedure suggested in this thesis iterates on the conduction period alone and avoids iterating on the induced e.m.f. The results obtained by this procedure are compared with those obtained using state space method [2]. Comparision with experimental results is also made. The stator voltage of a three phase induction motor can be controlled using thyristors and diodes in the stator circuit. A three thyristors - three diodes scheme is explained in Chapter 3. The stator voltage can be varied from rated value to zero by adjusting the firing angle of the thyristors. The various modes of operation of the system are explained. The state space procedure discussed in [3] is extended to the present system. A modified harmonic analysis method is also developed in Chapter 3 to obtain the steady state performance characteristic of the system. Analytical results are compared with experimental observations. The actual values of the machine parameters vary with frequency of excitation. Since the thyristor controlled machines are fed with distorted voltage and current waveforms, the effective values of the machine parameters vary with the amount of distortion present in the stator voltage. An attempt is made in Chapter 4 to consider the frequency dependency of the machine parameters using harmonic equivalent circuits.

The steady state harmonic equivalent circuits can also be applied for estimating the steady state performance characteristics of inverter driven systems. Chapter 5 discusses the applicability of the harmonic equivalent circuit method to voltage and current source driven systems. Here, iterative procedures are developed to study the behaviour of the system. The iterative procedures consider the input filter characteristic and the sixth harmonic ripples present in the dc supply for the performance calculations.

Phase controlled SCRs can be used in different configurations in the rotor circuit of the wound rotor induction motors to have wide range speed variations. Bridge and delta configurations are considered in the present thesis. A phase controlled resistance method of rotor impedance vcontrol is explained in Chapter 6. The scheme uses a fully controlled bridge and an external resistance in the rotor circuit. The effective rotor impedance is varied by adjusting the firing angle of the controlled rectifier. A large inductance is used in the dc side to keep the dc current continuous. The various modes of operation are also explained. A state space procedure is developed to obtain the rotor current and hence the performance characteristics of the system. The state variables used in the state space model are the actual rotor quantities of the machine. The procedure does not involve iterations. The imposition of current zero in the mathematical model is done as follows : When one of the phases of the machine with isolated neutral gets open circuited, the other two phase currents and their derivatives are equal and opposite to each other. This condition is made use of in the model. A simplified ac equivalent circuit is also developed in Chapter 6. The analytical results are compared with experimental values which were already available.

A continuous and smooth variation of rotor impedance can also be achieved by using data connected phase controlled SCRs at the open star point of the rotor circuit. The speed of the machine is adjusted by advancing or retarding the firing angle of the thyristors. Depending upon speed and firing angle, two different modes of operation are possible. They are (i) 2/1 mode, where two thyristor conduction and one thyristor conduction occur alternatively and (ii) 1/0 mode where one thyristor conduction is followed by an off period. For 1/0 mode, the analysis is simple. In the case of 2/1 mode of operation, the analysis becomes complicated because of the unknown current zero instants. The state space procedure developed in Chapter 6 is extended to this problem in Chapter 7. The problem is defined as, given the slip and length of the period of two thyristor conduction, the firing angle of the thyristor is to be obtained. Once α is known for the above given quantities, the initial state vector and hence the complete solution can be obtained easily. The harmonic analysis method is also applied to the present problem. Here the current zero instant is solved by iterations. The iterations are carried out until the r.m.s. value of the phase current during the off period is reasonably low. The analytical results of the scheme are compared with experimental observations.

In the case of rotor phase control schemes, synchronization of the firing pulses with the signals available across the slip rings is the problem because the magnitude and frequency of the rotor voltage change with the speed of rotor. A simple and reliable firing scheme suitable for delta connected configuratio is discussed in Chapter 8. The firing angles of the SCRs are adjusted automatically through suitable feed back to keep the speed of the machine at the pre-set value. The voltage proportional to the speed of the machine is compared with the referenc voltage and the error is amplified and given to the controller. The output of the controller is given to a delay circuit. The controller adjusts the delay to the required value. Both P and PI controllers are considered for the present study. The responses of the closed loop system for load and reference voltage perturbations are obtained analytically and the results are compared with experimental observations.

Concluding remarks and scope for further work are given in the last chapter. The major aims of this thesis are to develop proper control schemes suitable for variable speed operations and methods for steady state and dynamic analysis of SCR controlled induction motors.

CHAPTER 2

PHASE CONTROLLED SINGLE PHASE MACHINE

2.1 Introduction

Triac or a pair of SCRs in antiparallel is used in the stator circuit as shown in Fig. 2.1. for the speed control of single phase ac machines which drive loads like fans and pumps. The steady state analysis of this drive system is not easy because the conduction angle and the stator induced emf are not known. In [4], an analytical procedure which uses shifting theorem has been presented. A state space procedure has been explained in [2]. A harmonic analysis method which iterates on conduction angle and the stator induced emf has been discussed in [1]. In this chapter, the harmonic analysis method given in [1] is modified to avoid iterations on two variables. The induced emf is transformed into a dependent variable and iterations are made on the conduction angle.

The advantages of the harmonic analysis method over the other procedures are that this can be easily applied to systems which use nonsinusoidal excitations and the frequency dependency of the machine parameters can be easily taken into account by considering the harmonic equivalent circuits.

2.2 Mathematical Model

The performance equations of the single phase machine are derived in this section using the resolving field theory. A pulsating field is produced when the stator is excited by a single phase supply. This pulsating field, for the analysis purpose, can be imagined as two fields rotating in opposite directions at synchronous speed. The amplitude of each field is one - half of that of the main field. These two fields induce currents in the rotor circuit of the machine. When the machine is at standstill, torques equal in magnitude and opposite in direction are produced by these two fields. Therefore there is no resultant torque for starting. If the rotor is started by some auxiliary means, it will continue to run in one direction. The field which is rotating in the same direction as that of the rotor is known as 'forward' field and other one is called as 'backward' field. If the synchronous speed is n_s and the rotor speed is n, the slip of the rotor with respect to the forward field is given by $s_f = \frac{n_s - n}{n_s}$ and slip of the rotor with respect to the backward field is given by $s_b = \frac{n_s + n}{n_s}$.

$$= \frac{2n_s - (n_s - n)}{n_s} = (2 - s_f)$$

It is imagined that the two fields are acting on two separate rotors of equal impedance. If I_1, I_{r1} and I_{r2} are

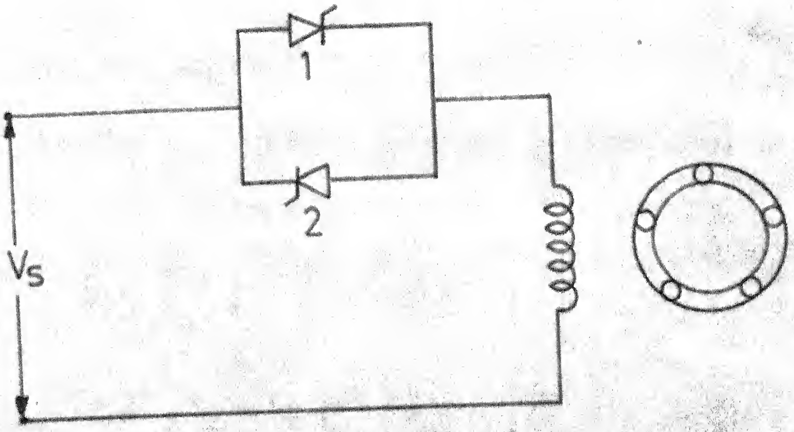

FIG.2.1 SCHEMATIC DIAGRAM

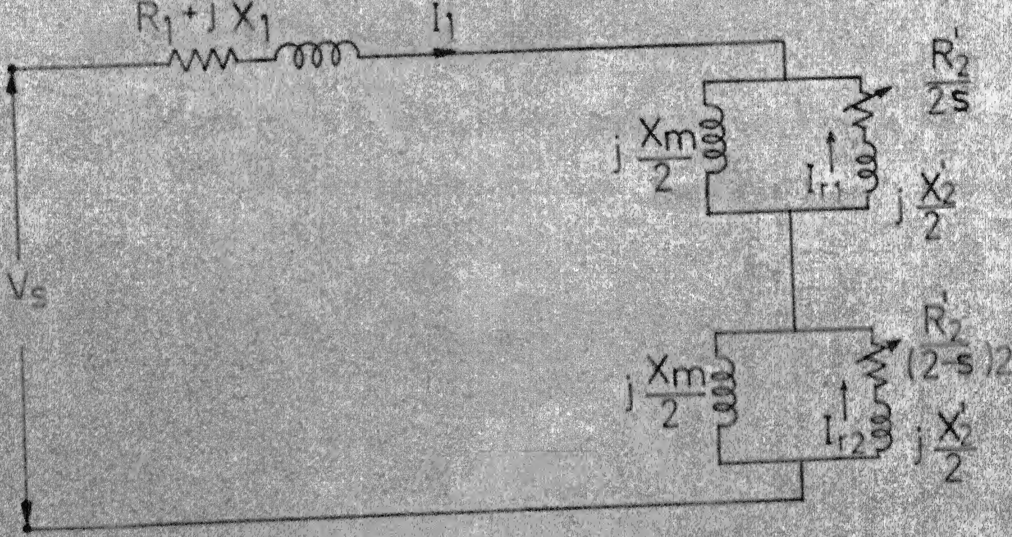
R1 + j X1
I1
R'2 / 2s
j Xm / 2
Ir1
j X'2 / 2
Vs
R'2 / (2-s)2
j Xm / 2
Ir2
j X'2 / 2

FIG.2.2 EQUIVALENT CIRCUIT OF SINGLE PHASE MACHINE

the stator, forward rotor and backward rotor currents respectively, the steady state voltage equations of the machine can be written as follows :

$$V_s = I_1 Z_1 + j\frac{X_m}{2}(I_1 + I_{r1}) + j\frac{X_m}{2}(I_1 + I_{r2}) \qquad (2.1)$$

$$0 = I_{r1} Z_f + j\frac{X_m}{2}(I_1 + I_{r1}) \qquad (2.2)$$

$$0 = I_{r2} Z_b + j\frac{X_m}{2}(I_1 + I_{r2}) \qquad (2.3)$$

where

$Z_1 = R_1 + jX_1$ is the stator winding impedance

$Z_f = R_2'/2s + j\,X_2'/2$ is the effective rotor impedance at slip s to the forward field

$Z_b = \frac{R_2'}{2(2-s)} + j\,X_2'/2$ is the effective rotor impedance at slip s to the backward field

The equivalent circuit satisfying equations (2.1 - 2.3) is given in Fig. 2.2. These equations can be arranged in matrix form as follows.

$$\begin{bmatrix} V_s \\ 0 \\ 0 \end{bmatrix} = \begin{bmatrix} (Z_1 + jX_m) & j\frac{X_m}{2} & j\frac{X_m}{2} \\ j\frac{X_m}{2} & (Z_f + j\frac{X_m}{2}) & 0 \\ j\frac{X_m}{2} & 0 & (Z_b + j\frac{X_m}{2}) \end{bmatrix} \begin{bmatrix} I_1 \\ I_{r1} \\ I_{r2} \end{bmatrix} \qquad (2.4)$$

Symbolically,

$$\underline{V} = \underline{Z}\,\underline{I}$$

$$\underline{I} = \underline{Z}^{-1}\,\underline{V} \qquad (2.5)$$

From equation (2.5), $I_1 = Y_{11}V_s$, $I_{r1} = Y_{21}V_s$ and $I_{r2} = Y_{31}V_s$

In the case of thyristor controlled machines, the voltage waveform applied to the stator of the machine contains fundamental and several other harmonic components. In the present case, the thyristors are fired symmetrically at an angle α measured from voltage zero and only one of the devices can conduct at a time during positive or negative half cycles. Therefore, odd harmonics alone are present. The equivalent circuit shown in Fig. 2.2 can be used to obtain the every harmonic current by applying the respective harmonic voltage and using appropriate slip and machine parameters. For the present analysis, it is assumed that the machine parameters are constant and the machine inertia is large enough to elliminate the speed fluctuations. The slip of the rotorfor the Nth harmonic stator excitation is $s_{N\pm} = \frac{N \pm (s_f - 1)}{N}$ (positive sign for forward field and negative sign for backward field).

In the present system, off periods are created in the stator current waveform by adjusting the firing angle. For the given speed and conduction angle, the firing angle and emf across the stator winding during the off period have to be known apriori to make use of harmonic equivalent circuits for performance calculations. Straight forward solution is not possible and therefore iterations are to be employed. In the next section an iterative procedure which iterates only on conduction angle for the given firing angle and slip) is developed.

The developed torque of the machine is given by

$$T_d = \sum_{N=1}^{M} [I_{rN+}^2 \frac{R_2'}{2s_{N+}} - I_{rN}^2 \frac{R'_2}{2s_{N-}}] \qquad (2.6)$$

where I_{rN+} is the Nth harmonic forward rotor current referred to stator

I_{rN-} is the Nth harmonic backward rotor current referred to stator.

and M is the order of the highest harmonic considered for the analysis.

2.3 Harmonic Analysis Method

In the present system, the voltage waveform that appears across the stator windings is not sinusoidal because of the off period introduced in the stator current waveform by the delayed firing. The harmonic analysis of the stator waveform is necessary to make use of the harmonic equivalent circuits for performance calculations. For this, the waveform is to be defined fully for the entire cycle. Referring to Fig. 2.3, for the given firing angle α, the conduction angle β and induced voltage waveform during the off period $(\pi - \beta)$ are not known initially. In [1 and 2], for the given conduction

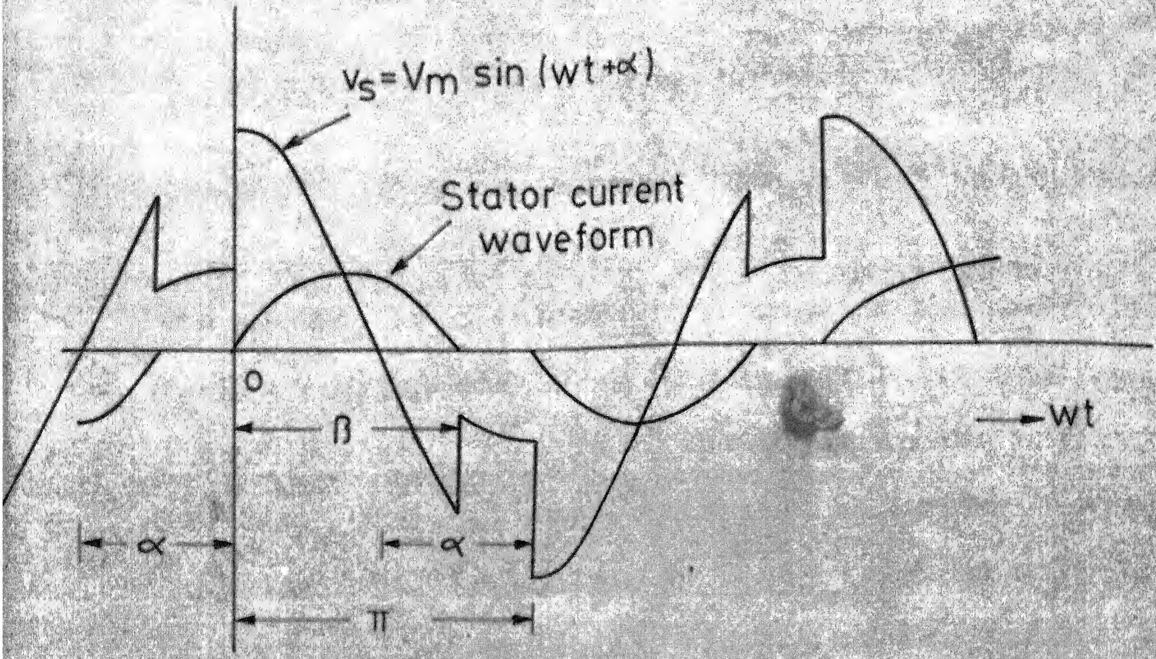

FIG. 2·3 VOLTAGE AND CURRENT WAVEFORM OF SINGLE PHASE MACHINE

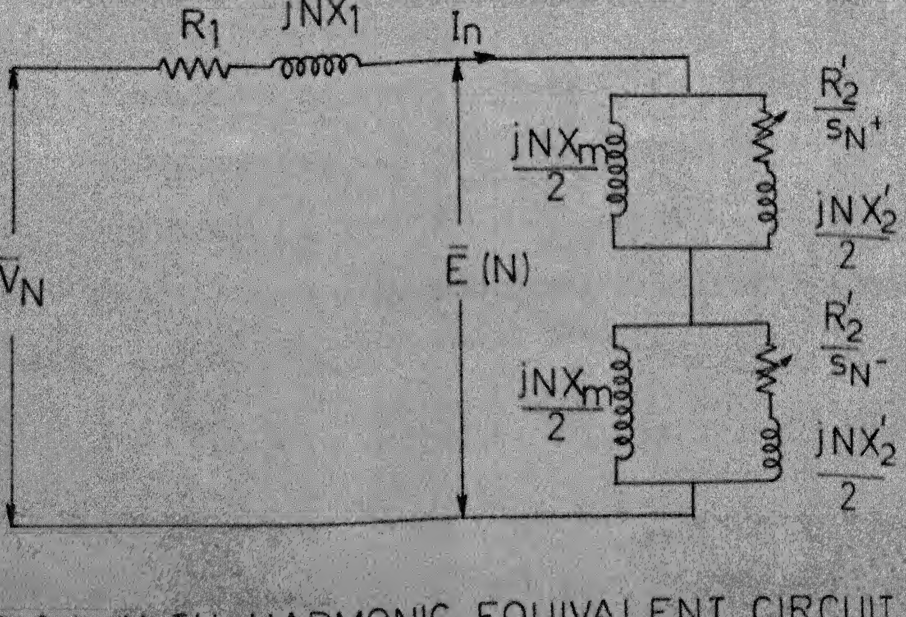

R_1
jNX_1
I_n
$\frac{R_2'}{s_N^+}$
$\frac{jNX_m}{2}$
$\frac{jNX_2'}{2}$
$\bar{V}_N$
$\bar{E}(N)$
$\frac{R_2'}{s_N^-}$
$\frac{jNX_m}{2}$
$\frac{jNX_2'}{2}$

FIG. 2·4 N TH HARMONIC EQUIVALENT CIRCUIT OF SINGLE PHASE MACHINE angle and slip, the current zero instant and hence the firing angle α is obtained using state space procedure. Iterations are avoided by eliminating the unknown induced voltage in the open circuited stator winding in terms of other known variables. However, this is not possible in the harmonic analysis methods. In [1], a procedure which iterates on conduction angle and the induced emf is presented. An attempt is made in this section to avoid iterating on the induced emf and thereby reduce the overall computation time. The procedure is explained below.

The iterative procedure developed in this section starts with aninitial guess value of the conduction angle β. This guess value can be obtained using static equivalent circuit of the machine as is explained in [1]. For the sake of immediate reference, the procedure for obtaining the initial guess is given in Appendix A. The actual value of β will be less than the value obtained from the static equivalent circuit.

The state space procedure solves for the exact current zero instant for the given slip and conduction angle without explicitly knowing the actual induced emf during the off period. Therefore, it should be possible in the harmonic analysis procedure also to obtain an approximate induced stator emf as the iterations on the conduction angle proceeds. The conduction angle β is reduced by a small amount from its initial guess towards its fairly accurate value. At every new value of β, first the induced emf during the off period is made zero and the harmonic analysis is made to obtain an approximate value for induced emf. This is obtained considering the steady state equivalent circuit and the stator voltage waveform with zero off period voltage. The induceed emf is obtained by the following procedure.

The induced emf during the off period is assumed to be a sinusoidal voltage in phase with the supply voltage [1]. Its amplitude EN may be obtained by the following ~~equation~~ relation.

$$EN = \sqrt{\sum_{N=1,3\ldots}^{M} E_N^2} \qquad (2.7)$$

where E_N is the amplitude of the Nth harmonic induced emf obtained using the equivalent circuit given in Fig. 2.4. In Fig. 2.4., $\bar{E}(N)$ is the Nth harmonic induced emf when Nth harmonic stator voltage is applied to the machine. For the same value of β, with the above value of induced emf the harmonic analysis is repeated and the harmonic stator currents are obtained. The r.m.s. value of the stator current during the off period (π-β) is calculated and is examined whether it is reasonably low. If it is reasonably low, solution is obtained and the developed torque of the machine at the given speed and conduction angle is calculated using the equation (2.6). If not, the value of β is reduced by a small amount and the above procedure is repeated.

Therefore, the procedure iterates only on β and for every value of β, the corresponding approximate induced emf is obtained considering the steady state harmonic equivalent circuit. The algorithm for the above procedure is given in the next section.

2.4 Algorithm for the Suggested Procedure

The algorithm for the procedure discussed in the previous section is given below :

1. Read the machine parameters, slips, firing angles and Δβ.
2. Choose slip and firing angle.
3. Decide the initial guess for β using the static equivalent circuit (Appendix A)
4. Assume induced emf during off period (π-β) as zero.
5. Do the harmonic analysis on stator voltage waveform. (Appendix B)
6. Calculate the harmonic stator and rotor currents using the harmonic voltages obtained in step 5 and the harmonic equivalent circuits.
7. Obtain the induced emf EN using equation 2.7.
8. Repeat the harmonic analysis on the stator voltage waveform [Appendix B : Equations (B.5, B.7, B.9 and

B.11) which are functions of induced voltage alone are to be evaluated. Equations (B.4, B.6, B.8 and B.10) which are the functions of supply voltage have been already evaluated in step 5].

9. Obtain the machine currents using the harmonic voltages and the harmonic equivalent circuits.

10. Obtain the rms value of the stator current during the off period. [Divide the off period into N number of intervals and obtain the value of the resultant stator current at the middle of each interval. The root of the mean value of the squared ordinates gives the required r.m.s. value].

11. Check whether the r.m.s. value calculated in step 10 is reasonably low.

12. If not, put $\beta = \beta - \Delta\beta$ and go to step 4. Otherwise go to 13.

13. Calculate the developed torque using equation 2.6.

14. Check whether performance calculations have been done for all given values of slip and α.

15. If not, choose the next set of slip and α and go to 3. Otherwise stop.

This procedure is simple and it is easy to implement in a digital computer program. The results obtained by this procedure are discussed below.

2.5 Comparision of Results

A digital computer program for the above procedure is prepared and the complete performance characteristic of the machine is obtained. For the purpose of comparing the results with the experimental values, a single phase capacitor start induction motor is chosen for the study. The details of the machine are given below.

230 V, 1ϕ, $.25$ hp

$R_1 = 7\Omega$ $X_1 = 15.7\Omega$

$R_2' = 9.63\Omega$ $X_2' = 15.7\Omega$ $X_m = 100\ \Omega$

The above parameters of the machine are obtained from the usual tests. The auxiliary winding is disconnected after starting the machine. The speed-torque characteristic of the machine obtained using the above procedure is shown in Fig. 2.5. The experimental values are marked in the figure. The results obtained using the state space procedure discussed in [2] are also given in Fig. 2.5. for the sake of comparision. The stator current waveform obtained by the suggested harmonic analysis method for the given set of slip and conduction angle is shown in Fig. 2.6. Fig. 2.7 gives the experimental current waveform.

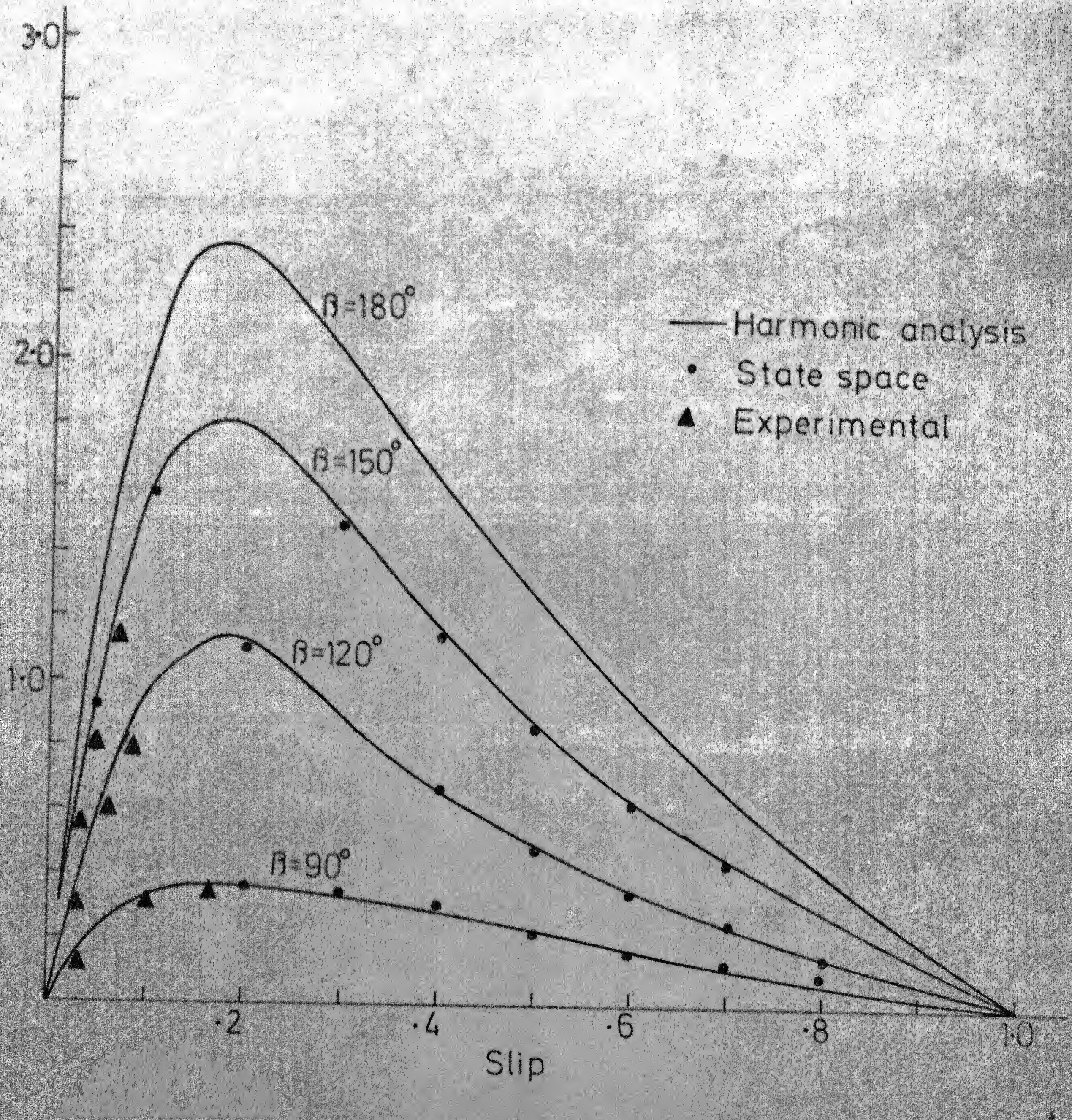

FIG. 2·5 SPEED–TORQUE CHARACTERISTIC OF SINGLE PHASE MACHINE

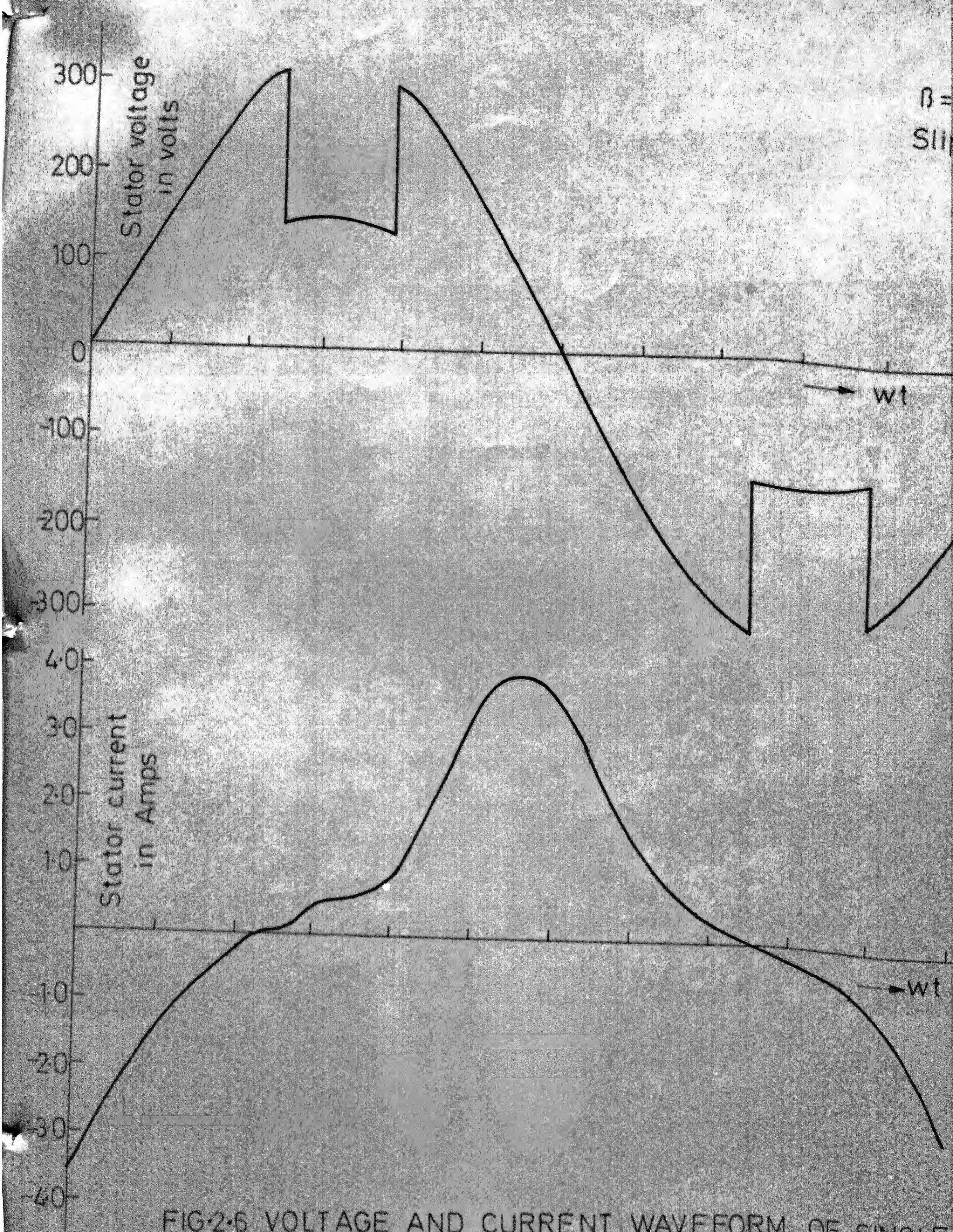

FIG·2·6 VOLTAGE AND CURRENT WAVEFORM OF SINGLE

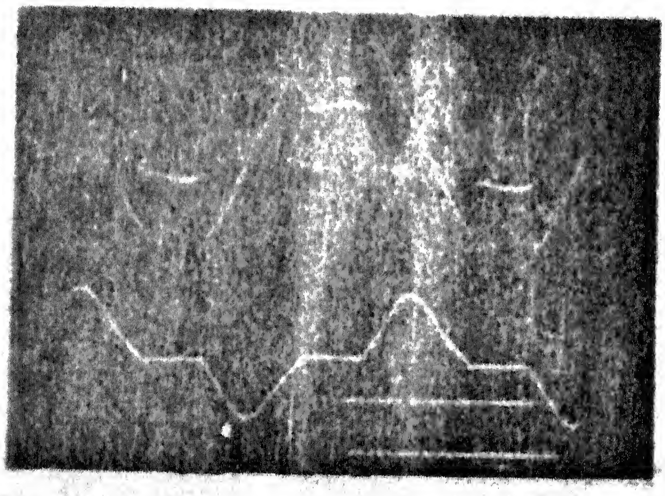

Fig. 2.7 Oscillograms of voltage and current waveform
Upper trace : Voltage, 165 V/division
Lower trace : Current, 3.5 A/division

The small deviation of the experimental results from the analytical values may be due to the error involved in the measuring procedures and the error in the parameters used for the analysis.

2.6 Conclusion

A harmonic analysis method suitable for phase controlled single phase machine has been developed in this chapter. The method iterates only on one variable instead on two. The performance characteristic of the system is obtained using the steady state harmonic equivalent circuits of the machine. The analytical results are compared with experimental values.

CHAPTER 3

PHASE CONTROLLED THREE PHASE INDUCTION MOTOR

3.1 Introduction

As discussed in the introductory chapter, the simplest, most economical and most straight forward method of varying the speed-torque characteristic of small and medium power induction motors which drive variable torque loads like fans and pumps is by adjusting the effective r.m.s. value of the voltage applied to the stator using phase controlled SCRs. Phase controlled SCRs can be used in different circuit configurations. The various circuit configurations demonstrated in [5] are given in Fig. 3.1. The analysis of these circuits is quite complicated because of the reason that the current zero instants and the e.m.f. that may come across the open circuited stator phase due to the rotor currents are not known initially. In [6], an attempt has been made for the exact analysis of a delta - connected system which uses a pair of SCRs connected in antiparallel in each line, but however,the solution of the resulting equations was not carried out. State space techniques have been employed successfully in [3,7] for the solution of star connected systems. Here also a pair of back-to-back connected SCRs is used in each line as shown in circuit 7 of Fig. 3.1. In [8], a four wire star

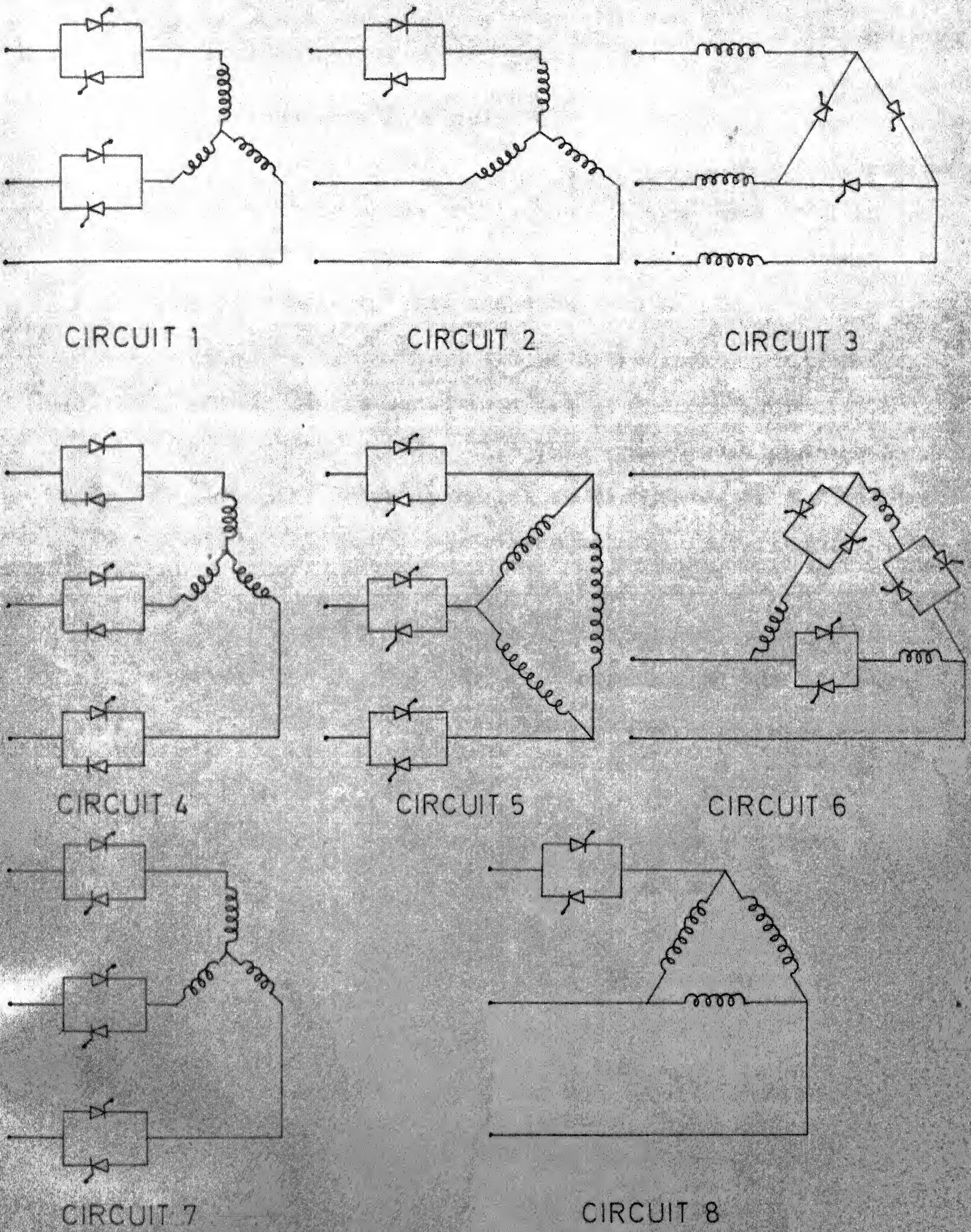
CIRCUIT 1
CIRCUIT 2
CIRCUIT 3
CIRCUIT 4
CIRCUIT 5
CIRCUIT 6
CIRCUIT 7
CIRCUIT 8

FIG. 3·1 VARIOUS CIRCUIT CONFIGURATIONS

connected system with thyristors in antiparallel in each line has been investigated. The analysis of a star connected machine using state space techniques has been explained in [9]. A comparative study of circuits which use six thyristors in different configurations has been made in [10].

In this chapter a three diodes - three thyristors voltage control scheme is discussed in detail. The configuration is shown in circuit 4 of Fig. 3.1. This scheme uses one diode and one thyristor in antiparallel in each phase of the machine. The effective stator voltage of the machine is varied by adjusting the firing angle of the thyristors. The various modes of operation of the system are explained. The state space procedure discussed in [3] is extended to the present study. A modified harmonic analysis method is also explained.

3.2 Various Modes of Operation

The schematic diagram of the three diodes - three thyristors voltage control scheme is shown in circuit 4 of Fig. 3.1. This scheme has the advantage of economy and wide range speed control. The stator voltage can be controlled from rated value to zero by adjusting the firing angle of the thyristors. The firing angle of the thyristors is measured from zero crossing of the phase voltages of the supply. The sequence of firing is given as T_1, T_2, T_3, T_1 and so on. Two different modes of operation are possible depending upon speed and firing angle. The system voltages and currents have three phase symmetry in both modes of operation. If the off period in the phase current of the machine is less than 120 electrical degrees, the system is subject to three phase and single phase operations alternatively. When the system is in three phase operation, three devices conduct. It may be one thyristor and two diodes or two thyristors and one diode. This happens during interval I in Fig. 3.2. During interval II in Fig. 3.2, the system is subject to single phase operation where one thyristor and one diode conduct. This mode of operation is called as 3/2 mode. The other mode of operation occurs when the off period in the phase current of the machine is more than 120 electrical degrees. Here the machine is subject to single phase operation and complete isolation from supply terminals alternatively. During interval I in Fig. 3.3; the machine is completely isolated from the supply terminals and during interval II the machine is single phasing. The mode of operation is called as 2/0 mode. In both the modes of operation three phase symmetry exists in system variables phase voltages and currents because of symmetrical firing of thyristors. The state space procedure developed in [5] is applied to the present study and is explained in the next section.

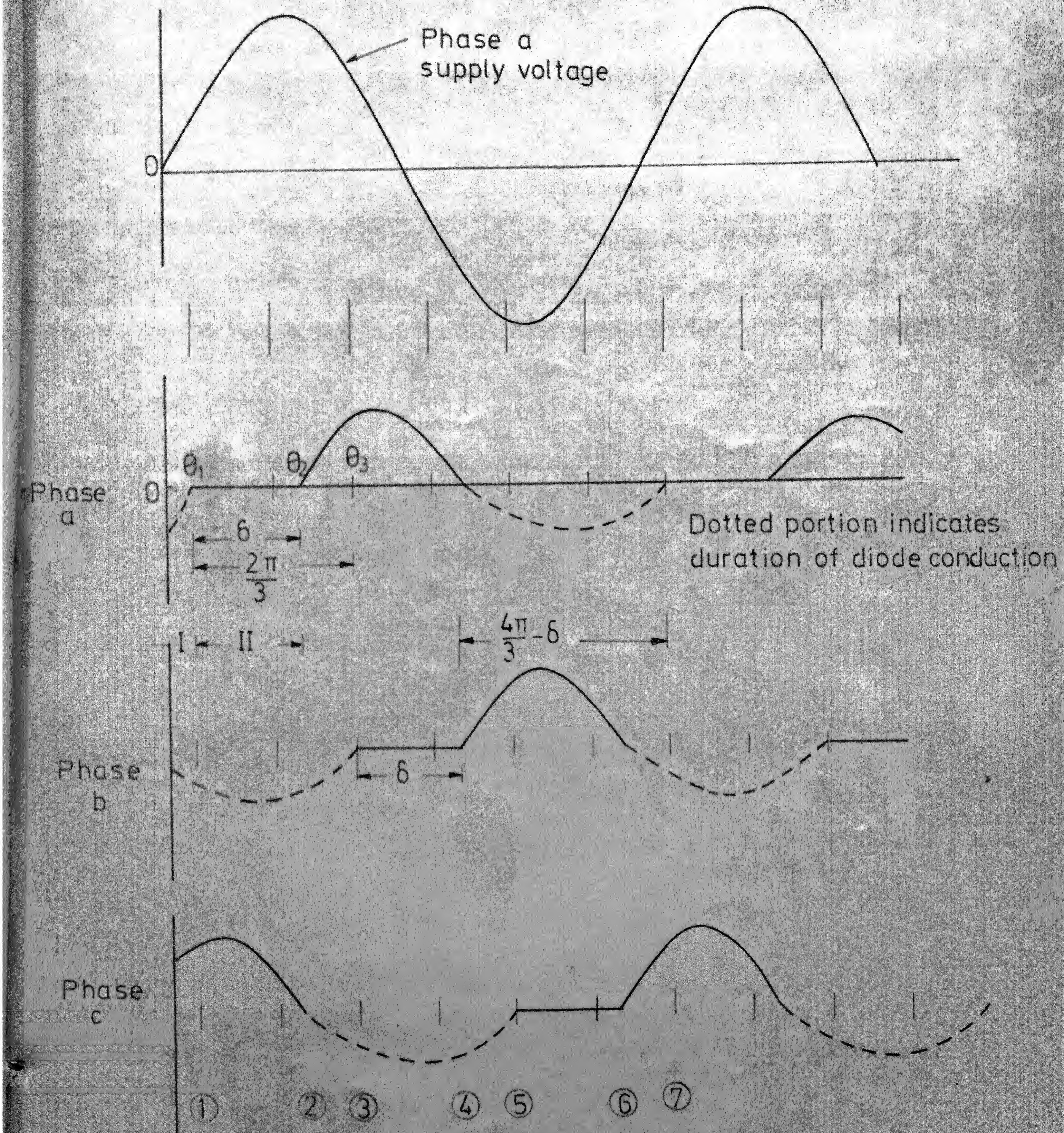
Phase a
supply voltage
0
θ1
θ2
θ3
Phase
a
0
δ
2π/3
Dotted portion indicates
duration of diode conduction
I
II
4π/3 - δ
Phase
b
δ
Phase
c
①
②
③
④
⑤
⑥
⑦

FIG. 3·2 CURRENT WAVEFORMS WHEN THE SYSTEM IS IN 3/2 MODE

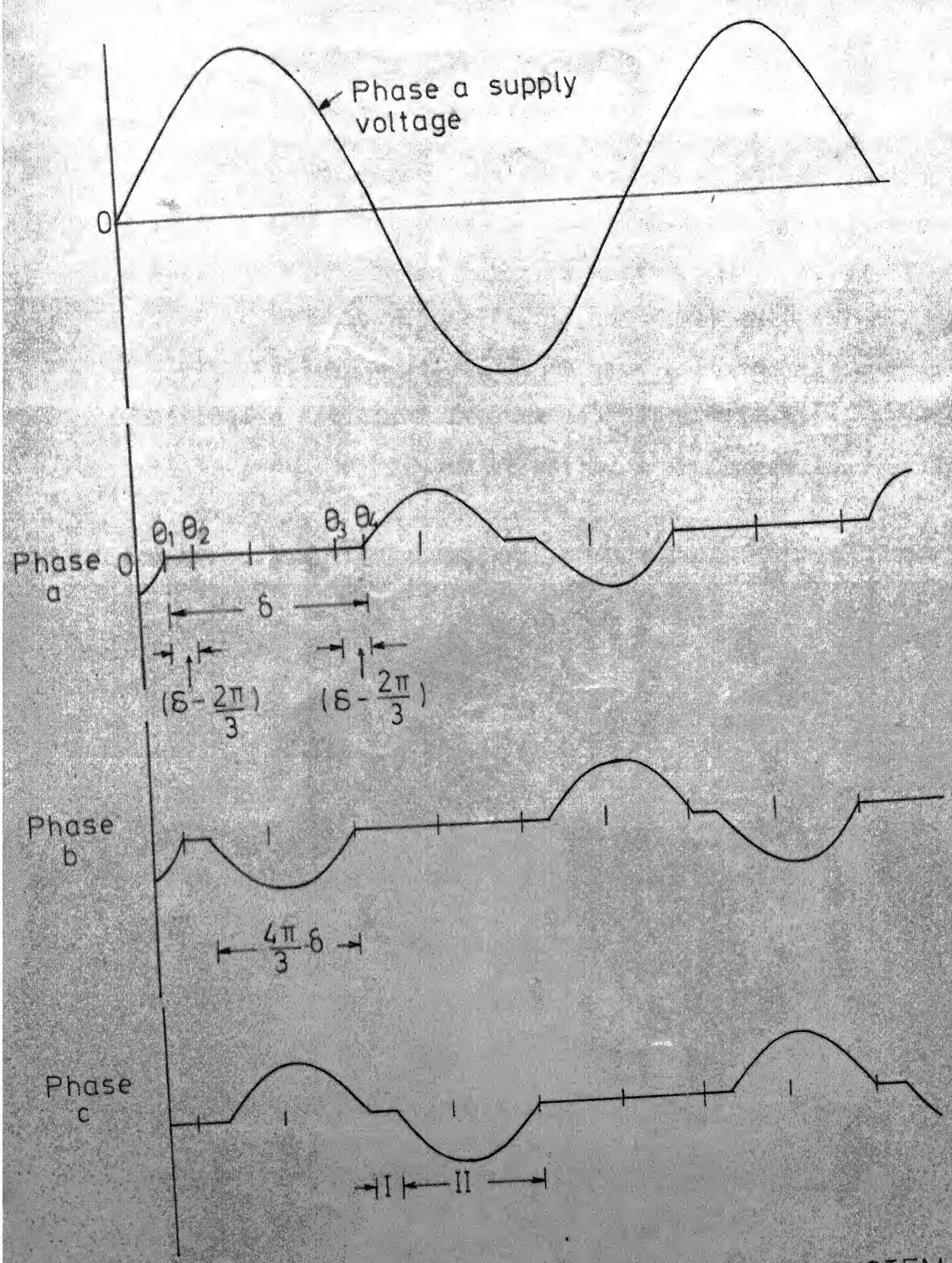
Phase a supply voltage
0
θ_1 θ_2
θ_3 θ_4
Phase a
0
δ
$(\delta - \frac{2\pi}{3})$
$(\delta - \frac{2\pi}{3})$
Phase b
$\frac{4\pi}{3}\delta$
Phase c
I
II

FIG.3.3 CURRENT WAVEFORMS WHEN THE SYSTEM IS IN 2/0 MODE

3.3 State Space Analysis

The state space analysis of the thyristor controlled ac machines can be done in terms of the d-q axes variables fixed in stator or rotor or in a frame rotating at synchronous speed with respect to stator. For the analysis of stator voltage control, it is convenient if the d-q axes variables are fixed in stator. The differential equations of the machine [3] can be arranged in matrix form as shown below.

$$\begin{bmatrix} v_{qs} \\ v_{ds} \\ 0 \\ 0 \end{bmatrix} = \begin{bmatrix} r_s+\frac{p}{\omega}x_s & 0 & \frac{p}{\omega}x_m & 0 \\ 0 & r_s+\frac{p}{\omega}x_s & 0 & \frac{p}{\omega}x_m \\ \frac{p}{\omega}x_m & -\frac{\omega_r}{\omega}x_n & r'_r+\frac{p}{\omega}x'_r & -\frac{\omega_r}{\omega}x'_r \\ \frac{\omega_r}{\omega}x_m & \frac{p}{\omega}x_m & \frac{\omega_r}{\omega}x'_r & r'_r+\frac{p}{\omega}x'_r \end{bmatrix} \begin{bmatrix} i_{qs} \\ i_{ds} \\ i'_{qr} \\ i'_{dr} \end{bmatrix} \qquad (3.1)$$

where

ω_r = speed of the rotor in electrical rad/sec

and ω = frequency of the supply in rad/sec

Equation (3.1) is expressed in perunit form. The actual stator phase voltages and currents are related to the d-q variables as given below

$$v_{qs} = v_{as} \qquad (3.2)$$

$$v_{ds} = \frac{1}{\sqrt{3}}(v_{cs} - v_{bs}) \qquad (3.3)$$

$$i_{qs} = i_{as} \qquad (3.4)$$

$$i_{ds} = \frac{1}{\sqrt{3}}(i_{cs} - i_{bs}) \tag{3.5}$$

The electromagnetic torque developed by the machine is given by

$$T_d = x_m(i_{qs}\, i'_{dr} - i_{ds}\, i'_{qr}) \tag{3.6}$$

In equation (3.6) the variables are to be substituted in per unit. The rated peak line-to-line voltage and rated peak current are chosen as the base quantities. Equation (3.1) can be rearranged as follows :

$$\begin{bmatrix} x_s & 0 & x_m & 0 \\ 0 & x_s & 0 & x_m \\ x_m & 0 & x'_r & 0 \\ 0 & x_m & 0 & x'_r \end{bmatrix} \begin{bmatrix} \frac{di_{qs}}{d\theta} \\ \frac{di_{ds}}{d\theta} \\ \frac{di'_{qr}}{d\theta} \\ \frac{di'_{dr}}{d\theta} \end{bmatrix} = \begin{bmatrix} -r_s & 0 & 0 & 0 \\ 0 & -r_s & 0 & 0 \\ 0 & \frac{\omega_r}{\omega}x_m & -r'_r & \frac{\omega_r}{\omega}x'_r \\ -\frac{\omega_r}{\omega}x_m & 0 & -\frac{\omega_r}{\omega}x'_r & -r'_r \end{bmatrix} \begin{bmatrix} i_{qs} \\ i_{ds} \\ i'_{qr} \\ i'_{dr} \end{bmatrix} + \begin{bmatrix} v_{qs} \\ v_{ds} \\ 0 \\ 0 \end{bmatrix} \tag{3.7}$$

Symbolically,

$$\underline{X}_3\, p\underline{i} = \underline{R}\,\underline{i} + \underline{v} \tag{3.8}$$

If the supply phase a voltage v_a is represented as $V_m \sin\theta$, phase b and phase c voltages are given by

$$v_b = V_m \sin(\theta - 2\pi/3) \quad \text{and}$$

$$v_c = V_m \sin(\theta + 2\pi/3)$$

In normal operation, phase voltages of the machine are the same as the supply voltages.

$$E_1 = V_m \sin\theta \tag{3.9}$$

and
$$E_2 = \frac{1}{\sqrt{3}}(v_c - v_b) = V_m \cos\theta \tag{3.10}$$

Equations (3.9) and (3.10) can be written in differential form as follows

$$\frac{dE_1}{d\theta} = E_2 \tag{3.11}$$

$$\frac{dE_2}{d\theta} = -E_1 \tag{3.12}$$

In vector matrix form,

$$\begin{bmatrix} \frac{dE_1}{d\theta} \\ \frac{dE_2}{d\theta} \end{bmatrix} = \begin{bmatrix} 0 & 1 \\ -1 & 0 \end{bmatrix} \begin{bmatrix} E_1 \\ E_2 \end{bmatrix} \tag{3.13}$$

Equations (3.8) and (3.13) are sufficient to represent the various states of the system. The following are the different states to which the system is put in the two modes of operation explained in the previous section : a) three phase state b) single phase state and c) off state.

a) Three phase state :

During three phase state of operation all the three machine terminals are connected to the supply terminals. Equations (3.8) and (3.13) are combined and arranged in matrix form as given below.

$$\begin{bmatrix} \frac{d\underline{i}}{d\theta} \\ \\ \frac{d\underline{E}}{d\theta} \end{bmatrix} = \begin{bmatrix} \underline{X}_3^{-1}\underline{R} & \underline{X}_3^{-1}\underline{C}_1 \\ \\ 0 & \begin{bmatrix} 0 & 1 \\ -1 & 0 \end{bmatrix} \end{bmatrix} \begin{bmatrix} \underline{i} \\ \\ \underline{E} \end{bmatrix} \qquad (3.14)$$

where

$$\underline{C}_1 = \begin{bmatrix} 1 & 0 \\ 0 & 1 \\ 0 & 0 \\ 0 & 0 \end{bmatrix} \qquad (3.15)$$

and $\underline{X}_3$ is already defined.

Equation 3.14 can be represented symbolically as,

$$\dot{\underline{x}} = A\ \underline{x} \qquad (3.16)$$

b) Single phase state

The system is subject to single phase operation when one of the machine phases gets open circuited due to delayed firing of thyristors. When a particular phase of the machine is isolated from supply, the corresponding phase current becomes zero and the imposition of this current zero in the mathematical model becomes a problem. This problem has been tackled in [3,7] by applying a voltage equal to the induced e.m.f. of the open circuited phase across it. The same technique is used in the present analysis also. However, an alternative method is suggested in Chapters 6 and 7 for a similar scheme. If phase a is open $i_a = 0$ and $\frac{di_a}{d\theta} = 0$.

That is

$$i_{qs} = 0 \qquad (3.17)$$

and

$$\frac{di_{qs}}{d\theta} = 0 \qquad (3.18)$$

Phase a induced emf $e_{as} = x_m \frac{di'_{qr}}{d\theta}$ (3.19)

The current zero is imposed by equating v_{qs} to the induced emf.

Therefore,

$$v_{qs} = x_m \frac{di'_{qr}}{d\theta} \qquad (3.20)$$

Phase b and phase c of the machine are connected to the supply terminals.

$$\begin{aligned} v_{ds} &= \frac{1}{\sqrt{3}} (v_c - v_b) \\ &= E_2 \qquad (3.21) \end{aligned}$$

Substituting equations (3.20) and (3.21) in (3.1) and rearranging,

$$\begin{bmatrix} \frac{d\underline{i}}{d\theta} \\ \\ \frac{d\underline{E}}{d\theta} \end{bmatrix} = \begin{bmatrix} \underline{X}_4^{-1}\underline{R} & \underline{X}_4^{-1}\underline{C}_2 \\ \\ \underline{0} & \begin{bmatrix} 0 & 1 \\ -1 & 0 \end{bmatrix} \end{bmatrix} \begin{bmatrix} \underline{i} \\ \\ \underline{E} \end{bmatrix} \qquad (3.22)$$

where

$$\underline{X}_4 = \begin{bmatrix} x_s & 0 & 0 & 0 \\ 0 & x_s & 0 & x_m \\ x_m & 0 & x_r' & 0 \\ 0 & x_m & 0 & x_r' \end{bmatrix} \quad (3.23)$$

$$\underline{C}_2 = \begin{bmatrix} 0 & 0 \\ 0 & 1 \\ 0 & 0 \\ 0 & 0 \end{bmatrix} \quad (3.24)$$

Equation (3.22) can be written in compact form as

$$\underline{\dot{x}} = \underline{B}\ \underline{x} \quad (3.25)$$

c) Off state :

During off state, the machine is completely disconnected from the supply. Since the phase currents of the machine are zero during this state of operation, the d-q axes currents vanish. The current zeros can be imposed in the model by equating d-q axes voltages to the respective induced emfs

$$v_{qs} = x_m \frac{di'_{qr}}{d\theta} \quad (3.26)$$

$$v_{ds} = x_m \frac{di'_{dr}}{d\theta} \quad (3.27)$$

Substituting equations (3.26) and (3.27) in (3.1)

$$\underline{X}_4 = \begin{bmatrix} x_s & 0 & 0 & 0 \\ 0 & x_s & 0 & x_m \\ x_m & 0 & x'_r & 0 \\ 0 & x_m & 0 & x'_r \end{bmatrix} \qquad (3.23)$$

$$\underline{C}_2 = \begin{bmatrix} 0 & 0 \\ 0 & 1 \\ 0 & 0 \\ 0 & 0 \end{bmatrix} \qquad (3.24)$$

Equation (3.22) can be written in compact form as

$$\underline{\dot{x}} = \underline{B}\ \underline{x} \qquad (3.25)$$

c) Off state :

During off state, the machine is completely disconnected from the supply. Since the phase currents of the machine are zero during this state of operation, the d-q axes currents vanish. The current zeros can be imposed in the model by equating d-q axes voltages to the respective induced emfs

$$v_{qs} = x_m \frac{di'_{qr}}{d\theta} \qquad (3.26)$$

$$v_{ds} = x_m \frac{di'_{dr}}{d\theta} \qquad (3.27)$$

Substituting equations (3.26) and (3.27) in (3.1)

$$\begin{bmatrix} \frac{d\underline{i}}{d\theta} \\ \\ \frac{d\underline{E}}{d\theta} \end{bmatrix} = \begin{bmatrix} \underline{X}_5^{-1}\ \underline{R} & \underline{0}^T \\ \\ \underline{0} & \begin{bmatrix} 0 & 1 \\ -1 & 0 \end{bmatrix} \end{bmatrix} \begin{bmatrix} \underline{i} \\ \\ \underline{E} \end{bmatrix} \tag{3.28}$$

where

$$\underline{X}_5 \quad \begin{bmatrix} x_s & 0 & 0 & 0 \\ 0 & x_s & 0 & 0 \\ x_m & 0 & x_r' & 0 \\ 0 & x_m & 0 & x_r' \end{bmatrix} \tag{3.29}$$

In state space form,

$$\dot{\underline{x}} = \underline{C}\ \underline{x} \tag{3.30}$$

3.3.1 Solution for 3/2 mode :

Every two firing instants are separated by $2\pi/3$ electrical radians. Referring to Fig. 3.2, the system is in single phase state from θ_1 to θ_2. During this period, phase a is disconnected from the supply. Duration of this interval is denoted as δ. The system is subject to three phase operation from θ_2 to θ_3. If the state of the system at θ_1 is denoted as $x(\theta_1)$, then the state of the system at θ_2 is given by

$$\underline{x}(\theta_2) = e^{(\theta_2 - \theta_1)\ \underline{B}}\ \underline{x}(\theta_1) \tag{3.31}$$

$$= e^{\delta \underline{B}}\ \underline{x}(\theta_1) \tag{3.32}$$

The state of the system at θ_3 is given by

$$\underline{x}(\theta_3) = e^{(\frac{2\pi}{3} - \delta)\,\underline{A}}\;\underline{x}(\theta_2) \tag{3.33}$$

$$= e^{(\frac{2\pi}{3} - \delta)\,\underline{A}}\; e^{\delta \underline{B}}\;\underline{x}(\theta_1) \tag{3.34}$$

Since the system is having three phase symmetry, any two state vectors separated by $2\pi/3$ electrical degrees can be related by a connection matrix $\underline{T}$. This connection matrix is obtained as follows.

In the d,q,0 model

$$i_{qs}(\theta) = I_m \sin\theta \quad \text{and}$$

$$i_{ds}(\theta) = I_m \cos\theta$$

$$\begin{aligned} i_{qs}(\theta + \tfrac{2\pi}{3}) &= I_m \sin(\theta + 120^\circ) \\ &= I_m[-\tfrac{1}{2}\sin\theta + \tfrac{\sqrt{3}}{2}\cos\theta] \end{aligned} \tag{3.35}$$

$$\begin{aligned} i_{ds}(\theta + \tfrac{2\pi}{3}) &= I_m \cos(\theta + 120) \\ &= I_m[-\tfrac{1}{2}\cos\theta - \tfrac{\sqrt{3}}{2}\sin\theta] \end{aligned} \tag{3.36}$$

Putting equations (3.35) and (3.36) in matrix form,

$$\begin{bmatrix} i_{qs}(\theta + 2\pi/3) \\ i_{ds}(\theta + 2\pi/3) \end{bmatrix} = \begin{bmatrix} -\frac{1}{2} & \frac{\sqrt{3}}{2} \\ -\sqrt{3}/2 & -\frac{1}{2} \end{bmatrix} \begin{bmatrix} i_{qs}(\theta) \\ i_{ds}(\theta) \end{bmatrix} \tag{3.37}$$

Considering all the six state variables i_{qs}, i_{ds}, i'_{qr}, i'_{dr}, E_1 and E_2, the $\underline{T}$ matrix becomes,

$$\underline{T} = \begin{bmatrix} -\frac{1}{2} & \sqrt{3}/2 & 0 & 0 & 0 & 0 \\ -\sqrt{3}/2 & -\frac{1}{2} & 0 & 0 & 0 & 0 \\ 0 & 0 & -\frac{1}{2} & \sqrt{3}/2 & 0 & 0 \\ 0 & 0 & -\sqrt{3}/2 & -\frac{1}{2} & 0 & 0 \\ 0 & 0 & 0 & 0 & -\frac{1}{2} & \sqrt{3}/2 \\ 0 & 0 & 0 & 0 & -\sqrt{3}/2 & -\frac{1}{2} \end{bmatrix} \qquad (3.38)$$

The state vectors $\underline{x}(\theta_3)$ and $\underline{x}(\theta_1)$ are related as follows

$$\underline{x}(\theta_3) = \underline{T}\,\underline{x}\,(\theta_1) \qquad (3.39)$$

From equations (3.34) and (3.39),

$$[\underline{T} - e^{(\frac{2\pi}{3} - \delta)\,\underline{A}}\; e^{\delta \underline{B}}]\;\underline{x}\,(\theta_1) = 0 \qquad (3.40)$$

Equation (3.40) can be written as

$$\begin{bmatrix} \underline{P}_1 & \underline{P}_2 \\ \underline{P}_3 & \underline{P}_4 \end{bmatrix} \begin{bmatrix} \underline{i}(\theta_1) \\ \underline{E}(\theta_1) \end{bmatrix} = \underline{0} \qquad (3.41)$$

From equation (3.41),

$$\begin{aligned} \underline{i}(\theta_1) &= -\,\underline{P}_1^{-1}\,\underline{P}_2\,\underline{E}(\theta_1) \\ &= \underline{Q}\,\underline{E}\,(\theta_1) \end{aligned} \qquad (3.42)$$

Since $i_{qs}(\theta_1) = 0$,

$$Q_{11}\,E_1(\theta_1) + Q_{12}\,E_2(\theta_1) = 0$$

that is, $$\frac{E_1(\theta_1)}{E_2(\theta_1)} = -\frac{Q_{12}}{Q_{11}} \qquad (3.43)$$

but $$E_1(\theta_1) = V_m \sin\theta_1 \qquad (3.44)$$

and $$E_2(\theta_1) = V_m \cos\theta_1 \qquad (3.45)$$

Therefore, $\frac{E_1(\theta_1)}{E_2(\theta_1)} = \tan(\theta_1) = -\frac{Q_{12}}{Q_{11}}$

$$\theta_1 = \tan^{-1}\left(-\frac{Q_{12}}{Q_{11}}\right) \qquad (3.46)$$

Once the instant of current zero θ_1 is computed, the initial state vector $\underline{x}(\theta_1)$ can be obtained using equations (3.42), (3.44) and (3.45). Having obtained the initial state vector, the complete solution can be computed using equations (3.16) and (3.25). Equation (3.6) gives instantaneous torque develoved by the machine for the given slip and off period δ. The average torque is obtained using the numerical technique.

3.3.2 Solution for 2/0 mode :

This mode of operation occurs when the off period in the stator phase current is more than 120 electrical degrees. The phase currents of the machines for this mode of operation are shown in Fig. 3.3. In Fig. 3.3, the system is subject to off state from θ_1 to θ_2 and to single phase state from θ_2 to θ_3. Now an equation similar to (3.40) is obtained using equations (3.25), (3.30) and (3.39) and is given below

$$\left[\underline{I} - e^{\left(\frac{4\pi}{3} - \delta\right)\underline{B}}\, e^{(\delta - 2\pi/3)\underline{C}}\right] \underline{x}(\theta_1) = \underline{0} \qquad (3.47)$$

The initial state vector and the complete solution are obtained using equations (3.25), (3.30) and (3.47). The speed torque characteristic of the test machine is obtained for various values of δ and it is given in Fig. 3.4.

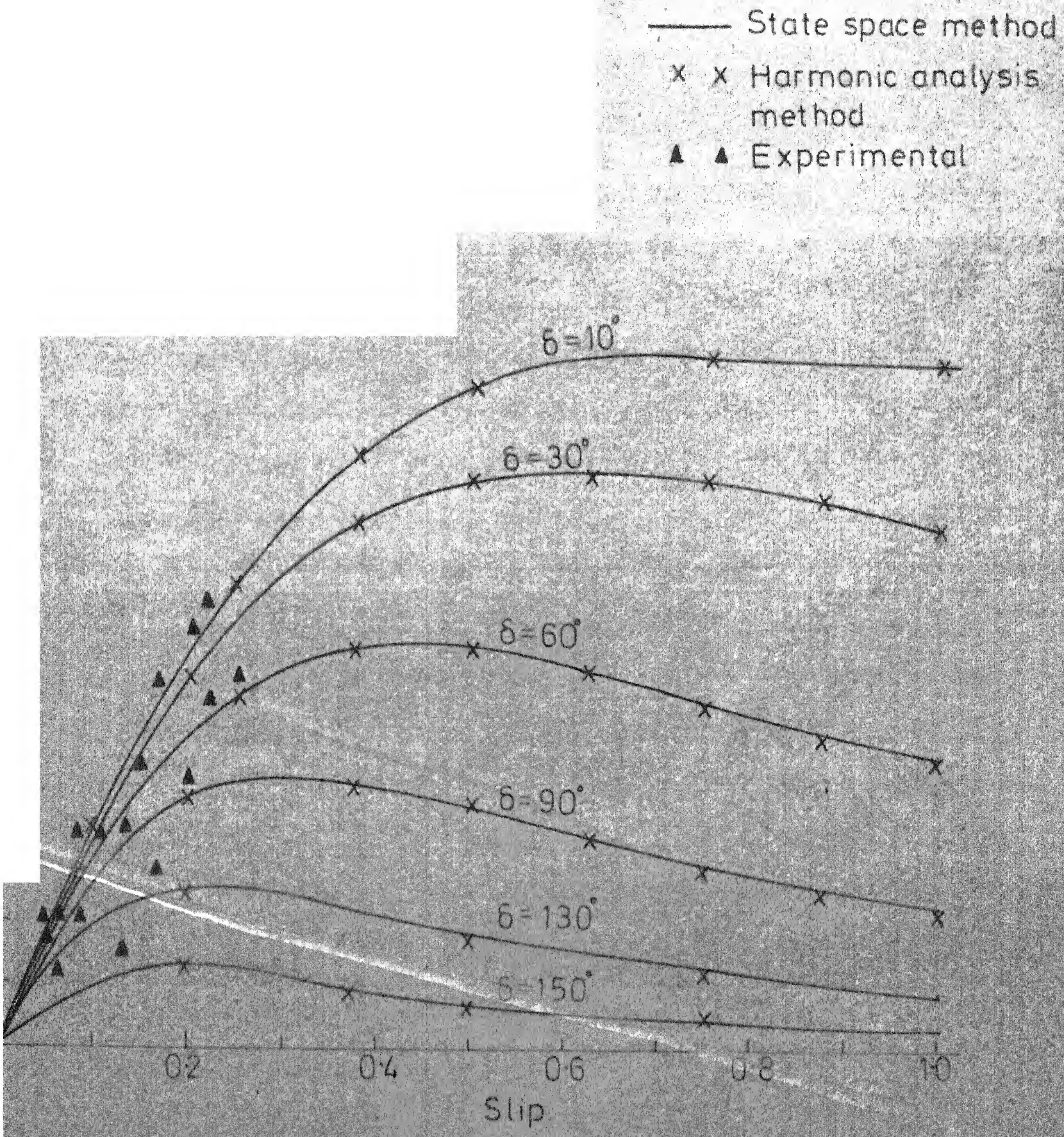

IG. 3·4 SPEED-TORQUE CHARACTERISTIC FOR 3 THYRISTORS 3 DIODES CASE

3.4 Method of Harmonic Analysis

The harmonic analysis method can be applied to all thyristor controlled machine problems. As explained in Chapter 2 for the analysis of single phase motor, the voltage waveform applied to the stator phase of the machine is resolved into several harmonic components and the resultant machine current and performance characteristic of the system are obtained using the harmonic equivalent circuits. The stator voltage waveform must be defined fully for the entire cycle. However, the stator voltage waveforms are not defined completely because of the unknown current zero instants and induced emf during the off period. In [7] iterative techniques are employed to solve for these unknown values. The practical waveform obtained from the actual system is used for the harmonic analysis in [11]. The iterative method discussed in Chapter 2 did not yield satisfactory results when applied to the present analysis. Therefore, in the present study, the current zero instants and induced emfs are obtained using the state space procedure and these informations are used in obtaining the harmonic components of the stator voltage waveform. No iteration on the off period or induced emf is made.

In the state space procedure, the instantaneous torque developed by the machine is computed and the average torque is obtained using a numerical technique, whereas in the present method the average torque is calculated easily using the harmonic equivalent circuits. Therefore, this method makes use of the advantage of both state space technique and harmonic equivalent circuit of the machine. The main advantage of this procedure is that the frequency dependency of the machine parameters can be easily taken into account. This is explained in the next chapter.

Considering the 3/2 mode of operation, phase a of the machine is disconnected from the supply from θ_1 to θ_2 as shown in Fig. 3.2. SCR 1 is triggered at (2) and the system enters into three phase operation. The three phase operation continues upto (3) when diode D_2 turns off. In between (3) and (4) phase b gets open circuited. At (4) SCR 2 is turned on and the system experience three phase operation until (5) when diode D_3 stops conduction. From (5) to (6) the system is single phasing and enters into three phase state at (6). The three phase state exists upto (7) when diode D_1 goes to off state and the above cycle of operation repeats. Now the line-to-line voltage v_{ab} appearing across the machine terminals can be defined as follows

$$\begin{aligned} v_{ab} &= e_1(\theta) && \theta_1 \leqslant \theta \leqslant \theta_1 + \delta \\ &= \sqrt{3}\, V_m \sin(\theta + \pi/6) && \theta_1 + \delta \leqslant \theta \leqslant \frac{2\pi}{3} + \theta_1 \\ &= e_2(\theta) && \frac{2\pi}{3} + \theta_1 \leqslant \theta \leqslant \frac{2\pi}{3} + \delta + \theta_1 \\ &= \sqrt{3}\, V_m \sin(\theta + \pi/6) && \frac{2\pi}{3} + \delta + \theta_1 \leqslant \theta \leqslant 2\pi + \theta_1 \qquad (3.48) \end{aligned}$$

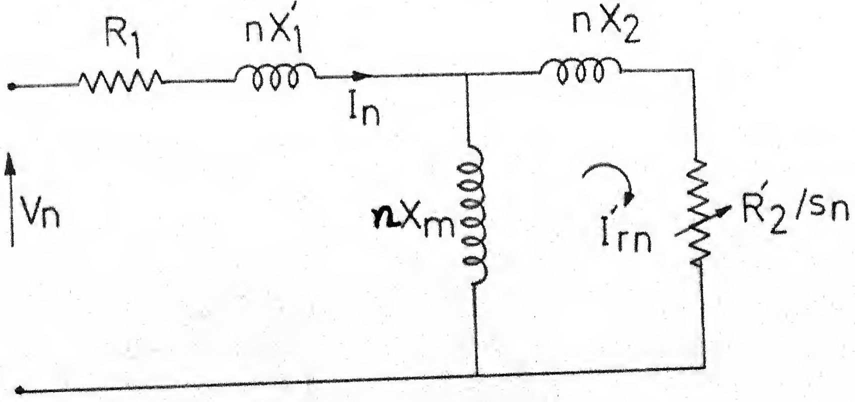
R_1
nX_1'
nX_2'
I_n
V_n
nX_m
I_{rn}'
R_2'/sn

FIG. 3·5 n th HARMONIC EQUIVALENT CIRCUIT

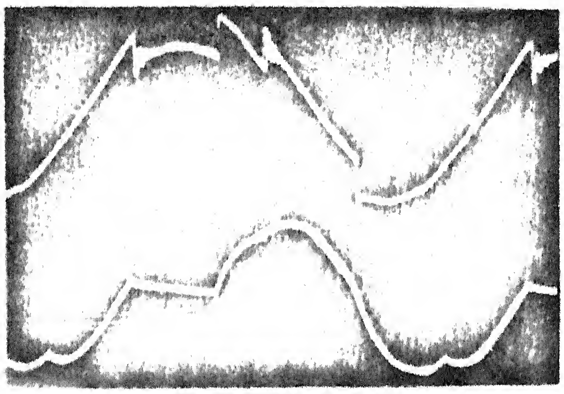

(a) 3/2 mode
Upper trace : Line-to-line voltage, .67 P.U./division
Lower trace : Line current, 1 P.U./division

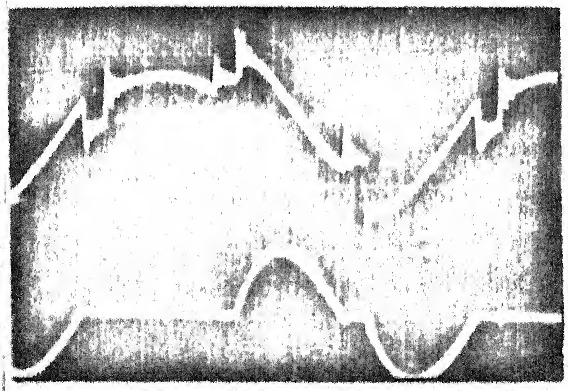

(b) 2/0 mode
Upper trace : Line-to-line voltage .67 P.U./division
Lower trace : Line current, 1 P.U./division

Fig. 3.6 Oscillograms demonstrating different modes of operation

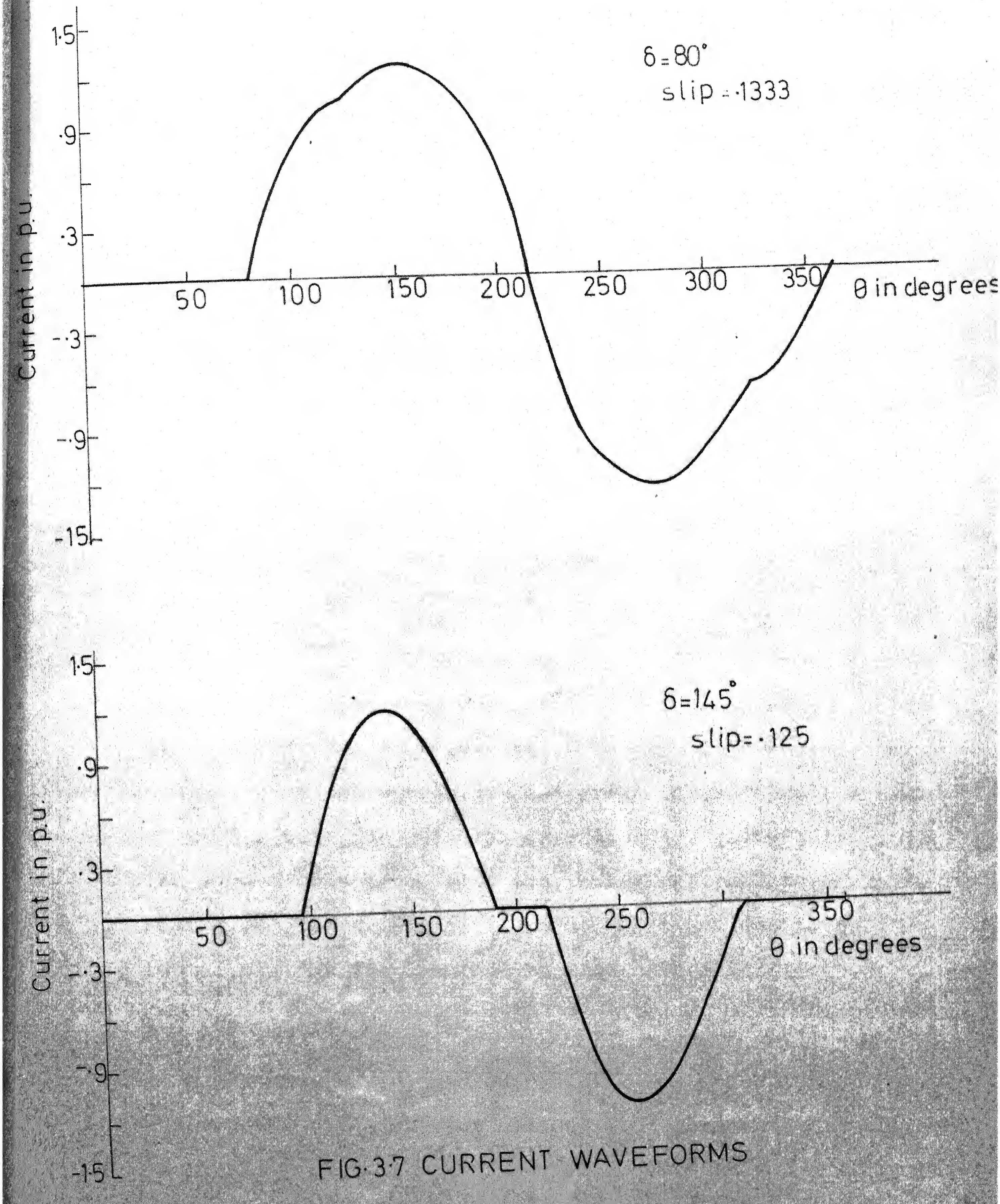

FIG·3·7 CURRENT WAVEFORMS

$$T_d = \sum_{n=1,4,7,..}^{N} \frac{I'^2_{rn}}{2} \cdot \frac{R'_2}{s_n} - \sum_{n=2,5,..}^{N} \left(\frac{I'_{rn}}{2}\right)^2 \frac{R'_2}{s_n} \qquad (3.53)$$

The negative harmonics produce braking torque and so -ve sign is introduced in the above equation.

3.5 Experimental Observations

The practical test of the three diodes - three thyristors voltage control scheme was carried out on a slip ring machine. The details of the test machine are given below

3 HP, 1400 rpm, 400 V slip ring machine

R_1 = 1.765 Ohms X_1 = 3.0 Ohms

R'_2 = 4.52 Ohms X'_2 = 3.0 Ohms

X_m = 650 Ohms

The machine parameters are obtained using the usual short circuit and open circuit tests. The two different modes of operation of the system are observed and the sample oscillograms for both the modes of operation are given in Fig. 3.6. These waveforms agree with the analitical results given in Fig. 3.7. The experimental values of the speed torque characteristic of the machine are also marked in Fig. 3.4.

3.6 Conclusion

The stator voltage control of three phase induction motor using one thyristor and one diode connected in anti-parallel in each line has been studied in this chapter. The various possible modes of operation of the system are discussed. A state space procedure and a modified harmonic analysis method are developed to obtain the performance characteristic of the machine. The actual test was conducted on a slip ring machine and the oscillograms demonstrating the various modes of operation are shown. The analytical results of the machine are compared with the experimental observations.

CHAPTER 4

FREQUENCY DEPENDENCY OF MACHINE PARAMETERS

4.1 Introduction

Thyristor controlled machines are fed with non-sinusoidal voltages and currents. In the case of phase controlled induction motors, the effective voltage applied to each phase of the machine is controlled by adjusting the phase position of the firing pulses to SCRs. As there is a definite off period in the current waveform due to the delayed firing of SCRs, the phase voltage waveforms are not smooth and are distorted. The amplitude of different harmonics which are present in these waveforms depends upon the circuit configuration used, the firing angle and other operating conditions of the machine. In the case of single phase thyristor controlled machine discussed in Chapter 2, the voltage waveform applied to the machine terminals is having only odd harmonics. The even harmonics are absent because of the halfwave symmetry present in the voltage waveform. The voltage waveform of the three thyristors - three diodes system discussed in Chapter 3 do have all nontriplen odd and even harmonics because the voltage waveform does not have halfwave symmetry and the neutral of the system is isolated. It is of interest to study the effects of these harmonics on the performance of the machine.

The machine parameters vary with the harmonic content of the waveforms due to the following reasons [12] : i) nonuniform current density distribution within the conductors of the machine winding and rotor bars, ii) increased leakage flux produced by harmonic currents, iii) saturation of magnetic paths due to harmonic leakage fluxes. The effective stator and rotor resistances of the machine increase and the magnetising inductance decreases with the presence of harmonics in the input voltage waveform. Therefore the frequency dependency of the machine parameters must be included in the analysis of thyristor controlled machines. Two methods of analysis, i) state space method and ii) harmonic analysis method have been discussed in the previous chapters for the phase controlled induction motors. The state space method gives exact current and voltage waveforms with less computational effort, but this method is not suitable to study the effects of frequency dependency of the machine parameters. The harmonic analysis method can conveniently take into account the effect of frequency dependency by substituting the appropriate resistances and inductances in the respective harmonic equivalent circuits. This is the major advantage of harmonic equivalent circuit method [7].

In this chapter, an attempt is made to study the effects of the frequency dependency of the machine parameters on the performance characteristic of the machine using harmonic equivalent circuits. Three thyristors - three diodes configuration and six thyristors configuration are used for the study.

4.2 Variation of Stator and Rotor Resistances with Frequency

The study is made on the same slipring machine used for the performance study of three thyristors - three diodes system discussed in Chapter 3. The effective stator and rotor resistance at different frequency of stator excitation was obtained as follows. The block rotor test was conducted at different frequency of excitation and the input power was noted. The effective equivalent resistances at the given frequency of excitation is obtained by equating this power to I^2 Req heat loss. R_{eq} is the equivalent resistance of the machine looking from stator terminals with the rotor blocked. A few observations were made between 50 Hz and 300 Hz. The ratio of stator to rotor resistance at the 50 Hz operation was obtained and the same ratio was used to divide the effective equivalent resistance into stator and rotor resistances at all other frequencies. It was observed that the variation of machine resistances with frequency was fairly linear for the range considered. This is shown in Fig. 4.1. The values given in this figure are used in the appropriate harmonic equivalent circuits for the present study.

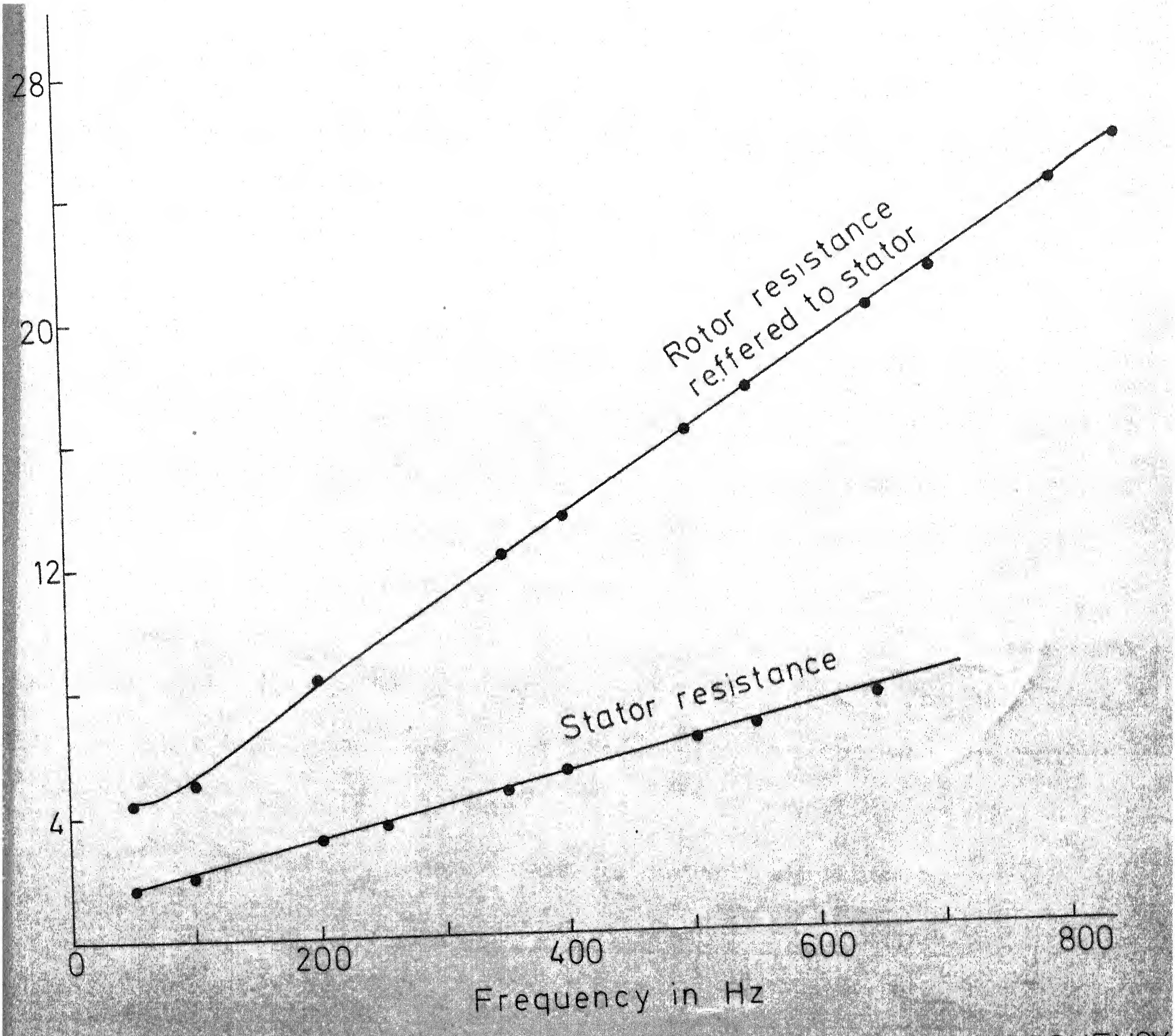

FIG.4.1 VARIATION OF MACHINE RESISTANCE WITH FREQUENCY

4.3 Effects of Harmonics on Machine Inductances

It has been discussed in [12] that the leakage inductances of the machine decreases with the presence of harmonics. In the present analysis these values are assumed as constant as there was not much reduction in inductances observed in the range of frequencies considered for the blocked rotor test discussed in the previous section. The magnetising inductance to fundamental frequency excitation is also assumed to be unaltered by the presence of harmonics.

4.4 Harmonic Equivalent Circuits and Harmonic Torques

The fundamental frequency equivalent circuit of the induction motor is shown in Fig. 4.2. The harmonic equivalent circuits can be simplified as follows : the slip of therotor to all of the harmonics is approximately equal to unity. Therefore, the harmonic equivalent circuit reduces to the form similar to the blocked rotor equivalent circuit for the particular harmonics being considered. The approximate equivalent circuit is shown in Fig. 4.3.

The nth harmonic machine current is given by

$$\bar{I}_n = \frac{\bar{V}_n}{(R_{1k} + R'_{2k}) + j2\pi\ fn(L_{1k} - L_{2k})} \qquad (4.1)$$

The developed torque for each harmonic can be obtained using the following equation

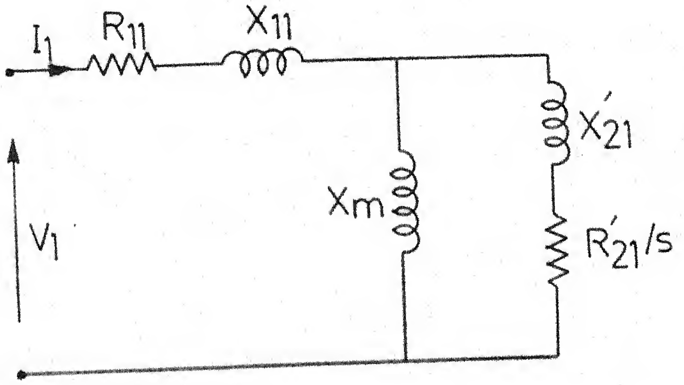
I_1
R_{11}
X_{11}
X'_{21}
X_m
V_1
R'_{21}/s

FIG.4.2 FUNDAMENTAL FREQUENCY EQUIVALENT CIRCUIT

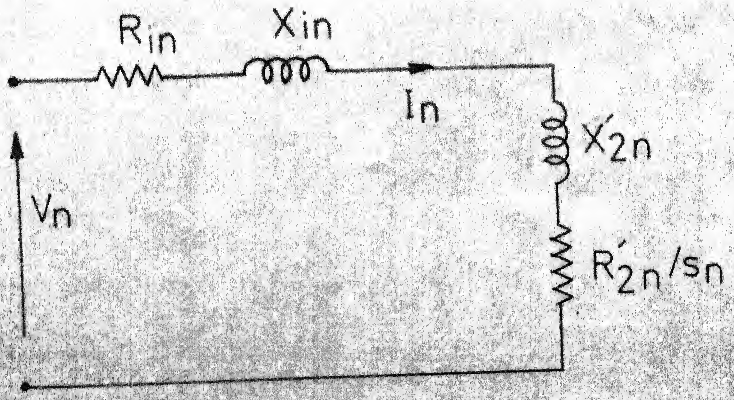
R_{in}
X_{in}
I_n
X'_{2n}
V_n
R'_{2n}/s_n

FIG.4.3 nTH HARMONIC EQUIVALENT CIRCUIT

$$T_{dn} = \pm \frac{3\ I_n^2\ R'_{2k}}{S_n 2\pi n . n_s} \qquad \text{Nm} \qquad (4.2)$$

where –ve sign is used for the backward revolving fields and +ve sign is used for forward fields.

T_{dn}	is the average torque for nth harmonic
R_{1k}	is the per phase stator resistance to nth harmonic
R'_{2k}	is the per phase rotor resistance to nth harmonic referred to stator
L_{1k}	is the stator leakage inductance to nth harmonic
L'_{2k}	is the rotor leakage inductance to nth harmonic referred to stator
n_s	is the synchronous speed corresponding to fundamental frequency excitation in r.p.s.

The harmonic torques are quite small and are alternatively positive and negative as the order of possible harmonics increase. Therefore the total effective harmonic torque is negligibly small. The interaction of every harmonic current with the air-gap flux of another harmonic will result in pulsating torques. In the case of three thyristors - three diodes case all nontriplen odd and even harmonics are present. Therefore, the lowest harmonic present in the system is third harmonic and is contributed by those harmonic rotor currents and air-gap fluxes which differ in speed of rotation by three times the fundamental synchronous speed.

4.5 Three thyristors - three Diodes System

The modified harmonic analysis method discussed in Chapter 3 is used for the present study. The induced emf across the open circuited machine phase is obtained using the state space techniques and fundamental frequency machine parameters. Then, the harmonic analysis is done on the voltage waveform appearing across the machine terminals. Assuming that the leakage inductances remain unaltered, the appropriate machine resistances are substituted in the harmonic equivalent circuits. The various harmonic currents are obtained using equation 4.1. The total average torque is obtained using the following equations.

$$T_d = \sum_{n=1,2,4,\ldots}^{N} \pm \frac{I_n^2 \, R'_{2k}}{S_n \, 2\pi\eta n_s} \quad \text{Nm} \qquad (4.3)$$

where +ve sign is for +ve sequence and -ve sign for -ve sequence currents.

The developed torques thus obtained at various slips and off periods are shown in Fig. 4.4. The speed torque characteristic obtained without considering the frequency dependency is also shown in the figure. It is noted that when the off period is small the frequency dependency of the machine parameters do not have much effect, but at larger ~~frequencies~~ off period. there is some difference between the two characteristics. In the case of large HP squirrel machines the rotor bar resistance may change

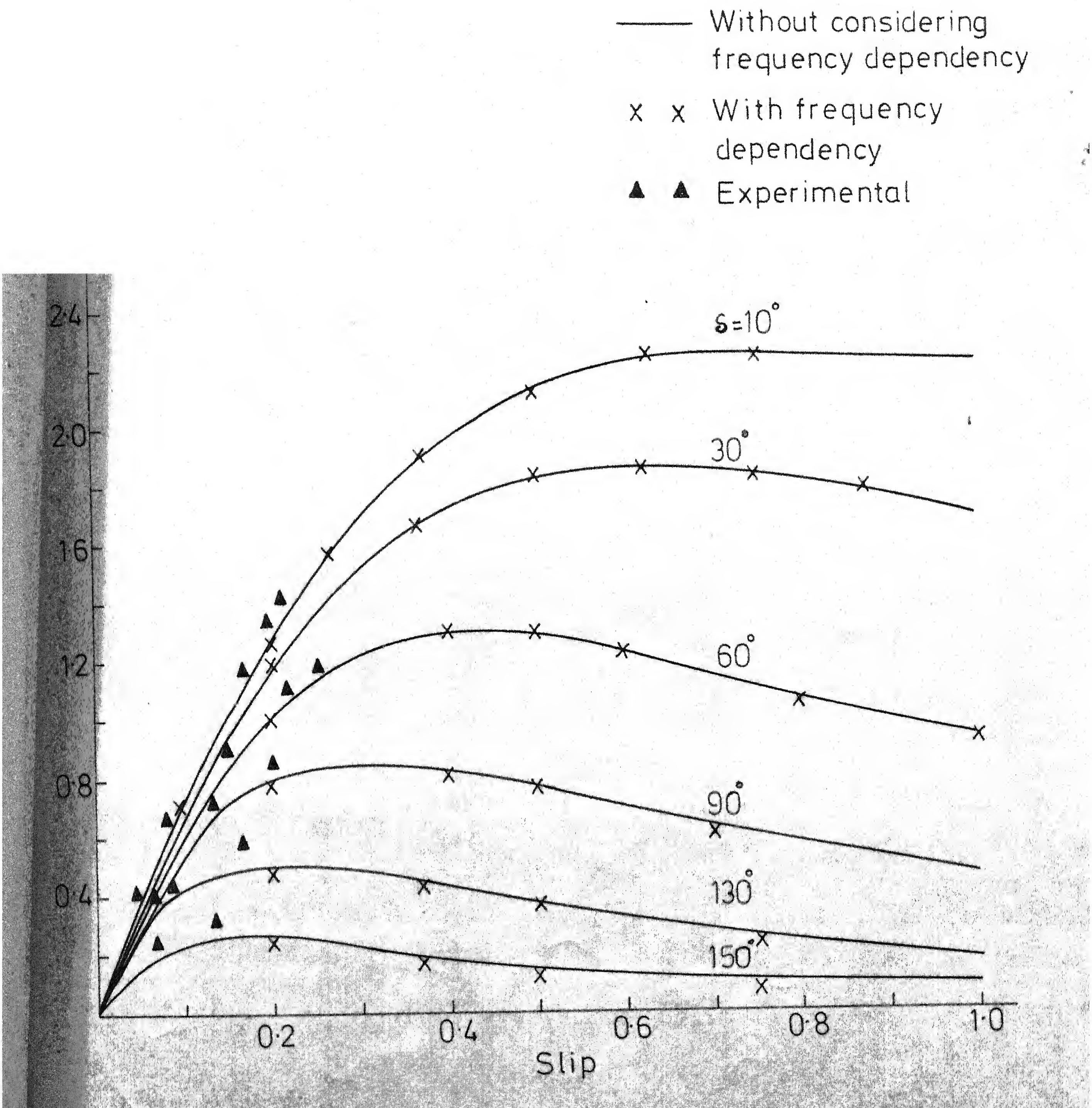

FIG.4.4 SPEED TORQUE CHARACTERISTIC FOR 3 THYRISTORS-3 DIODES CASE

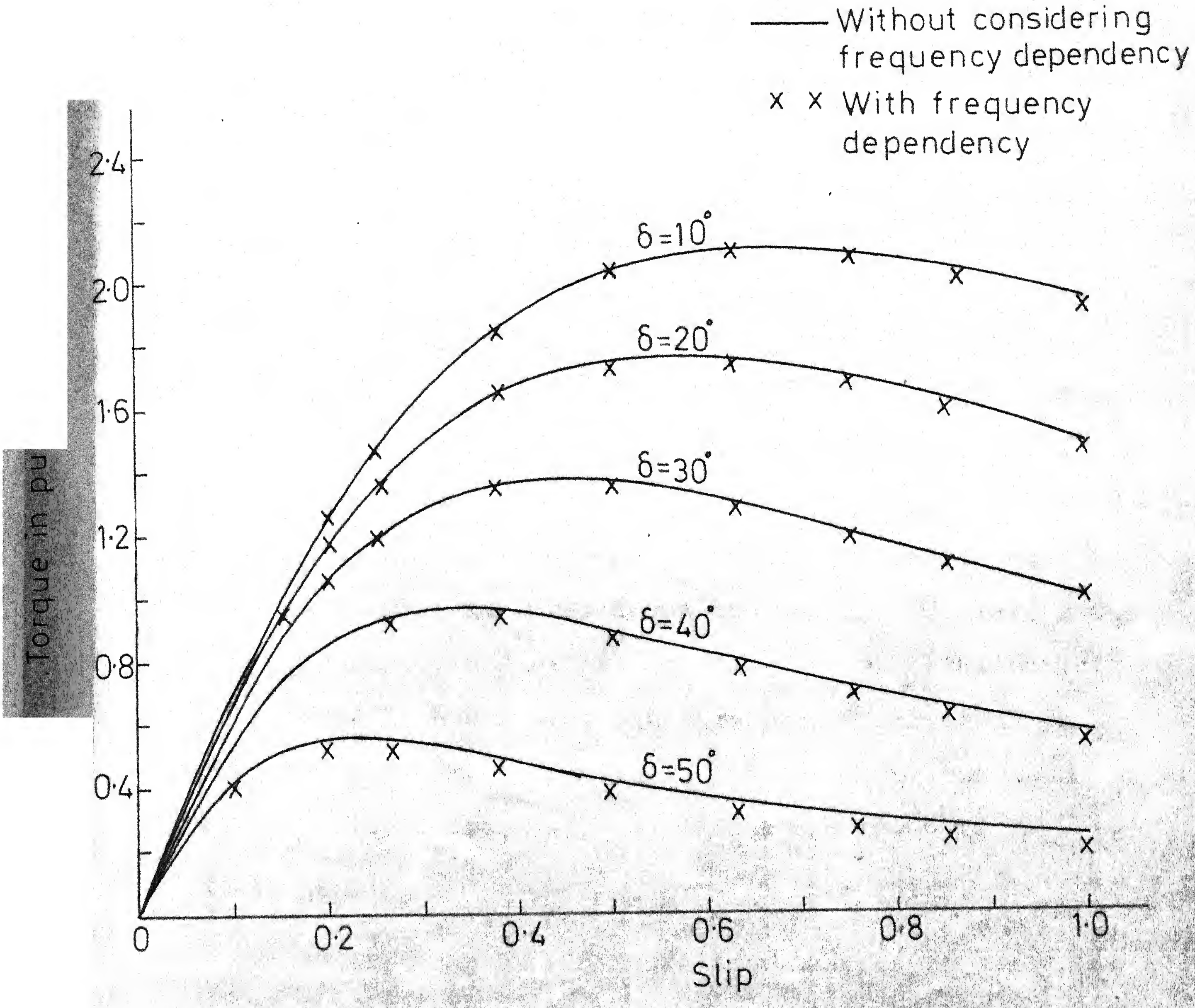

FIG. 4·5 SPEED-TORQUE CHARACTERISTIC FOR 6 THYSISTOR CAS considerably with the degree of distortion present in the input voltage waveform and for these cases the frequency dependency may affect the performance considerably.

4.6 Six Thyristors Configuration

Similar investigation is also carried out on the six thyristor configuration shown in circuit 7 of Fig. 3.1. The induceed emf during off period is obtained using the state space technique and fundamental frequency parameters. The harmonic analysis is carried out on the input voltage waveform. The harmonic currents and torques are obtained using equations (4.1) and (4.2). In this case nontriplen odd harmonics alone are present. The speed torque characteristics with and without frequency dependency are shown in Fig. 4.5.

4.7 Conclusion

An attempt has been made in this chapter to study the effect of frequency dependency of the machine parameters in the case of phase controlled systems. The test machine used for the study is a slipring machine. It is noted that there is not much change in the speed torque characteristic at low values of off period, but the developed torque gets reduced at larger values of off period. The procedure can be conveniently extended to large squirrel cage machines where the rotor bar resistances and inductances may vary considerably with distortions in input voltage and may affect the performance of the machine to a larger extent. For the squirrel cage machine also the induced emf necessary for the harmonic analysis may be obtained using the state space procedure and the fundamental frequency machine parameters.

CHAPTER 5

ITERATIVE METHOD APPLIED TO INVERTER DRIVEN SYSTEMS

5.1 Introduction

As the speed of the induction motors is decided mainly by the frequency of stator excitation, variable frequency ac sources are being used for the wide range speed control of large power ac drive systems. The sources may be voltage or current controllable. Most of the present day drives are voltage fed. Recently, current source inverters has become popular because of its regenerative capability, controllability, simplicity and reliability. Some of the important problems associated with these drive systems are : i) instability due to improper choice of system parameters [13], ii) increase in motor losses [12,14] and iii) steady state torque pulsations [15,16,17]. The problem of torque pulsations and increased losses are due to the presence of harmonics in the output of the inverters. The phenomena of torque fluctuations has been analysed in [15] using d-q model of the machine. The single phase steady state equivalent circuit is used in [16] for the calculation of torque pulsations in voltage driven induction motor drive systems. In this paper an ideal voltage source is assumed. It has been shown in [16,17,18] that the single phase steady state equivalent circuit model is the simple and convenient tool for studying the complete steady state performance of the machine.

The presence of harmonic voltages in the machine phases introduces additional distortions in the output of the inverters. The dc link voltage and current have sixth and multiples of sixth harmonic components. Since the sixth harmonic component is predominant it must be considered in the analysis. In [15], the input filter transients are included in the overall state space equations for the evaluation of steady state characteristics. The d,q,o model is used for the analysis. In this chapter, a simple and fast converging iterative procedure is explained using the steady state equivalent circuit for the calculation of steady state average and pulsating torque for the inverter driven induction motor including the input filter transients.

The method is applied to a voltage fed and a current fed drive systems. The iterative procedure estimates the amount of sixth harmonic ripple present in the dc link and includes its effect in calculating the performance characteristics. The single phase steady state harmonic equivalent circuits are used for this purpose. The following are the assumptions made for the study.

i) The commutation interval of the inverter is negligibly small.

ii) The induction machine is star-connected. If delta-connected, the machine windings can be represented by an equivalent star-connection. The effects of saturation in the machine can be taken into account by using the appropriate saturated magnetising reactance.

iii) The rotor inertia is sufficiently large to minimize the speed fluctuations.

iv) The machine parameters are constant for a given operating point. However, the frequency dependency of the parameters can be considered by substituting the appropriate values in the respective steady state harmonic equivalent circuit of induction machine.

v) The input voltage to the filter is assumed to be pure dc.

5.2 Voltage Source Driven System

5.2.1 System description

The system considered for investigation is represented by the circuit diagram given in Fig. 5.1. The system consists of a three phase controlled rectifier, an LC filter, a three phase inverter, and a three phase induction machine. The commutating components of the inverter are not shown in the circuit diagram. The output of the inverter is assumed as a six-stepped waveform. The r.m.s. value of the output voltage waveform is adjusted by varying the firing angle of the controlled rectifier. The

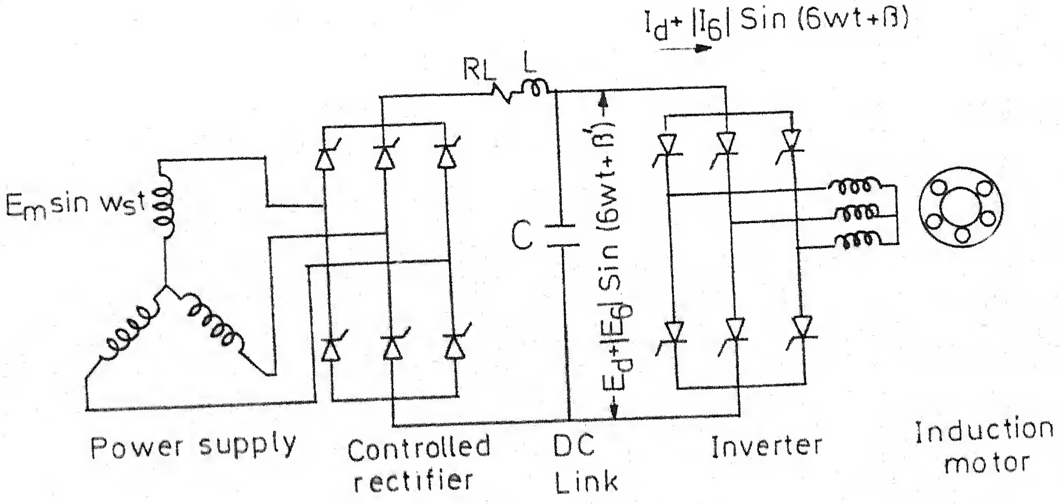
$I_d + |I_6| \sin(6wt+\beta)$
RL
L
$E_m \sin w_s t$
C
$E_d + |E_6| \sin(6wt+\beta')$
Power supply
Controlled rectifier
DC Link
Inverter
Induction motor

FIG.5.1 SYSTEM REPRESENTATION

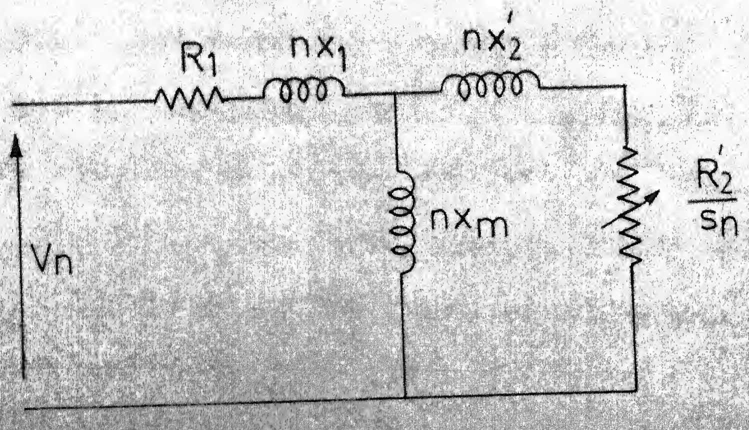
R_1
nx_1
nx_2'
nx_m
$\frac{R_2'}{s_n}$
V_n

FIG.5.2 STEADY STATE EQUIVALENT CIRCUIT

frequency of the stator excitation is varied by changing the frequency of the inverter.

5.2.2 Prediction of dc link current waveform

In an ideal case, the input voltage of the inverter is a smooth dc and the output voltage is a stepped waveform free from fluctuations. However, for the present analysis the inverter input will have super imposed harmonic ripples. The presence of this ripple voltage is due to the flow of harmonic currents generated in the induction machine through the filter. The necessary explanation can be given as follows: The induction machine considered for the analysis is symmetrical and is supplied with the voltage waveform which has 5,7,11, 13th order harmonics. All triplen harmonics are absent because of neutral isolation. For fundamental and every other harmonic, the induction machine can be represented by the respective single phase steady state equivalent circuit shown in Fig. 5.2. The harmonic current flowing into the machine is obtained by the application of corresponding harmonic voltages to the respective equivalent circuit. The condition $i_a + i_b + i_c = 0$ is to be satisfied for all harmonic components. Considering the fundamental components alone and applying the condition given above, the waveform of the current in the dc link is obtained as shown in Fig. 5.3. This current waveform consists of a d.c. sixth harmonic and

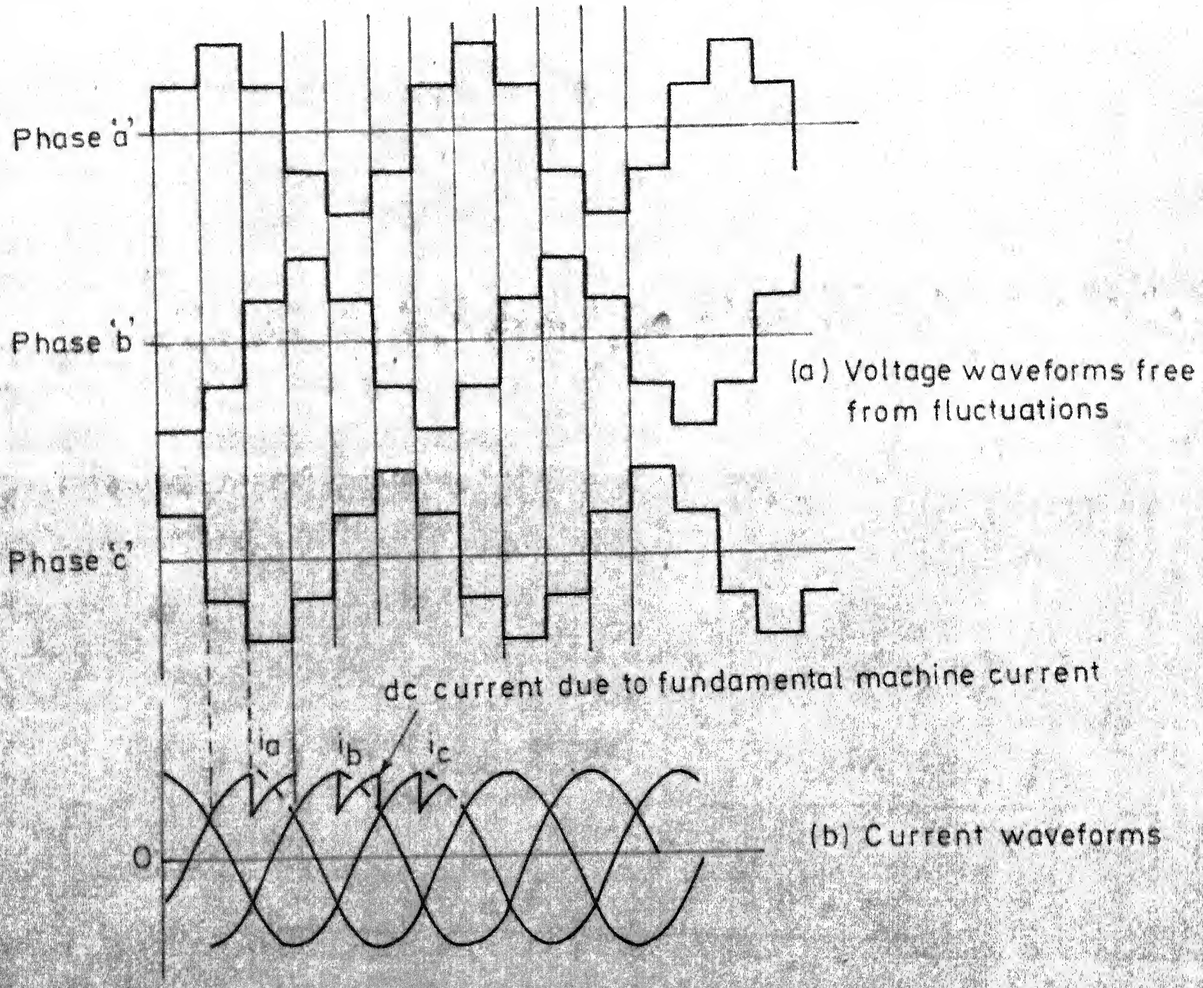
Phase 'a'
Phase 'b'
Phase 'c'
(a) Voltage waveforms free from fluctuations
dc current due to fundamental machine current
i_a
i_b
i_c
0
(b) Current waveforms

FIG.5.3 VOLTAGE AND CURRENT WAVEFORMS

multiples of sixth harmonics components. Similarly, we consider the contribution to the dc and sixth harmonic by each of the harmonic machine current. The dc and the sixth harmonic current can be calculated using the following relations.

Let the current in phase 'a' of the machine be

$$i_a = \sum_{n=1,5,7}^{N} I_n \sin(n\theta + \psi_n)$$

From Fig. 5.3,

$$I_d = \sum_{n=1,5,7}^{N} \frac{1}{\pi/3} \int_{\pi/3}^{2\pi/3} I_n \sin(n\theta + \psi_n)\, d\theta$$

$$= \sum_{n=1,5,7}^{N} \frac{I_n}{(\pi/3)n} \left[-\cos(n.\frac{2\pi}{3} + \psi_n) + \cos(\frac{n\pi}{3} + \psi_n)\right] \qquad (5.1)$$

$$I_{6c} = \sum_{n=1,5,7}^{N} \frac{1}{\pi/6} \int_{\pi/3}^{2\pi/3} I_n.\sin(n\theta + \psi_n) \cdot \cos 6\theta\, d\theta$$

$$= \sum_{n=1,5,7}^{N} \frac{3I_n}{\pi} \left[- \frac{\cos(\overrightarrow{6+n}\frac{2\pi}{3} + \psi_n)}{(6+n)} + \frac{\cos(\overline{6+n}\frac{\pi}{3} + \psi_n)}{(6+n)} + \frac{\cos(\overline{6-n}\frac{2\pi}{3} - \psi_n)}{(6-n)} - \frac{\cos(\overrightarrow{6-n}\frac{\pi}{3} - \psi_n)}{(6-n)}\right] \qquad (5.2)$$

$$I_{6s} = \sum_{n=1,5,7}^{N} \frac{1}{\pi/6} \int_{\pi/3}^{2\pi/3} I_n \sin(n\theta + \psi_n) \cdot \sin 6\theta \cdot d\theta$$

$$= \sum_{n=1,5,7}^{N} \frac{3I_n}{\pi}\left[\frac{\sin(\overline{6-n}\frac{2\pi}{3} - \psi_n)}{(6-n)} - \frac{\sin(\overline{6-n}\frac{\pi}{3} - \psi_n)}{(6-n)} - \frac{\sin(\overrightarrow{6+n}\frac{2\pi}{3} + \psi_n)}{(6+n)} + \frac{\sin(\overrightarrow{6+n}\frac{\pi}{3} - \psi_n)}{(6+n)}\right] \qquad (5.3)$$

The resultant sixth harmonic current is given by

$$I_6 = |I_6| \sin(6\theta + \beta) \qquad (5.4)$$

where

$\beta = \tan^{-1}(I_{6c}/I_{6s})$ and $I_6 = \sqrt{I_{6c}^2 + I_{6s}^2}$. Neglecting all other harmonic currents except the sixth harmonic, we get the resultant dc link current as

$$I_{dc} = I_d + |I_6| \sin(6\theta + \beta) \qquad (5.5)$$

5.2.3 Iterative procedure to solve for the sixth harmonic voltage

In the present analysis, the main aim of the investigation is the estimation of the sixth harmonic voltage component present in the input of the inverter and to consider its effect on the performance characteristic of the motor example sixth harmonic torque pulsation. The iterative procedure explains how the estimation is done. The output voltage of the controlled rectifier when it is supplying a dc current of I_d is given by the expression,

$$E_d = \frac{3\sqrt{3}\,E_m}{\pi} \cos\alpha - \frac{3}{\pi} X_s I_d - I_d R_L \qquad (5.6)$$

As explained in the previous section, the sixth harmonic voltage appears in the input voltage of the inverter due to the flow of sixth harmonic current through the filter. The sixth harmonic voltage $\bar{E}_6$ is given by

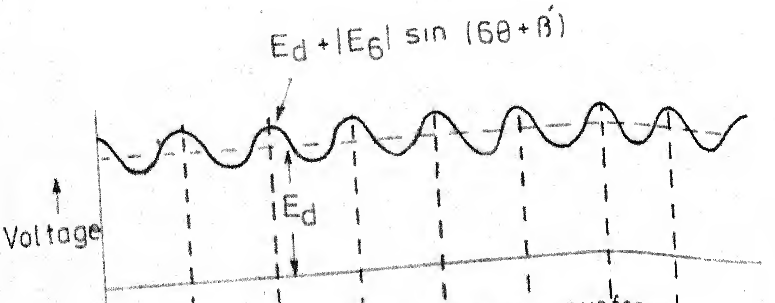
Ed + |E6| sin (6θ + β')
Voltage
Ed

(a) D.C. Link voltage waveform

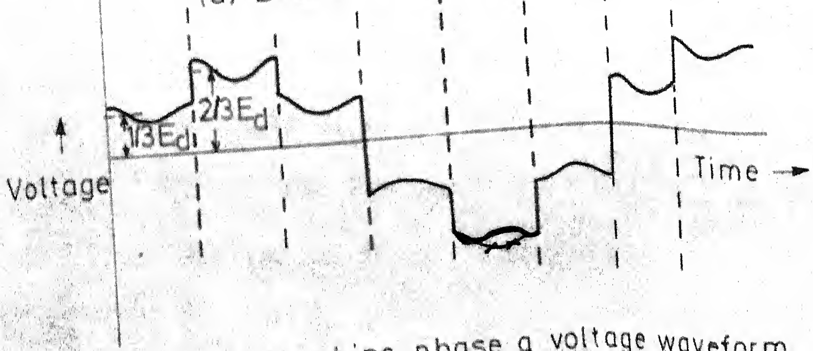
1/3Ed
2/3Ed
Voltage
Time

(b) Machine phase a voltage waveform

FIG. 5·4 VOLTAGE WAVEFORM

$$\bar{E}_6 = \bar{I}_6 \frac{X_1 X_2}{X_1+X_2}$$

$$E_6 = |I_6| \left| \left(\frac{X_1 X_2}{X_1+X_2}\right) \right| \sin (6\theta + \beta') \qquad (5.7)$$

where $X_1 = -j/6\omega C$ and $X_2 = j6\omega L$

The dc link voltage waveform, when the sixth harmonic ripple alone is considered, is shown in Fig. 5.4(a) and Fig. 5.4(b) gives the corresponding phase a machine voltage waveform. The firing angle of the controlled rectifier is chosen so that the amplitude of the machine phase voltage without considering the ripple in the dc link divided by frequency is constant. In otherwords, $2/\pi \left(\frac{3\sqrt{3}\, E_m}{\pi}\right) \cdot \cos \alpha / f$ is kept constant. The following is the iterative procedure.

1. Choose E_d. Assume $E_6 = 0$ $\left(E_d \simeq \frac{3\sqrt{3}}{\pi} E_m \cdot \cos \alpha\right)$
2. Perform the harmonic analysis (Appendix C) on the waveform shown in Fig. 5.4(b).
3. $\overline{E_{61}} = \bar{E}_6$
4. Calculate I_6, E_d and E_6 using equations (5.1), (5.4), (5.6) and (5.7).
5. Check whether $\bar{E}_6 - \bar{E}_{61}$ is less than or equal to a pre-assigned value.
6. If the answer for step 5 is 'YES' go out of the loop.
7. If 'NO' go to 2.

The iterative procedure is simple and it converges very fast. The E_d and $\bar{I}_6$ thus obtained are used to calculate the sixth harmonic torque.

5.2.4 Sixth harmonic torque

The electromagnetic torque is produced because of the interaction between the air gap flux and rotor currents. The sixth harmonic torque is generated when these two quantities differ in their frequency by six times the synchronous speed [16]. The total instantaneous sixth harmonic torque considering upto 13th order harmonic is given by

$$T_6 = T_{61} \sin 6\theta + T_{62} \cos 6\theta \qquad (5.8)$$

where

$T_{61} = -\varphi_1 I_5^r + \varphi_1 I_7^r + \varphi_{11} I_5^r - \varphi_5 I_{11}^r + \varphi_7 I_{13}^r - \varphi_{13} I_7^r$ and

$T_{62} = \varphi_7 I_1^r + \varphi_5 I_1^r$

In the above equations φ_n and $I_n{}^r$ are the amplitude of the nth harmonic air gap flux and rotor current respectively. These are calculated from the steady state equivalent circuit for each harmonic. The amplitude of sixth harmonic torque is given by

$$T_6 = \sqrt{T_{61}^2 + T_{62}{}^2} \qquad (5.9)$$

The method is applied to a system whose parameters are given below [15]

r_s = .025 p.u.
x_s = 2.075 p.u.
x_m = 2.0 p.u.
X_s = .016 p.u.
X_L = .5 p.u.

r_r' = .02 p.u.
x_r' = 2.075 p.u.
R_L = .025 p.u.
X_c = .05 p.u.

The sixth harmonic torque is calculated for various values of frequency and slip. For the different operating conditions the average torque T_d is also calculated using the equivalent circuit. The average torque is given by

$$T_d = \sum \pm \frac{3}{2} (I_n^r)^2 \cdot \frac{R_2'}{S_n} \qquad (5.10)$$

The variation of sixth harmonic torque T_6 with output power for different frequency of operation is plotted in Fig. 5.5. The sixth harmonic torque is significant when the machine is lightly loaded. For the present analysis it is assumed that the machine speed is constant due to large inertia. A few solution points obtained using hybrid computer in [15] are also marked in Fig. 5.5. In [15] both speed and voltage fluctuations are considered. In the method discussed above the commutation reactance drop and the dc voltage drop across the filter inductance are also considered. At every frequency of operation, to keep the air gap flux constant $\frac{2}{\pi} (\frac{3\sqrt{3}E_m}{\pi})$ $\cos \alpha/f$ is kept constant.

5.3 Current Source Driven System

5.3.1 System description

The current source inverter was introduced by ward [19] in 1957. The interest towards current source inverters for drive applications is due to the ease of protection, regenerative capability and reliability. The schematic diagram of a

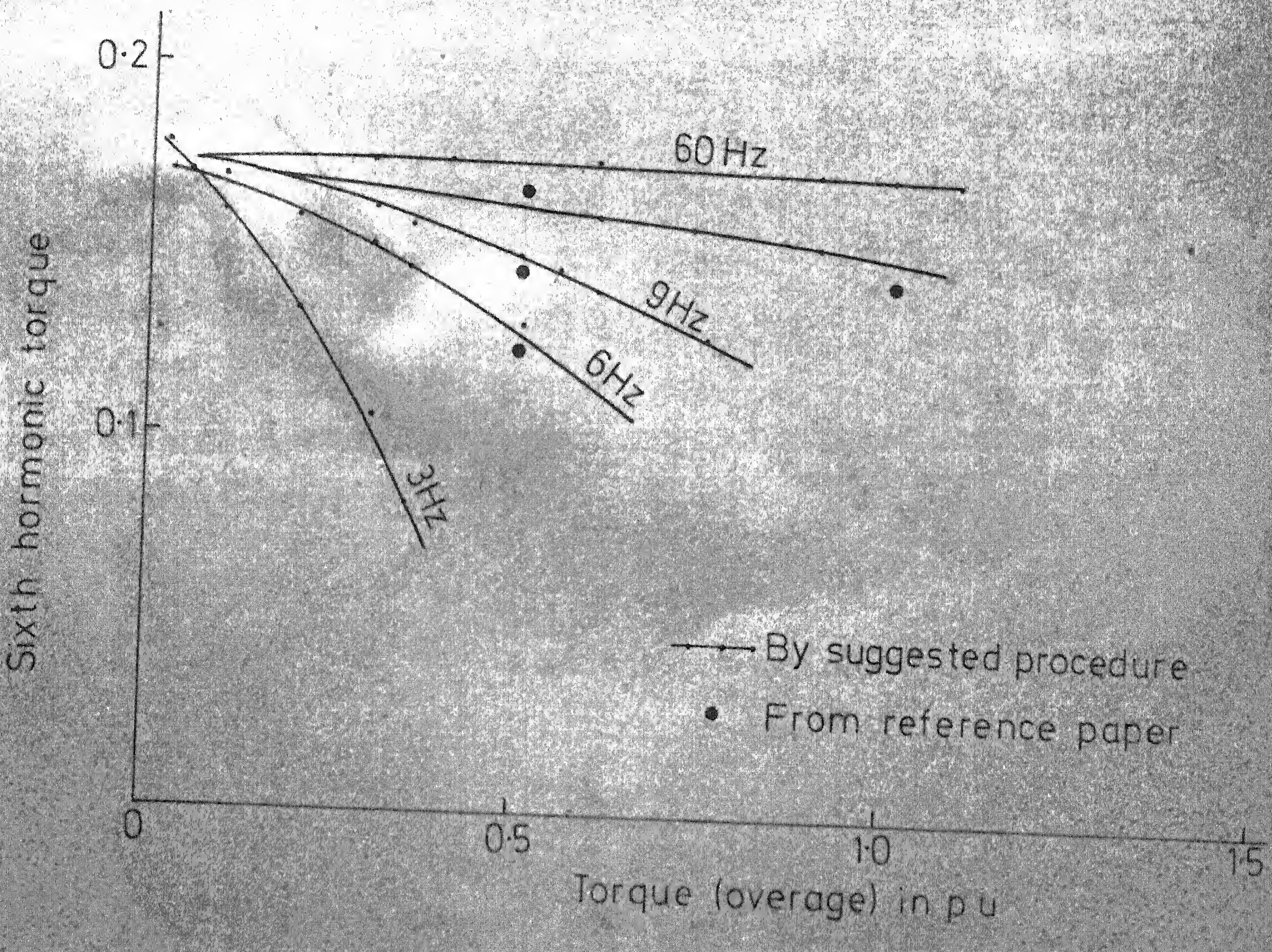

FIG.5·5 VARIATION OF SIXTH HARMONIC TORQUE WITH AVERAGE TORQUE DEVELOPED drive system taken for the present study is given in Fig. 5.6. The system consists of a controlled rectifier, a dc link containing a smoothing reactor, a variable frequency three phase inverter and a three phase induction motor. The controlled rectifier and the large dc link inductance together forms the current source. The magnitude of the dc link current is controlled by adjusting the firing angle of the controlled rectifier. The dc current is converted into three phase ac current and is supplied to the machine. The frequency of the output ac current is controlled by adjusting the frequency of operation of the inverter. The inverter uses autosequential commutation introduced by Ward [19]. The commutating components are shown in Fig. 5.6.

The current fed ac drive systems have been discussed in literature [20 - 24]. The advantages of the current fed induction motor variable speed drive has been explained in [20]. In [21], current source driven synchronous motor drive has been discussed. A state space procedure is discussed in [22] for induction motor drive to obtain the machine voltages and the other performance characteristics. The performance of the current source driven induction motor system has been studied in [23] by simulating the drive system on the analog computer and comparing the results with the actual system performance. A boundary value approach is presented in [24]. In the above papers, for the analysis purpose it has been assumed that the

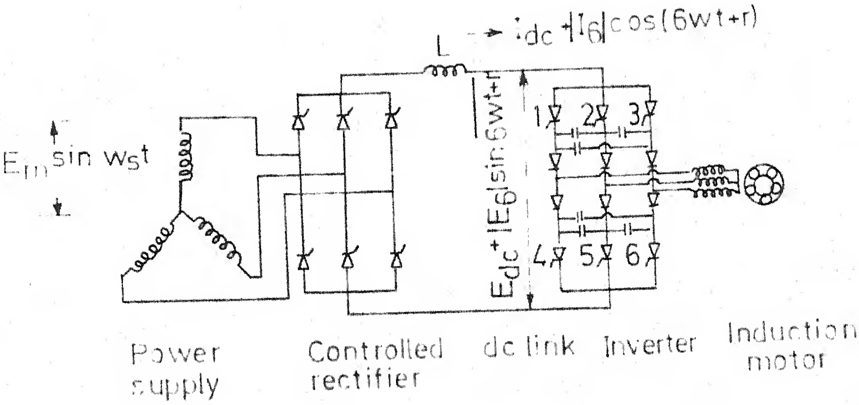
L
Idc + |I6| cos(6wt+r)
Em sin wst
1 2 3
4 5 6
Edc + |E6| sin(6wt+r)
Power supply
Controlled rectifier
dc link
Inverter
Induction motor

Fig. 5·6 System reprentation

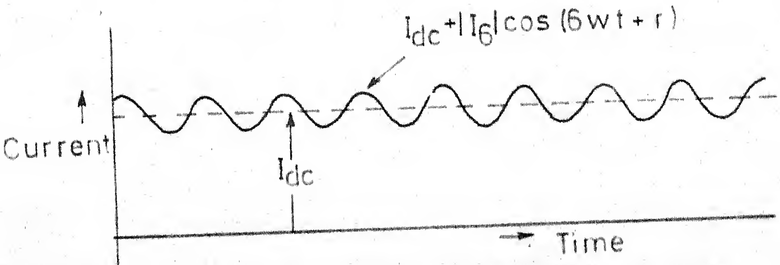

(a) Current waveform at dc link

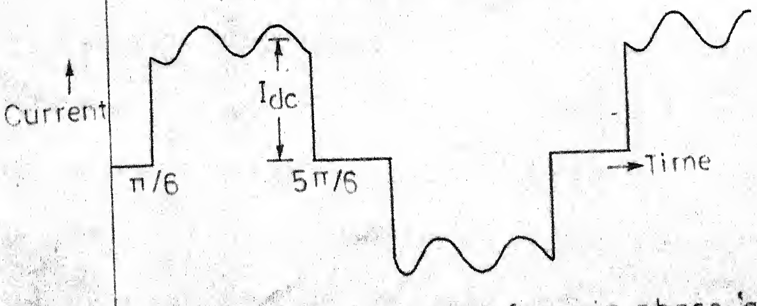

(b) Current waveform in phase 'a'

Fig. 5·7 System current waveforms

dc link current is ripple free. In the actual system sixth and multiples of sixth harmonic currents are present. In this chapter, an iterative procedure is described to estimate the sixth harmonic ripple content using the single phase harmonic equivalent circuits of the induction motor.

5.3.2 Prediction of dc link voltage waveform

The 120° current waveform given in Fig. 5.7 is assumed for the study. Only sixth harmonic ripple is considered. There are six different states in each cycle. The firing sequence of the thyristors is given as 1 and 5, 1 and 6, 2 and 6, 2 and 4, 3 and 4, 3 and 5, 1 and 5, and so on. The machine terminals are brought to the dc side through the conducting thyristors in the following sequence: ab, ac, bc, ba, ca, cb, ab and so on. For the given dc link current waveform, the voltage induced in each phase of the machine for every harmonic current can be calculated using the respective steady state harmonic equivalent circuit. Referring to Fig. 5.7, the terminals a and b of the machine are connected to the dc terminals for a duration of 60 electrical degrees in every cycle. Therefore, the dc voltage waveform during this period can be obtained considering the machine phase voltages. This voltage waveforms repeats six times in every cycle because of the symmetry in the machine voltages. The triplen harmonic currents are absent because of neutral isolation. The expression for average dc link voltage E_d is given below.

$$v_{ab} = \sqrt{3}\, V_1 \sin(\theta + \alpha_1 + \pi/6) + \sqrt{3}\, V_5 \sin(5\theta + \alpha_5 - \pi/6) + \sqrt{3}\, V_7 \sin(7\theta + \alpha_7 + \pi/6) + \sqrt{3}\, V_{11} \sin(11\theta + \alpha_{11} - \pi/6) + \ldots\ldots\ \text{and so} \tag{5.11}$$

$$E_d = \sum_{n=1,5,7}^{N} \left[\frac{1}{\pi/3} \int_{\pi/6}^{\pi/2} v_{ab}\, d\theta\right]$$

$$= \sum_{1,5,7}^{N} \left[\frac{3}{\pi} \int_{\pi/6}^{\pi/2} \sqrt{3}\, V_n \sin(n\theta + \alpha_n \pm \pi/6)\, d\theta\right]$$

$$= \sum_{1,5,7}^{N} \frac{3\sqrt{3}}{\pi}\left[\frac{-\cos(\frac{n\pi}{2} + \alpha_n \pm \pi/6)}{n} + \frac{\cos(\frac{n\pi}{6} + \alpha_n \pm \pi/6)}{n}\right] \tag{5.12}$$

where V_n is the per phase voltage (maximum) obtained from the nth harmonic equivalent circuit and n takes values 1,5,7,11 and 13. α_n is the phase angle of the nth harmonic voltage $+\pi/6$ is used for positive sequence harmonics like 1,7,13 etc $-\pi/6$ is used for negative sequence harmonics like 5,11 etc. The sixth harmonic voltage for the given current waveform is obtained using the following expressions.

$$E_{6s} = \sum_{n=1,5,7}^{N} \frac{6}{\pi} \int_{\pi/6}^{\pi/2} \sqrt{3}\, V_n \sin(n\theta + \alpha_n \pm \pi/6) \sin 6\theta \cdot d\theta$$

$$= \sum_{n=1,5,7}^{N} \frac{3\sqrt{3}\, V_n}{\pi} \int_{\pi/6}^{\pi/2} [\cos(\overline{6-n}\theta - \alpha_n \mp \pi/6) - \cos(\overline{6+n}\,\theta + \alpha_n \pm \pi/6]\, d\theta$$

$$= \sum_{n=1,5,7}^{N} \frac{3\sqrt{3}V_n}{\pi}\left[\frac{\sin(\overline{6-n}\;\theta - \alpha_n \mp \pi/6)}{(6-n)} - \frac{\sin(\overline{6+n}\;\theta + \alpha_n \pm \pi/6)}{(6+n)}\right]_{\pi/6}^{\pi/2}$$

$$= \sum_{n=1,5,7}^{N} \frac{3\sqrt{3}\,V_n}{\pi}\left[\frac{\sin(\overline{6-n}\;\pi/2 - \alpha_n \mp \pi/6)}{(6-n)} - \frac{\sin(\overline{6-n}\;\pi/6 - \alpha_n \mp \pi/6)}{(6-n)} - \frac{\sin(\overline{6+n}\;\pi/2 + \alpha_n \pm \pi/6)}{(6+n)} + \frac{\sin\;(\overline{6+n}\;\pi/6 + \alpha_n \pm \pi/6)}{(6+n)}\right] \tag{5.13}$$

$$E_{6c} = \sum_{n=1,5,7}^{N} \frac{6}{\pi}\int_{\pi/6}^{\pi/2} \sqrt{3}\,V_n \sin(n\theta + \alpha_n \pm \pi/6)\cos 6\theta \cdot d\theta$$

$$= \sum_{n=1,5,7}^{N} \frac{3\sqrt{3}\,V_n}{\pi}\int_{\pi/6}^{\pi/2}\left[\sin(\overline{6+n\theta} + \alpha_n \pm \pi/6) - \sin(\overline{6-n}\;\theta - \alpha_n - \pi/6)\right] d\theta$$

$$= \sum_{n=1,5,7}^{N} \frac{3\sqrt{3}\,V_n}{\pi}\left[-\frac{\cos(\overline{6+n}\;\theta + \alpha_n \pm \pi/6)}{(6+n)} + {} + \frac{\cos(\overline{6-n}\;\theta - \alpha_n \mp \pi/6)}{(6-n)}\right]_{\pi/6}^{\pi/2}$$

$$= \sum_{n=1,5,7}^{N} \frac{3\sqrt{3}\,V_n}{\pi}\left[-\frac{\cos(\overline{6+n}\;\pi/2 + \alpha_n \pm \pi/6)}{(6+n)} + \frac{\cos(\overline{6+n}\;\pi/2 + \alpha_n \pm \pi/6)}{(6+n)} + \frac{\cos(\overline{6-n}\;\pi/2 - \alpha_n \mp \pi/6)}{(6-n)} - \frac{\cos(\overline{6-n}\;\pi/6 - \alpha_n \pm \pi/6)}{(6-n)}\right] \tag{5.14}$$

$$E_6 = \sqrt{E_{6s}^2 + E_{6c}^2}\;\sin(6\theta + \gamma) \tag{5.15}$$

where $\gamma = \tan^{-1}(E_{6c}/E_{6s})$.

Equations (5.12) and (5.15) give E_d and E_6 for a given dc current. The sixth harmonic ripple content of the dc link current waveform of a given dc value is estimated by the following iterative procedure.

5.3.3 Iterative procedure for the estimation of sixth harmonic dc link current

The iterative procedure follows the following steps.

1. Choose I_d
2. Assume $I_6 = 0$
3. Perform the harmonic analysis (Appendix D)
4. Find out E_d and E_6 using equations 5.12 and 5.15
5. $\overline{I_{61}} = \overline{I_6}$
6. Calculate $\overline{I_6}$ ($\overline{I_6} = \frac{\overline{E_6}}{X_6}$), where X_6 is the impedance to the sixth harmonic current by the smoothing reactor.
7. Check whether ($\overline{I_{61}} - \overline{I_6}$) is less than or equal to a pre-assigned value.
8. If step 7 says 'YES' go out of the loop
9. If step 7 says 'NO' go to 3

The procedure is simple and fast converging. The method is applied to an example taken from [23]. The data given in the example are :

$R_1 = .014$ ohm $\quad R_2' = .116$ ohm $\quad L_1 = .32$ mh

$L_2' = .61$ mh $\quad L_m' = 98.0$ mh $\quad$ dc link choke = 4.2 mh

For the purpose of comparis~~ion~~on, the operating point chosen in [23] is considered for the present study also. The steady state operating point is defined as : slip frequency = .85 Hz, machine line frequency = 52.85 Hz and the dc link current = 100 A. The dc link voltage for the above operating point is calculated using the present method. It is approximately equal to 181.6 volts. The value obtained using analog computer in the reference paper is 180.0. There is close agreement. Fig. 5.8 gives the line ab voltage waveforms of the machine at two different frequencies. The dc value of the dc link current and the slip of the machine are kept constant. The voltage spikes which are present in the actual line a-b voltage waveform due to switching are absent in Fig. 5.8. The line a-b voltage is sinusoidal for frequency of operation around 10 Hz. There are more fluctuations in line a-b voltage waveform around 60 Hz operation for the same dc current. Fig. 5.9 gives the voltage waveform at the input side of the inverter. It is for the same operating point given above. The sixth harmonic voltage amplitude in the above waveform is found out as 18.06 volts. It is 9.95 percent of the dc value. The sixth harmonic current is calculated using the relation $I_6 = \frac{E_6}{X_6}$ and it comes to 2.15 . It is 2.15% of the given dc value. With the decrease of frequency, the harmonic content increases and becomes 9.2 percent at 10 Hz operation. So it becomes significant to warrant consideration in obtaining the steady state performance at low frequencies.

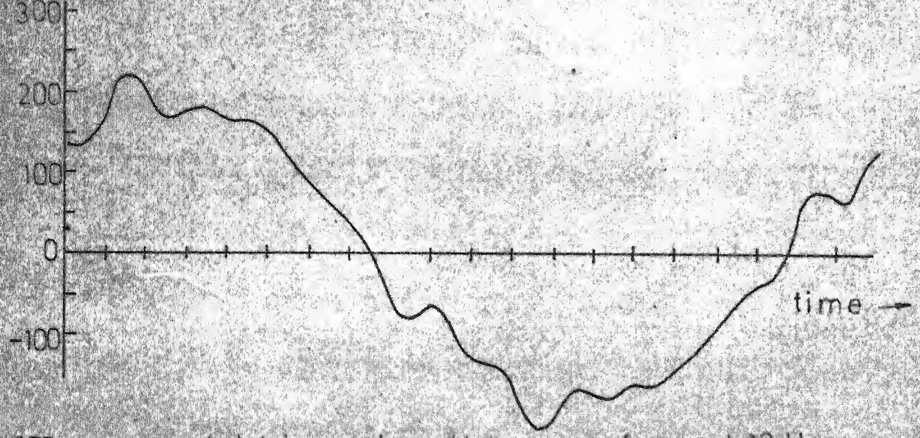

(a) Line a-b voltage waveform at 10 Hz

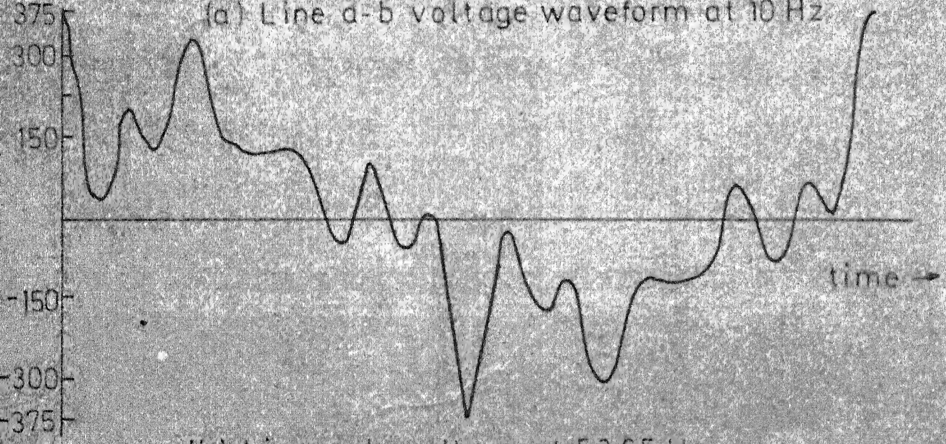

(b) Line a-b voltage at 52·65 Hz

FIG. 5·8 LINE a-b VOLTAGE WAVEFORMS

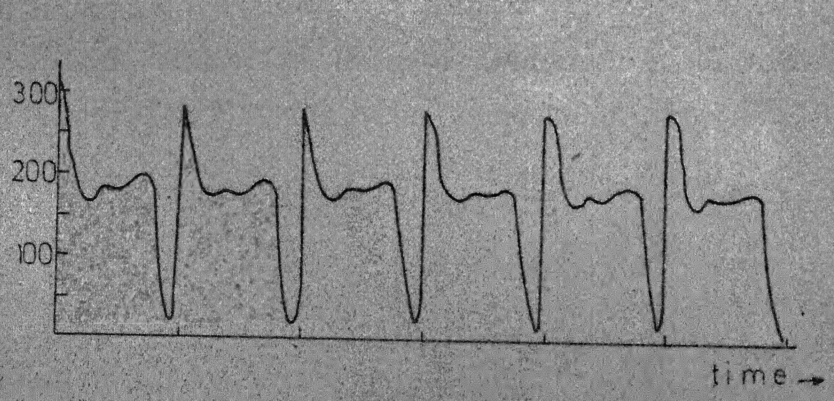

FIG. 5·9 VOLTAGE WAVEFORM AT DC LINK

5.4 Conclusion

In both voltage and current source driven systems, the sixth harmonic ripple contents are present in the dc link A simple and fast converging iterative procedure has been explained in this chapter for the estimation of these quantities. The method is applied to suitable examples and it has been noted that the percentage of sixth harmonic components becomes appreciable at low frequency operations. The various voltage waveforms computed using the suggested procedure are also shown.

CHAPTER 6

SPEED CONTROL USING PHASE CONTROLLED RESISTANCE IN THE ROTOR

6.1 Introduction

The rotor power control and rotor impedance control methods [25,26,27] give wide range speed variation for wound rotor induction motors. The rotor power control method is quite efficient and gives satisfactory variable speed-torque characteristic, but the speed control system is expensive because it involves a considerable amount of auxiliary equipments. Comparatively simpler and economical speed control schemes can be realized by employing rotor impedance control technique. The speed-torque characteristic of the wound rotor machine can be varied by controlling the effective resistance included in the rotor circuit. In the conventional scheme, the rotor impedance is varied by adjusting the external resistance included in the rotor circuit. This scheme provides high starting torque, low starting current and wide speed variation, but the drawback of the conventional scheme is that the speed variation is not continuous and it is not suitable for closed loop operations.

With the development of power semiconductor technology, it has become possible to have continuous and contactless control over the effective impedance included in the rotor circuit of the wound rotor induction motors. A few attempts have been made recently to use SCR circuits in various configurations in the rotor of the machine for wide range speed control [28,29,30,31,32]. In [28], a pair of SCRs connected in antiparallel is placed in series with each phase of the rotor circuit to control the effective impedance. The speed variation is achieved by adjusting the firing angle of the phase controlled SCRs. The chopper controlled resistance method of speed control has been discussed in [29,30]. In the chopper controlled schemes the rotor power is rectified using a diode bridge and fed to the chopper controlled external resistance. The chopper is connected across the external resistance. When the chopper is ON the effective resistance included in the circuit is zero and when it is OFF the entire external resistance comes into the rotor circuit. The chopper is periodically regulated by a control module which in every chopper period keeps the chopper ON for a definite duration and OFF for the rest of the period. The effective rotor impedance is varied by adjusting the duty cycle of the chopper. Thus a continuous and contactless control over the effective rotor impedance is achieved. In [29] a thorough analysis on a chopper controlled scheme in open loop mode has been done using dc and ac equivalent circuits. The closed loop performance of the chopper controlled scheme has been investigated in [30].

In the present chapter a phase controlled resistance method of speed control is discussed. In this scheme, the rotor power is fed to the external resistance through a controlled bridge. A smoothing choke is used in the dc side to keep the dc current continuous. The effective rotor impedance is controlled by adjusting the firing angle of the controlled rectifier. The scheme is simple and economical for low and medium power applications. However, the analysis of this scheme is not simple because the instant at which the conducting SCR goes off is not known apriori. In this chapter a closed form solution for the present problem is obtained using state space techniques [31]. The state variables used in the mathematical model are the actual rotor variables and the suggested procedure completely avoids iterations. The procedure solves for the current zero instants and then obtains the initial state vector. Once the initial state vector is known, the per phase rotor current waveform and the developed torque can be calculated easily. A simplified ac equivalent circuit suitable for the present scheme is also developed in this chapter. The analytical results obtained by the above procedures are compared with the experimental values given in [32].

A half controlled bridge can also be used for this control as there is no power reversal through the bridge. Since the experimental results were available for the machine with a fully controlled bridge circuit in the rotor, the present analysis is done for a fully controlled bridge circuit. However, the same method of analysis can be extended to motor speed control with half controlled bridge.

The following are the assumptions made for the study.

1. The machine parameters are assumed constant
2. The voltage drop across the stator winding due to stator harmonics is negligible
3. The distortion in the air gap flux wave is negligible
4. The forward drop across the SCRs is negligibly small
5. The rotor induced emfs are balanced
6. The rotor inertia is sufficiently large to smoothen the speed fluctuations.

6.2 System Representation

The schematic diagram of the present system is shown in Fig. 6.1. It concists of a three phase fully controlled bridge, a smoothing choke L and an external resistance R. The rotor phases of the three phase induction motor is connected to the input terminals of the controlled rectifier. The smoothing choke is sufficiently large to keep the dc current continuous.

The equivalent circuit used for the analysis is the per phase equivalent circuit with parameters referred to secondary. The same equivalent circuit is used in [29,30] for the study of chopper controlled systems. The equivalent circuit is shown in Fig. 6.2. The parameters of the equivalent circuit can be

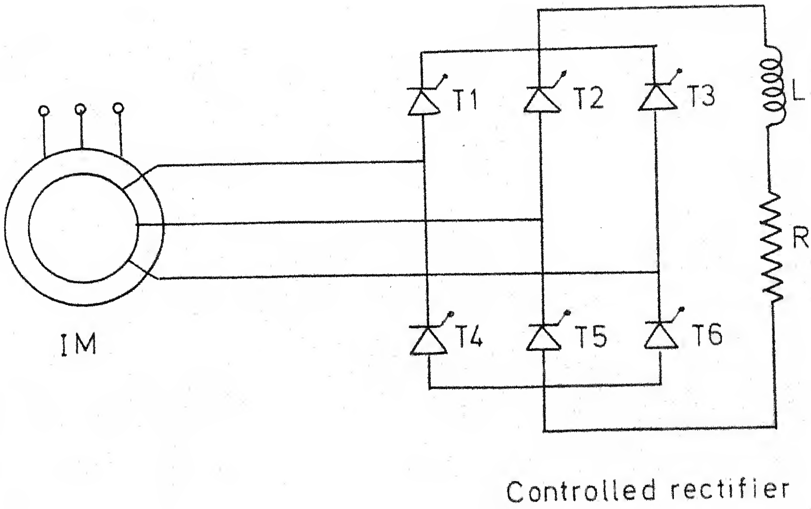
T1
T2
T3
L
R
T4
T5
T6
IM
Controlled rectifier

FIG.6.1 SCHEMATIC DIAGRAM

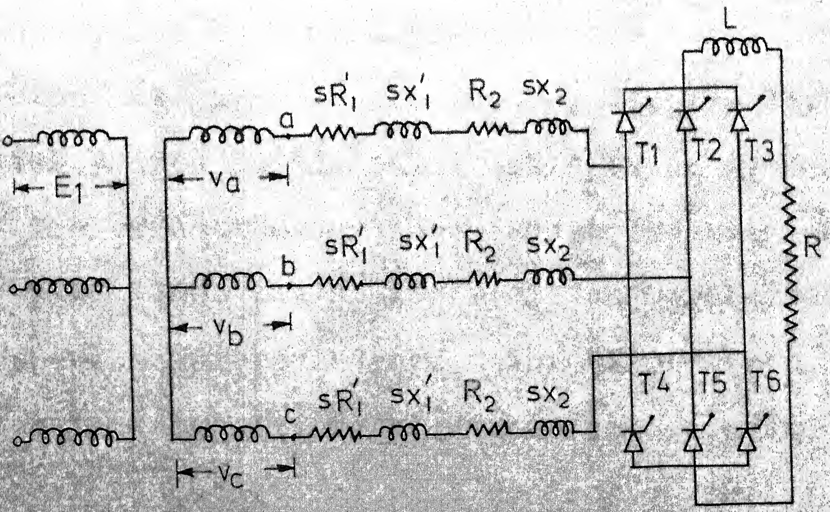
L
E1
sR'1
sx'1
R2
sx2
a
va
T1
T2
T3
R
sR'1
sx'1
R2
sx2
b
vb
T4
T5
T6
sR'1
sx'1
R2
sx2
c
vc

FIG.6.2 EQUIVALENT CIRCUIT WITH PARAMETERS REFERRED TO SECONDARY

obtained by conducting the short circuit and open circuit tests on the machine. The induced rotor voltages v_a,v_b and v_c are sinusoidal and are displaced from each other by 120 electrical degrees. The system now reduces essentially to a three phase thyristor converter system with large source impedance. The operation of the thyristor converter system is reviewed in the following section.

6.3 Operation of the Converter System-Review

The operation of the converter system shown in Fig. 6.2 is similar to that of conventional bridge. The induced rotor voltages v_a,v_b and v_c are shown in Fig. 6.3. The firing angle α of the controlled bridge is measured from the 30° point of the voltage waveform. The firing angle is controlled using suitable control circuits. Referring to Fig. 6.2, phase a of the rotor is connected to thyristors 1 and 4 of the bridge. Thyristor 1 is fired when the phase a voltage is positive and thyristor 4 is fired when phase a is becoming negative. The firing sequence of the thyristors is given as T1, T6, T2, T4, T3, T5, T1 and so on. The actual source impedance of the present system varies with speed. The effective per phase source resistance is the summation of slip times the stator resistance referred to rotor and the per phase rotor resistance. The effective source reactance is slip times the total standstill reactance of the machine referred to secondary. The conduction period of each SCR varies from zero to the maximum of 180 electrical degrees

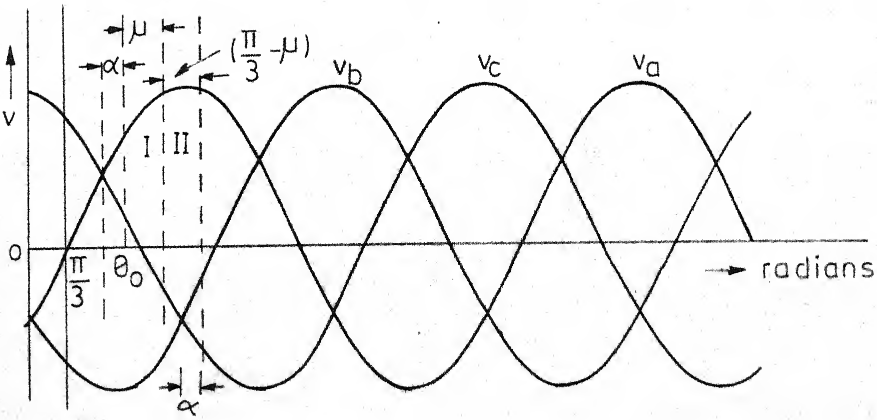

FIG.6·3 ROTOR INDUCED VOLTAGE WAVEFORMS

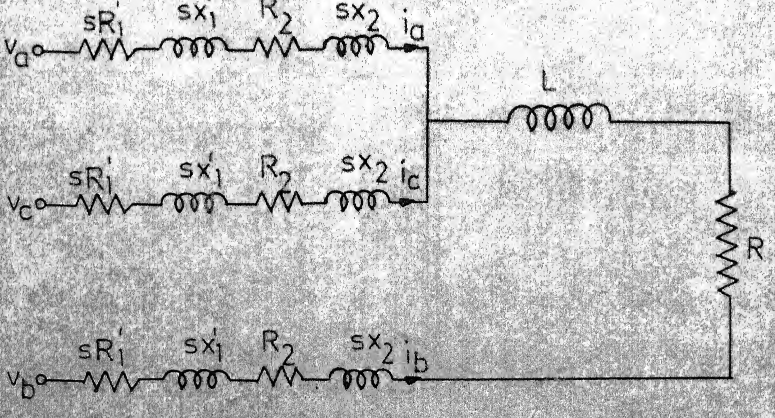

v_a
sR_1'
sx_1'
R_2
sx_2
i_a
v_c
i_c
v_b
i_b
L
R

FIG.6·4 THE EQUIVALENT CIRCUIT WHEN T1, T3 AND T5 CONDUCT depending upon speed and firing angle. When the dc current is continuous a minimum of 2 SCRs conduct at any time. The transfer of load current from outgoing SCR to incoming SCR can take place instantaneously only if the source reactance is negligibly small. With the presence of source reactance, the current transfer does not take place instantaneously, but it takes definite time decided by speed and firing angle. This interval of current transfer is known as commutation interval or overlap period μ. In the normal operation of the bridge, in between successive triggerings, three SCRs conduct during the commutation interval and two SCRs conduct during the rest of the period. The commutation interval varies from zero to a maximum of 60 electrical degrees in the normal operation of the bridge. If the commutation interval exceeds beyond 60°, four SCRs conduction will occur and this results in periodic short circuits across the ac terminals. This mode of operation is normally avoided. In the present analysis only 3 SCR and 2 SCR conductions are considered.

6.4 State Space Analysis

6.4.1 Modes of operation

The system may be subject to three different states depending upon the operating conditions. They are (i) three phase state, (ii) single phase state, and (iii) off state. The three phase state occurs when all the three rotor phases carry current and the system is said to be single phasing when one of the rotor phases gets open circuited. The system is subject to off state when the three rotor phase currents are zero. If the smoothing choke is sufficiently large, the system will never be put into off state. When the dc current is continuous and the commutation interval is less than 60°, the system will alternate between three phase state and single phase state. During the commutation period three SCRs conduct and all the three rotor phases carry current. Immediately after the commutation interval the system is single phasing until the next SCR is turned ON. Since three SCR conduction and two SCR conduction occur alternatively, this mode of operation is known as 3/2 mode of operation. The SCR conduction occurs in the following sequence: T3T5, T1T3T5, T1T5, T1T5T6, T1T6, T1T2T6, T2T6, T2T4T6, T2T4, T2T3T4, T3T4, T3T4T5, T3T5 and so on. Therefore there are totally six three phase states and six single phase states occur in every cycle of operation. The complete performance characteristic of the system can be obtained if the rotor current is known for one complete cycle. It is assumed that the rotor induced emfs are having three phase symmetry. Because of the symmetry in firing sequence, the rotor phase currents are also similar with equal phase displacement and halfwave symmetry. When the system variables are having three phase symmetry and halfwave symmetry, it is sufficient if the rotor currents are solved for only 60 electrical degrees, that is, one sixth of a cycle. The mathematical model used for the present analysis is derived in the following sections.

6.4.2 Three thyristor conduction

Referring to Fig. 6.3, T1, T3 and T5 conduct for the duration μ, the commutation interval when the system is in three phase operation. This is the interval I in Fig. 6.3. During this interval all the three rotor phases carry current. The rotor phases a and c are shorted and brought to phase b through the dc side choke and external resistance. The equivalent circuit of the system reduces to the form shown in Fig. 6.4. The differential equation of the system can be written as follows :

$$v_{ab} = (sR_1' + R_2)\, i_a + (sX_1' + sX_2)\frac{di_a}{d\theta} - (sR_1' + R_2 + R)\, i_b - (sX' + sX_2 + X)\frac{di_b}{d\theta} \qquad (6.1)$$

$$v_{bc} = (sR_1' + R_2 + R)i_b + (sX_1' + sX_2 + X)\frac{di_b}{d\theta} - (sR_1' + R_2)i_c - (sX_1' + sX_2)\frac{di_c}{d\theta} \qquad (6.2)$$

$$v_{ca} = (sR_1' + R_2)i_c + (sX_1' + sX_2)\frac{di_c}{d\theta} - (sR_1' + R_2)i_a - (sX_1' + sX_2)\frac{di_a}{d\theta} \qquad (6.3)$$

Subtracting equation (6.2) from equation (6.3),

$$v_{ca} - v_{bc} = -(sR_1' + R_2)i_a - (sX_1' + sX_2)\frac{di_a}{d\theta} - (sR_1' + R_2 + R)i_b - (sX_1' + sX_2 + X)\frac{di_b}{d\theta} + (2sR_1' + 2R_2)i_c + (2sX_1' + 2sX_2)\frac{di_c}{d\theta} \qquad (6.4)$$

As the summation of rotor currents is zero at any instant of time,

$$i_c = -(i_a + i_b) \text{ and } \frac{di_c}{d\theta} = -(\frac{di_a}{d\theta} + \frac{di_b}{d\theta})$$

Substituting the above conditions in equation (6.4),

$$v_{ca} - v_{bc} = -(sR_1' + R_2)i_a - (sX_1' + sX_2)\frac{di_a}{d\theta} - (sR_1' + R_2 + R)i_b -$$
$$(sX_1' + sX_2 + X)\frac{di_b}{d\theta} - (2sR_1' + 2R_2)i_a - (2sR_1' + 2R_2)i_b -$$
$$(2sX_1' + 2sX_2)\frac{di_a}{d\theta} - (2sX_1' + 2sX_2)\frac{di_b}{d\theta} \qquad (6.5)$$

$$= -3(sR_1' + R_2)i_a - 3s(X_1' + X_2)\frac{di_a}{d\theta} - (3sR_1' + 3R_2 + R)i_b -$$
$$(3sX_1' + 3sX_2 + X)\frac{di_b}{d\theta} \qquad (6.6)$$

where $X = s2\pi fL$

Substituting $V_1 = v_{ab}$ and $V_2 = v_{ca} - v_{bc}$ in equations (6.1) and (6.6)

$$V_1 = (sR_1' + R_2)i_a + s(X_1' + X_2)\frac{di_a}{d\theta} - (sR_1' + R_2 + R)i_b -$$
$$(sX_1' + sX_2 + X)\frac{di_b}{d\theta} \qquad (6.7)$$

$$V_2 = -3(sR_1' + R_2)i_a - 3s(X_1' + X_2)\frac{di_a}{d\theta} - (3sR_1' + 3R_2)i_b -$$
$$(3sX_1' + 3sX_2 + X)\frac{di_b}{d\theta} \qquad (6.8)$$

As the rotor induced emfs are having three phase symmetry, the line-to-line rotor induced emfs can be written as,

$$v_{ab} = V_m \sin \theta$$

$$v_{bc} = V_m \sin (\theta - 120)$$

$$v_{ca} = V_m V_m \sin(\theta + 120)$$

Therefore $V_1(\theta) = v_{ab} = V_m \sin\theta$ (6.9)

and $V_2(\theta) = v_{ca} - v_{bc} = \sqrt{3}\, V_m \cos\theta$ (6.10)

where $\theta = s2\pi f$

Differentiating equations (6.9) and (6.10) with respect to θ,

$$\frac{dV_1(\theta)}{d\theta} = V_m \cos\theta$$

$$= 1/\sqrt{3}\, V_2(\theta)$$

$$\frac{dV_2(\theta)}{d\theta} = -\sqrt{3}\, V_m \sin\theta$$

$$= -\sqrt{3}\, V_1(\theta)$$

that is, $V_1(\theta)$ and $V_2(\theta)$ can be written in differential form as follows ,

$$V_1(\theta) = -1/\sqrt{3}\, \frac{dV_2(\theta)}{d\theta} \qquad (6.11)$$

$$V_2(\theta) = \sqrt{3}\, \frac{dV_1(\theta)}{d\theta} \qquad (6.12)$$

Equations (6.7), (6.8), (6.11) and (6.12) can be arranged in matrix forms as follows :

$$\begin{bmatrix} (sX_1 + sX_2) & -(sX_1' + sX_2 + X) & 0 & 0 \\ -(3sX_1' + 3sX_2) & -(3sX_1'+3sX_2 + X) & 0 & 0 \\ 0 & 0 & 1 & 0 \\ 0 & 0 & 0 & 1 \end{bmatrix} \begin{bmatrix} \frac{di_a}{d\theta} \\ \frac{di_b}{d\theta} \\ \frac{dV_1}{d\theta} \\ \frac{dV_2}{d\theta} \end{bmatrix} =$$

contd...

$$\begin{bmatrix} -(sR_1' + R_2) & (sR_1' + R_2 + R) & 1 & 0 \\ 3(sR_1' + R_2) & (3sR_1' + 3R_2 + R) & 0 & 1 \\ 0 & 0 & 0 & \frac{1}{\sqrt{3}} \\ 0 & 0 & -\sqrt{3} & 0 \end{bmatrix} \begin{bmatrix} i_a \\ i_b \\ V_1 \\ V_2 \end{bmatrix} \qquad (6.13)$$

Symbolically,

$$\begin{aligned} \underline{A}\,\underline{\dot{x}} &= \underline{B}\,\underline{x} \\ \underline{\dot{x}} &= \underline{A}^{-1}\,\underline{B}\,\underline{x} \\ \dot{x} &= C\,\underline{x} \end{aligned} \qquad (6.14)$$

Equation (6.14) represents the system when it is in three phase operation during interval I in Fig. 6.3. The mathematical model for two thyristor conduction is derived in the next section.

6.4.3 Two thyristor conduction

During inyerval II in Fig. 6.3 thyristors T_1 and T_5 conduct. The duration of this interval is $(\pi/3 - \mu)$ radians. Phase c of the rotor gets open circuited during this interval. Phases a and b are connected through the smoothing choke L and external resistance R. The equivalent circuit of the system can now be redrawn as shown in Fig. 6.5. The differential equation of the system is written down as

$$V_1 = v_{ab} = (sR_1' + R_2)\, i_a + (sX_1' + sX_2)\,\frac{di_a}{d\theta} - (sR_1' + R_2 + R)\, i_b - (sX_1' + sX_2 + X)\,\frac{di_b}{d\theta} \qquad (6.15)$$

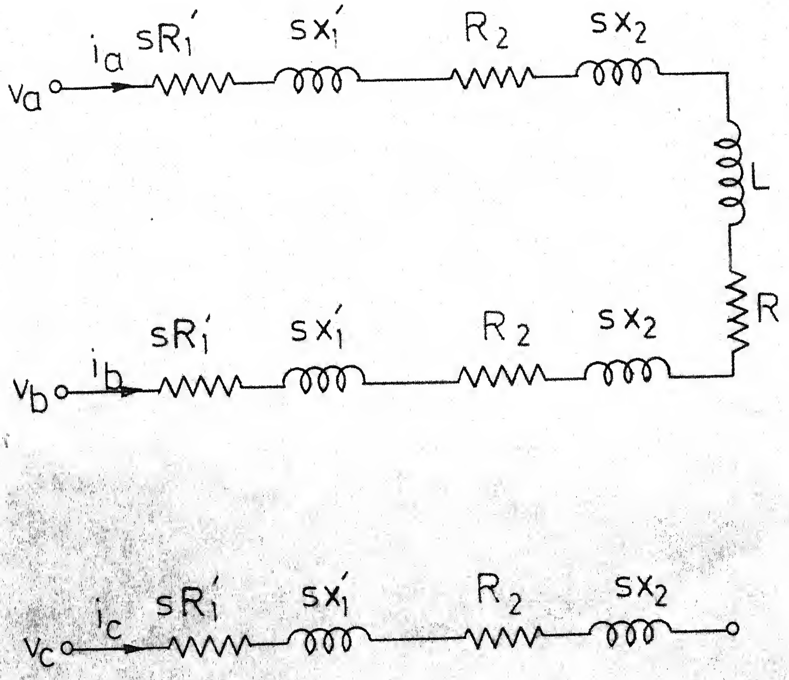
v_a
i_a
sR_1'
sx_1'
R_2
sx_2
L
R
v_b
i_b
sR_1'
sx_1'
R_2
sx_2
v_c
i_c
sR_1'
sx_1'
R_2
sx_2

FIG.6·5 THE EQUIVALENT CIRCUIT WHEN T1 AND T5 CONDUCT

Since phase c is disconnected from the bridge, the phase c current is zero during this interval. Now the problem is to impose this current zero condition in the mathematical model. In [3], this is imposed by applying a voltage equal to the induced emf across the open circuited phase. In the present study an alternative procedure is followed. When phase c is open, the other two phase currents and their derivatives are equal and opposite to each other. Therefore one more differential equation is available and is made use of in the model.

That is, $\frac{di_a}{d\theta} = -\frac{di_b}{d\theta}$ (6.16)

Equations (6.11), (6.12), (6.15) and (6.16) can be arranged in matrix form as follows

$$\begin{bmatrix} (sX_1' + sX_2) & -(sX_1' + sX_2 + X) & 0 & 0 \\ 1 & 1 & 0 & 0 \\ 0 & 0 & 1 & 0 \\ 0 & 0 & 0 & 1 \end{bmatrix} \begin{bmatrix} \frac{di_a}{d\theta} \\ \frac{di_b}{d\theta} \\ \frac{dV_1}{d\theta} \\ \frac{dV_2}{d\theta} \end{bmatrix} =$$

$$\begin{bmatrix} -(sR_1' + R_2) & +(sR_1' + R_2 + R) & 1 & 0 \\ 0 & 0 & 0 & 0 \\ 0 & 0 & 0 & \frac{1}{\sqrt{3}} \\ 0 & 0 & -\sqrt{3} & 0 \end{bmatrix} \begin{bmatrix} i_a \\ i_b \\ V_1 \\ V_2 \end{bmatrix} \quad (6.17)$$

Symbolically,

$$\underline{D}\,\dot{\underline{x}} = \underline{E}\,\underline{x}$$

$$\dot{\underline{x}} = \underline{D}^{-1}\,\underline{E}\,\underline{x}$$

$$\dot{\underline{x}} = \underline{F}\,\underline{x} \tag{6.18}$$

Equations (6.18) represents the system when it is single phasing during interval II in Fig. 6.3.

6.4.4 State space solution

The present problem can be defined as follows : Given the commutation interval μ and speed of the machine, the firing angle of the thyristors and the rotor per phase current waveform are to be obtained. The performance characteristic of the system can be easily obtained once the rotor current waveform is known. The first step in the state space analysis is to solve for the initial state vector using the system symmetry. The system symmetry also simplifies the computational effort required to obtain the complete rotor current waveform The positive lobe of the rotor current is similar to the negative lobe. This property can be represented mathematically as follows.

$$i_a(\theta) = -i_a(\theta + \pi) \tag{6.19}$$

$$i_b(\theta) = -i_b(\theta + \pi) \tag{6.20}$$

$$i_c(\theta) = -i_c(\theta + \pi) \tag{6.21}$$

The three phase symmetry of the rotor current waveform can be written down mathematically as follows,

$$i_a(\theta + \pi/3) = i_b(\theta + \pi) \qquad (6.22)$$

$$i_b(\theta + \pi/3) = i_c(\theta + \pi) \qquad (6.23)$$

$$i_c(\theta + \pi/3) = i_a(\theta + \pi) \qquad (6.24)$$

Substituting equations (6.22) to (6.24) in equations (6.19) to (6.21),

$$i_a(\theta + \pi/3) = -i_b(\theta) \qquad (6.25)$$

$$i_b(\theta + \pi/3) = -i_c(\theta) \qquad (6.26)$$

$$i_c(\theta + \pi/3) = -i_a(\theta) \qquad (6.27)$$

Since i_c is not taken as a state variable, equations (6.26) is rewritten in terms of i_a and i_b.

$$\begin{aligned} i_b(\theta + \pi/3) &= -i_c(\theta) \\ &= i_a(\theta) + i_b(\theta) \qquad (6.28) \end{aligned}$$

The state variables chosen for the analysis are i_a, i_b, V_1 and V_2. V_1 and V_2 have been already defined. The relations similar to (6.25) to (6.27) can now be obtained for the variables V_1 and V_2 as follows

$$\begin{aligned} V_1(\theta + \pi/3) &= v_{ab}(\theta + \pi/3) \\ &= -v_{bc}(\theta), \text{ following the notations} \end{aligned}$$

in equations (6.25) - (6.27)

$$V_1(\theta + \pi/3) = -v_{bc}(\theta) \qquad (6.29)$$

Adding equations (6.9) and (6.10),

$$v_{ab}(\theta) + v_{ca}(\theta) - v_{bc}(\theta) = V_1(\theta) + V_2(\theta)$$

That is $-2\, v_{bc}(\theta) = V_1(\theta) + V_2(\theta)$

$$v_{bc}(\theta) = -\tfrac{1}{2}\, V_1(\theta) - \tfrac{1}{2}\, V_2(\theta)$$

That is, $V_1(\theta + \pi/3) = \tfrac{1}{2}\, V_1(\theta) + \tfrac{1}{2}\, V_2(\theta)$ (6.30)

$$V_2(\theta + \pi/3) = v_{ca}(\theta + \pi/3) - v_{bc}(\theta + \pi/3)$$

$$V_2\ (\theta + \pi/3) = -v_{ab}(\theta) + v_{ca}(\theta) \qquad (6.31)$$

Substituting equation (6.9) from equation (6.10),

$$v_{ca}(\theta) - v_{bc}(\theta) - v_{ab}(\theta) = V_2(\theta) - V_1(\theta)$$

$$2v_{ca}(\theta) = V_2(\theta) - V_1(\theta)$$

$$v_{ca}(\theta) = \tfrac{1}{2}[V_2(\theta) - V_1(\theta)] \qquad (6.32)$$

Substituting equation (6.32) in equation (6.31),

$$V_2(\theta + \pi/3) = -V_1(\theta) + \tfrac{1}{2}\, V_2(\theta) - \tfrac{1}{2}\, V_1(\theta)$$

$$V_2(\theta + \pi/3) = -\tfrac{3}{2}\, V_1(\theta) - \tfrac{1}{2}\, V_2(\theta) \qquad (6.33)$$

Equations (6.25), (6.28), (6.30) and (6.33) can be arranged in matrix form as given below

$$\underset{\theta = \theta_1 + \pi/3}{\begin{bmatrix} i_a \\ i_b \\ V_1 \\ V_2 \end{bmatrix}} = \begin{bmatrix} 0 & -1 & 0 & 0 \\ 1 & 1 & 0 & 0 \\ 0 & 0 & \tfrac{1}{2} & \tfrac{1}{2} \\ 0 & 0 & -3/2 & \tfrac{1}{2} \end{bmatrix} \underset{\theta = \theta_1}{\begin{bmatrix} i_a \\ i_b \\ V_1 \\ V_2 \end{bmatrix}} \qquad (6.34)$$

Symbolically

$$\underline{x}(\theta + \pi/3) = \underline{T}\ \underline{x}(\theta) \tag{6.35}$$

The matrix $\underline{T}$ is called as connection matrix. Equation (6.34) shows that any two state vectors separated by 60 electrical degrees is related by the connection matrix $\underline{T}$. Therefore if the solution is known for any 60° interval, then the solution for the entire cycle can be obtained by using equation (6.35) repetitively. Therefore, it is sufficient if we solve for the rotor currents for any 60 electrical intervals. To start with, we should know the initial state vector. This is obtained as explained below.

Referring to Fig. 6.3, if $\underline{x}\ (\theta_o)$ is the state of the system at θ_o, when T_1 is turned on, then the state of the system at $(\theta_o + \mu)$ is given by,

$$\underline{x}(\theta_o + \mu) = e^{\underline{C}\mu}\ \underline{x}(\theta_o) \tag{6.36}$$

The state of the system at the end of interval II is

$$\begin{aligned} \underline{x}(\theta_o+\pi/3) &= e^{\underline{F}(\pi/3 + \theta_o - \theta_o - \mu)}\ \underline{x}(\theta_o + \mu) \\ &= e^{\underline{F}(\pi/3 - \mu)}\ \underline{x}(\theta_o + \mu) \end{aligned} \tag{6.37}$$

Substituting equation (6.36) in equation (6.37),

$$\underline{x}(\theta_o + \pi/3) = e^{\underline{F}(\pi/3 - \mu)}\ e^{\underline{C}\mu}\ \underline{x}(\theta_o)$$

$$\underline{x}(\theta_o + \pi/3) = \underline{G}\ \underline{x}(\theta_o) \tag{6.38}$$

From equations (6.35) and (6.38),

$$\underline{G}\ \underline{x}(\theta_o) = \underline{T}\ \underline{x}(\theta_o)$$

$$(\underline{G} - \underline{T})\ \underline{x}(\theta_o) = \underline{0} \qquad (6.39)$$

Now the initial state vector $\underline{x}(\theta_o)$ is obtained for the given slip and commutation angle. Equation (6.39) is rearranged as follows

$$\begin{bmatrix} \underline{H1} & \underline{H2} \\ \underline{H3} & \underline{H4} \end{bmatrix} \begin{bmatrix} i(\theta_o) \\ V(\theta_o) \end{bmatrix} = \underline{0} \qquad (6.40)$$

$$\underline{H1}\ \underline{i}(\theta_o) + \underline{H2}\ \underline{V}(\theta_o) = \underline{0} \qquad (6.41)$$

$$\underline{i}(\theta_o) = -\underline{H1}^{-1}\ \underline{H2}\ \underline{V}(\theta_o)$$

$$\underline{i}(\theta_o) = \underline{U}\ \underline{V}(\theta_o) \qquad (6.42)$$

At θ_o, the phase current i_a is zero.

Therefore, $i_a(\theta_o) = 0 = U_{11}\ V_1(\theta_o) + U_{12}\ V_2(\theta)$ (6.43)

$$\frac{V_1(\theta)}{V_2(\theta)} = -\ \frac{U_{12}}{U_{11}} \qquad (6.44)$$

From Fig. 6.3, $V_1(\theta_o) = V_m \sin(\alpha + \pi/3)$ (6.45)

$$V_2(\theta_o) = \sqrt{3}\ V_m \cos(\alpha + \pi/3) \qquad (6.46)$$

Substituting (6.45) and (6.46) in (6.44),

$$\tan(\alpha + \pi/3) = -\sqrt{3}\ \frac{U_{12}}{U_{11}} \qquad (6.47)$$

Equation (6.47) gives the triggering angle α for the given μ and slip. The initial state vector $\underline{x}(\theta_o)$ can be derived from equations (6.42), (6.45) and (6.46). Having obtained the initial state vector, the system equations (6.14) and (6.18) are to be integrated through 60 electrical degrees to obtain the current waveform. If we start with an arbitrary initial state vector, then we will have to do the integration on the system equations for many cycles until the solution reaches steady state. The present procedure simplifies the computation effort to a large extent. The rotor current waveform thus obtained for a given set of parameters is shown in Fig. 6.6. This current waveform agrees closely with the experimental waveform given in [32].

6.4.5 Speed-torque characteristic

The current waveform obtained using the procedure explained in the previous section is the actual rotor current waveform in phase a of the machine. The torque developed by the machine is obtained by calculating the total air gap power. For this, the rotor current waveform obtained in the previous section is resolved into harmonic components and the fundamental component and the resultant r.m.s. values are used in the torque calculations. These values are obtained using numerical methods. The total period of the current waveform is divided into 2N equal interval. As the current waveform is having half wave symmetry

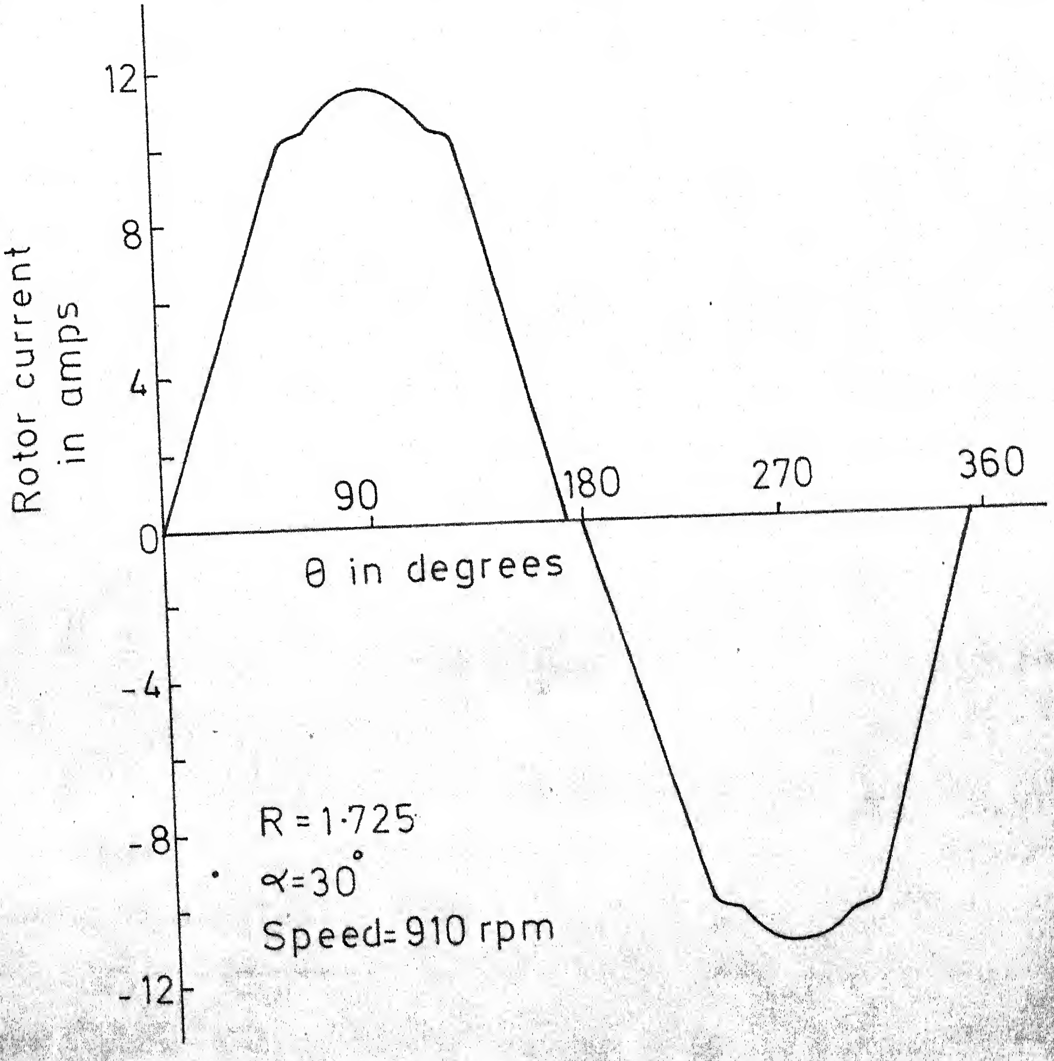

FIG. 6·6 ROTOR CURRENT WAVEFORM

and three phase symmetry, only non triplen odd harmonics alone are present. The following equations are used for the harmonic analysis of the function $f(\theta)$.

$$a_n = \frac{1}{\pi} \int_0^{2\pi} f(\theta) \cdot \cos n\theta \cdot d\theta \tag{6.48}$$

$$b_n = \frac{1}{\pi} \int_0^{2\pi} f(\theta) \cdot \sin n\theta \cdot d\theta \tag{6.49}$$

where a_n and b_n are the nth harmonic cosine and sine terms respectively. As numerical integration is employed for the present analysis, equations (6.48) and (6.49) are rewritten in summation form as follows

$$a_n = \frac{1}{N} \sum_{K=1}^{k=2N} f_K \cos \left[(nk)\left(\frac{360}{2N}\right) \right] \tag{6.50}$$

$$b_n = \frac{1}{N} \sum_{K=1}^{K=2N} f_K \sin \left[(nK) \left(\frac{360}{2N}\right) \right] \tag{6.51}$$

The rms value of the rotor current is given by

$$I_{rms} = \sqrt{\frac{1}{2N} \sum_{K=1}^{K=2N} f_K^2} \tag{6.52}$$

where f_K is the ordinate of the current waveform at mid point of the Kth interval. It is easy to implement the above equations as subroutines in the digital computer program. The total air gap power is obtained using the following equations.

$$P_g = (3sE_1 I_1 \cos \varphi_1 - I^2_{rms}\ sR_1')/s \qquad (6.53)$$

where s is the slip of the rotor

E_1 is the stator per phase applied voltage(rms and value)

φ_1 is the phase difference between rotor induced emf and fundamental rotor current

I_1 is the fundamental current (rms value)

The air gap power is also known as torque in synchronous watts. The developed torque in Nm is given by

$$T_d = P_g/2\pi n_s \quad \text{Nm} \qquad (6.54)$$

where n_s is the synchronous speed in rps

For the given slip s and commutation angle μ, the developed torque is calculated using equation (6.54). The practical speed torque characteristics available from [32] are for various values of firing angle α. Therefore, for the purpose of comparision, for every slip a number of values for μ are chosen and the corresponding α and T_d are obtained using equations (6.47) and (6.54) respectively. Now for every slip the developed torque for the required value of α is obtained by interpolation. The speed-torque characteristic thus obtained is shown in Fig. 6.7. The experimental values [32] are also marked in the figure. There is close agreement between the state space results and the experimental values. The computational effort required is simplified to a great extent as the solution is obtained

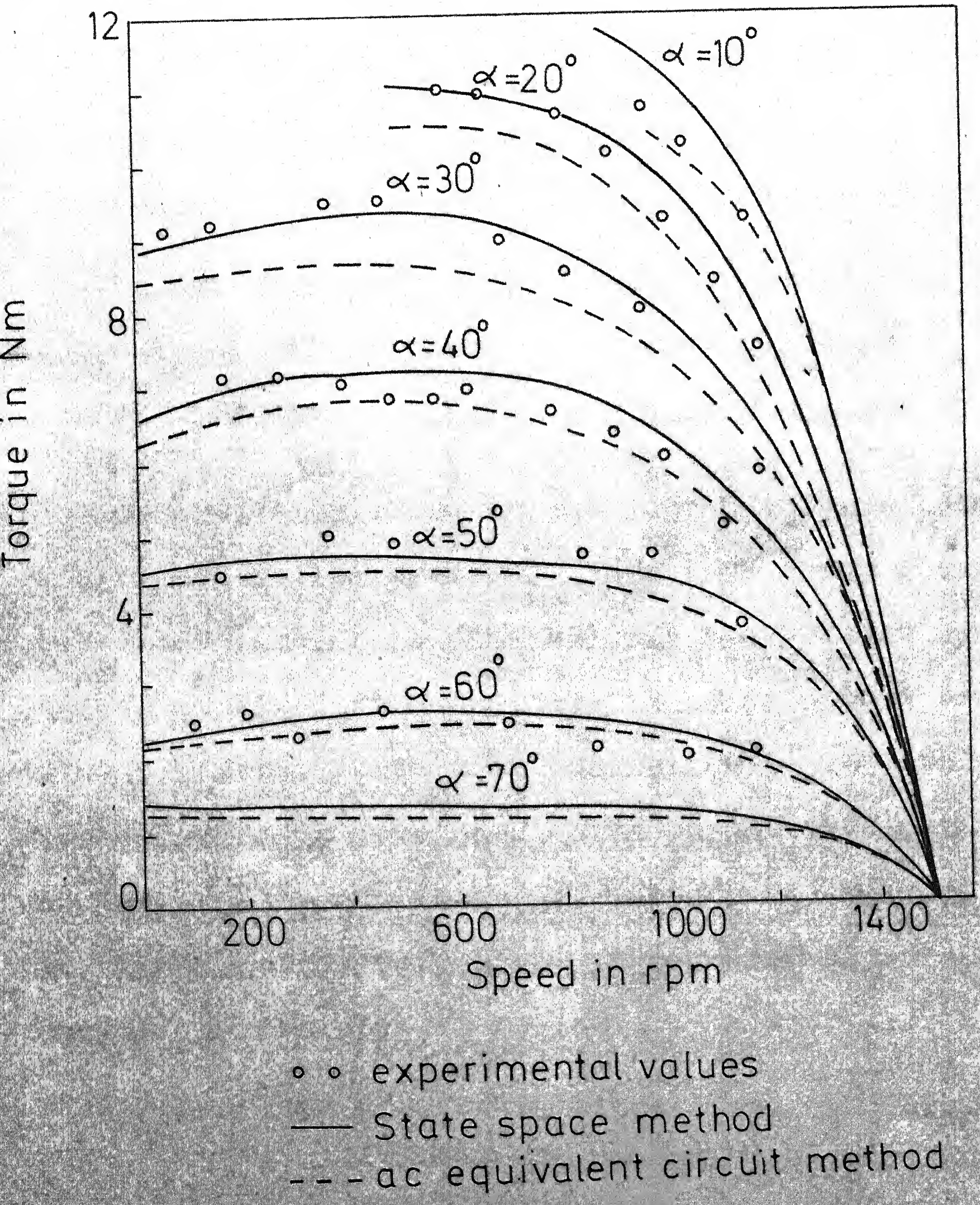

FIG.6.7 SPEED TORQUE CHARACTERISTIC

directly without iterations.

The important features of the present method of analysis are the following :

1) It avoids completely iterations.
2) It makes use of steady state per phase equivalent circuit.
3) It makes use of the symmetry that exists in the system to simplify the computational efforts and
4) It obtains the solution directly in terms of the actual system variables.

In the following section an attempt is made to further simplif the analysis of the phase controlled system.

6.5 Simplified ac Equivalent Circuit

In [29] simplified ac and dc models have been developed for chopper controlled systems. In this section a simplified ac equivalent circuit is obtained for the present system. For the purpose of simplified analysis it is assumed that the dc current is ripple free. With this assumption the equivalent circuit of the system is developed. The parameters of the equivalent circuit are the equivalent resistance and reactance when the fundamental ac current alone is considered. The equivalent circuit is developed as follows.

When the dc current is ripple free due to a large reactance in the dc side and the commutation angle is negligible, the ac current is of square pulses of $2\pi/3$ duration as shown in Fig. 6.8. If the dc current is I_d, r.m.s. value of the fundamental component of the ac current is given by

$$I_1 = \frac{1}{\sqrt{2}} \left\{ \frac{2}{\pi} \int_{\pi/6}^{5\pi/6} I_d \cdot \sin\theta \cdot d\theta \right\}$$

$$= \frac{\sqrt{2} I_d}{\pi} \left[-\cos\theta \right]_{\pi/6}^{5\pi/6}$$

$$I_1 = \frac{\sqrt{6}}{\pi} I_d \tag{6.55}$$

In the actual systems the pulses are not rectangular because of the commutation interval introduced due to source reactance. The error involved in the calculation of I_1 using equation (6.55) is 4.3 percent at the commutation angle of 60° [33]. Now the thyristor converter and the external resistance are to be replaced by an equivalent resistance and reactance as shown in Fig. 6.9. The equivalent resistance is obtained by equating the dc power to the power to be dissipated in the equivalent ac circuit when I_1 alone is made to flow.

That is,

$$3 I_1^2 R_{eq} \doteq I_d^2 R \tag{6.56}$$

Substituting I_1 from equation (6.55),

$$3\left(\frac{6}{\pi^2}\right) I_d^2 \cdot R_{eq} = I_d^2 R$$

$$R_{eq} = \frac{\pi^2}{18} \cdot R \tag{6.57}$$

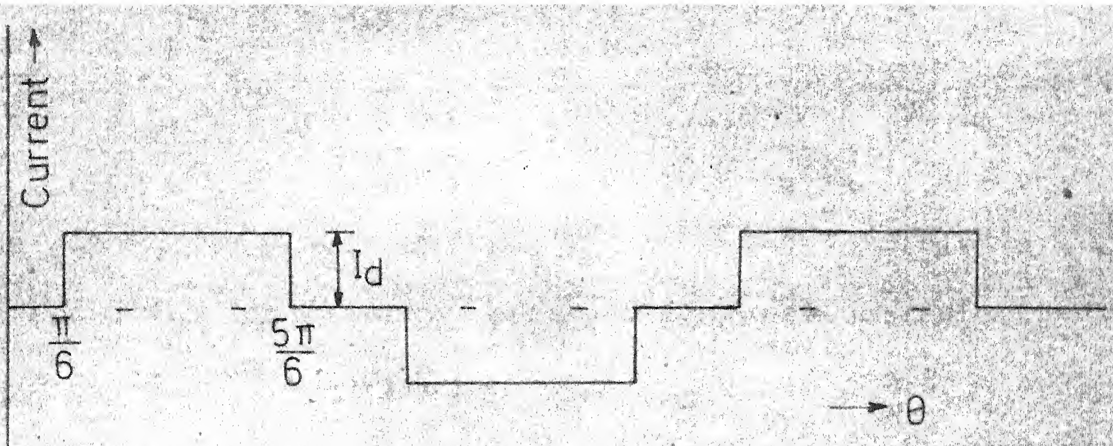

FIG. 6·8 PER PHASE ac CURRENT WAVEFORM WHEN THE ac CURRENT IS RIPPLE FREE AND COMMUTATION INTERVAL NEGLECTED

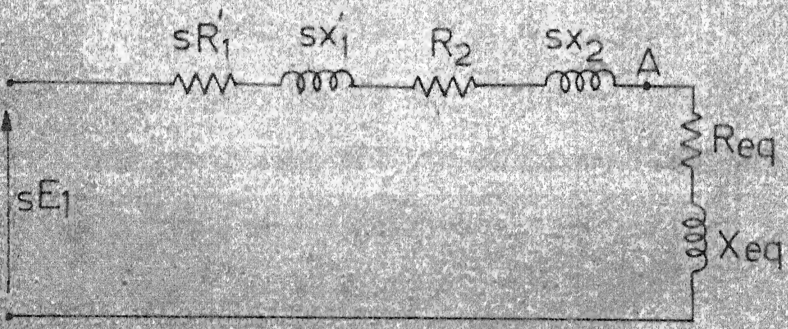
sR_1'
sx_1'
R_2
sx_2
A
R_{eq}
sE_1
X_{eq}

FIG.6·9 a c EQUIVALENT CIRCUIT

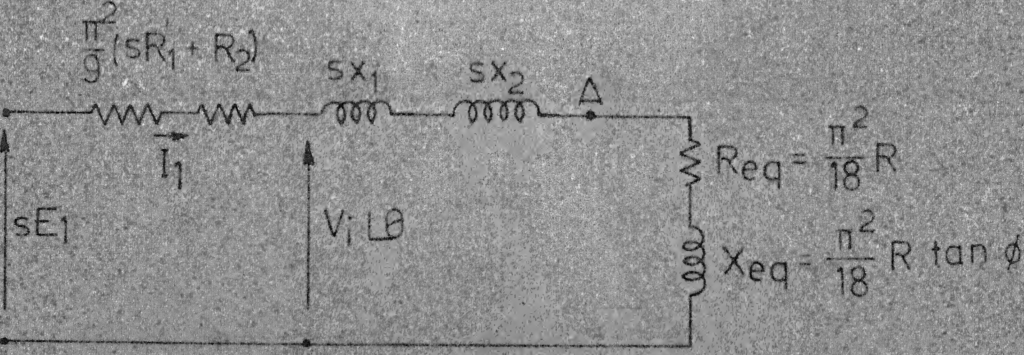
$\frac{\pi^2}{9}(sR_1' + R_2)$
sx_1
sx_2
A
I_1
sE_1
$V_i \angle \theta$
$R_{eq} = \frac{\pi^2}{18} R$
$X_{eq} = \frac{\pi^2}{18} R \tan \phi$

FIG.6·10 a c EQUIVALENT CIRCUIT WITH PARAMETERS REARRANGED

In Fig. 6.9, the powerfactor at A is unknown. It is equal to the firing angle only if the commutation angle is zero. In practice the commutation angle is not zero and it depends upon the operating conditions. When the commutation angle is not small, the power factor is given by

$$\cos \varphi = \frac{\cos \alpha + \cos \mu}{2} \tag{6.58}$$

The equivalent reactance $X_{eq} = R_{eq} \cdot \tan \varphi$. The winding resistances sR_1' and R_2 are replaced by the equivalent values considering the power equivalence. In the ac equivalent circuit the fundamental current alone is considered. Therefore the equivalent resistance that will dissipate the same amount of power as that when the rectangular ac pulses flow through the actual resistance is given by

$$I_1^2 R' = I_{rms}^2 (sR_1' + R_2) \tag{6.59}$$

$$I_{rms} = \sqrt{I_d^2 \cdot \frac{2\pi}{3} \cdot \frac{1}{\pi}}$$

$$I_{rms}^2 = I_d^2 \cdot \frac{2}{3} \tag{6.60}$$

Substituting equations (6.55) and (6.60) in (6.59),

$$\left(\frac{\sqrt{6}}{\pi}\right)^2 I_d^2 R' = \frac{2}{3} I_d^2 (sR_1' + R_2)$$

$$R' = \frac{\pi^2}{9} (sR_1' + R_2) \tag{6.61}$$

In the equivalent circuit shown in Fig. 6.9 X_{eq} is unknown. For the sake of analysis the present problem is defined as follows : Given the slip and powerfactor at A, the current in the ac equivalent circuit, firing angle α, commutation angle μ and developed torque are to be calculated.

The equivalent circuit shown in Fig. 6.9 is redrawn as shown in Fig. 6.10. In Fig. 6.10, the equivalent resistances are grouped together. Now the voltage that appears after the equivalent resistances can be related to the dc voltage $I_d \cdot R$ by the following equations [34].

$$\frac{3\sqrt{6}\, V_i \cos\alpha'}{\pi} - I_d \frac{3}{\pi}(sX_1' + sX_2) = I_d R \qquad (6.62)$$

Substituting for I_d from equation (6.55) in (6.62),

$$\frac{3\sqrt{6}\, V_i \cos\alpha'}{\pi} - \frac{\pi}{\sqrt{6}} I_1 \frac{3}{\pi}(sX_1' + sX_2) = \frac{\pi}{\sqrt{6}} I_1 R \qquad (6.63)$$

and
$$\frac{3\sqrt{6}\, V_i \cos(\alpha' + \mu)}{\pi} + \frac{\pi}{\sqrt{6}} I_1 \cdot \frac{3}{\pi}(sX_1' + sX_2) = \frac{\pi}{\sqrt{6}} I_1 R \qquad (6.64)$$

where $V_i \angle\theta$ is the voltage that will appear after the equivalent winding resistances in Fig. 6.10.

The ac equivalent circuit current I_1 is obtained using the following equations

$$\bar{I}_1 = \frac{sE_1}{[(R' + R_{eq}) + j(X_{eq} + sX_1' + sX_2)]} \qquad (6.65)$$

The firing angle α' and commutation angle μ are obtainined using equations (6.63), (6.64) and (6.65)

Actual firing angle $\alpha = \alpha' - \theta$ (6.66)

The developed torque in synchronous watts is obtained using the following equation

$$T_d = \frac{\text{Rotor Copper Loss}}{\text{Slip}}$$

$$T_d = 3I_1^2 \, [\frac{\pi^2}{9} R_2 + R_{eq}]/\text{slip} \qquad (6.67)$$

Torque in $\text{Nm} = 3I_1^2 \, [\frac{\pi^2}{9} R_2 + R_{eq}]/(\text{slip} \;\; 2\pi n_s)$ (6.68)

Thus for the given slip and fundamental power factor at point A of the equivalent circuit, firing angle α, commutation angle μ and and developed torque are obtained. In the above analysis, the commutation angle μ is assumed to be less than 60°. For values of μ greater than 60°, periodic short circuits take place on the dc side and the expressions derived earlier are not valid. Hence the present analysis of motor is confined to the region where the value of μ is less than or equal to 60°. Similar assumption is also made for the state space method Therefore in the above calculations, if the commutation angle μ exceeds 60°, the corresponding α and torque values are ignored. The characteristic thus obtained is shown as dotted curves in Fig. 6.7. Fig. 6.11 gives the variation of torque with firing angle at various speeds of the machine. The lowest firing

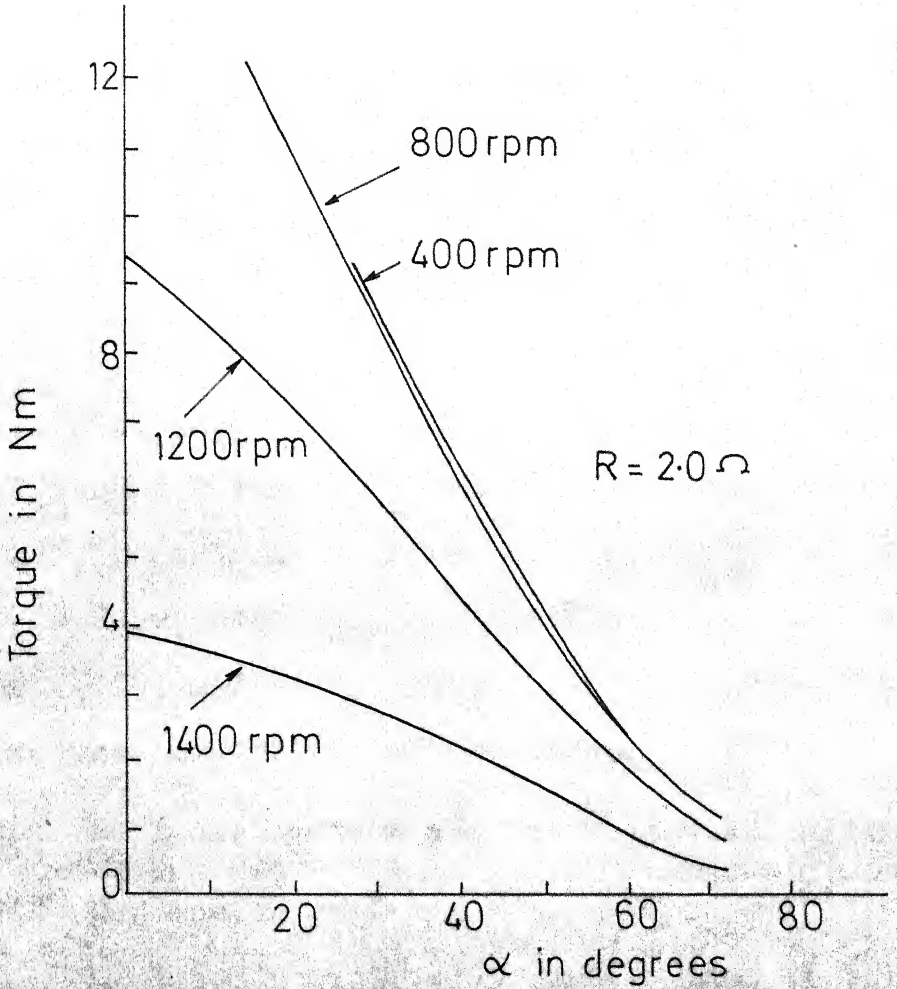

FIG·6·11 VARIATION OF TORQUE WITH FIRING ANGLE

angle is that value at which the commutation angle exceeds 60°.

6.6 Comparison with Chopper Controlled Scheme

1. As the present system uses only phase controlled SCRs which employ line commutation in the rotor circuit the system is simple and economical. Instead of fully controlled bridge half bridge can be conveniently used which will make the system still more economical whereas in the chopper controlled scheme forced commutation is employed which involves additional commutating elements and an auxiliary SCR.

2. The power factor of the scheme decreases with the increase of firing angle and becomes low at large firing angle whereas in chopper controlled drive the powerfactor is always quite high. This drawback of the present system can be eliminated by providing additional capacitors to improve the power factor. The half controlled bridge circuit will give better power factor.

3. Both the systems are convenient for closed loop operations.

6.7 Conclusion

The phase controlled & resistance method of speed control has been discussed in this chapter. The system is simple and economical for low and medium power applications. The scheme provides high starting torque and wide speed variations. A detailed analysis has been made using state space procedure.

The state variables used in the analysis are the actual rotor variables and the procedure does not involve iterations. The single phase steady state equivalent circuit with parameters referred to rotor is used for the development of the mathematical model. A simplified ac equivalent circuit is also derived. The results obtained using the equivalent circuit and the state space model are compared with the experimental values. The state space results agree closely with the experimental values. The results obtained using the simplified ac equivalent circuit agree closely with the experimental values at larger firing angles, but, there is error at low firing angles because of the assumptions made for the development of the equivalent circuit. The ac equivalent circuit is convenient for hand calculations.

CHAPTER 7

SPEED CONTROL USING DELTA CONNECTED PHASE CONTROLLED SCRs IN THE ROTOR

7.1 Introduction

Phase controlled SCRs can be used in different circuit configurations in the rotor circuit of the wound rotor induction motors to control the effective rotor impedance. A phase controlled resistance method of speed control has been discussed in the previous chapter. This method provides a wide speed variation and high starting torque. The SCRs are connected in bridge configuration to control the rotor impedance. The speed control is obtained by varying the firing angle of the controlled bridge. In this chapter, another scheme which uses delta connected phase controlled SCRs placed at the open star point of the rotor circuit is discussed. This scheme involves less number of components as compared to the one discussed earlier. The effective rotor impedance and hence the speed of the machine is varied by adjusting the firing angle of the SCRs. The possible modes of operation of the system are discussed. The steady state analysis of the present system is carried out using state space and harmonic analysis methods. The state space procedure discussed in this chapter is similar that developed in Chapter 6. The harmonic analysis method involves iterations to solve for the rotor current waveform. The developed procedures are first applied to a passive load and the phase current waveforms obtained by both the methods are compared. Then, these procedures are applied to the equivalent circuit of the induction motor to obtain the speed torque characteristic of the system. The analytical values are compared with the experimental values. The oscillograms of the actual rotor current waveforms are given to demonstrate the various modes of operation of the system. For the present study the following assumptions are made. These assumptions are similar to that made for the study of the previous system which uses phase controlled resistance in the rotor.

1. The machine parameters are constant.
2. The voltage drop across the stator winding is small
3. The distortion in the air gap flux wave due to harmonic currents through the stator windings is negligible.

7.2 System Representation

The schematic diagram of the present scheme is shown in Fig. 7.1. The system consists of a slipring induction motor, three equal external resistances one in each rotor phase and three phase controlled SCRs connected in delta and placed at the open star point of the rotor circuit of the machine. A firing scheme suitable for the present system is discussed in

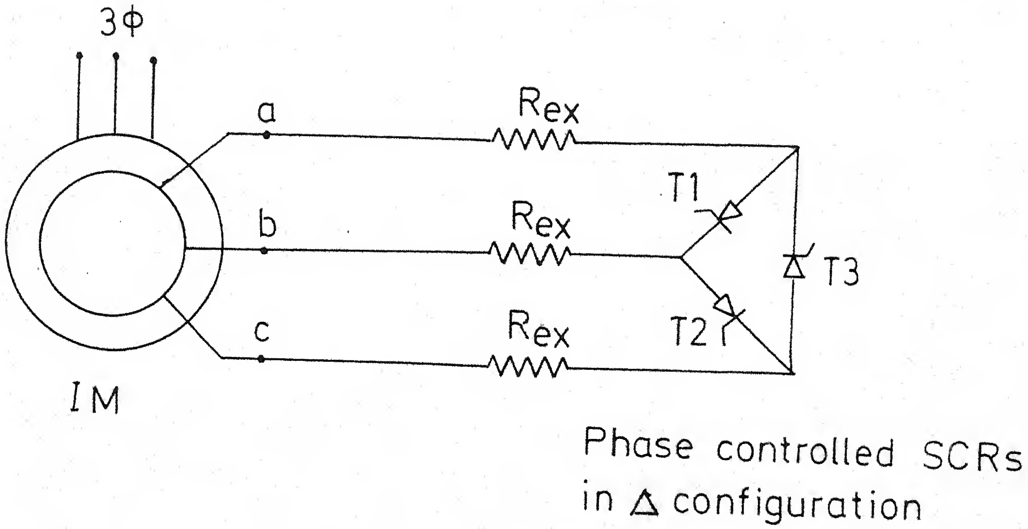
3Φ
a
b
c
Rex
Rex
Rex
T1
T2
T3
IM
Phase controlled SCRs
in Δ configuration

FIG. 7·1 SCHEMATIC DIAGRAM

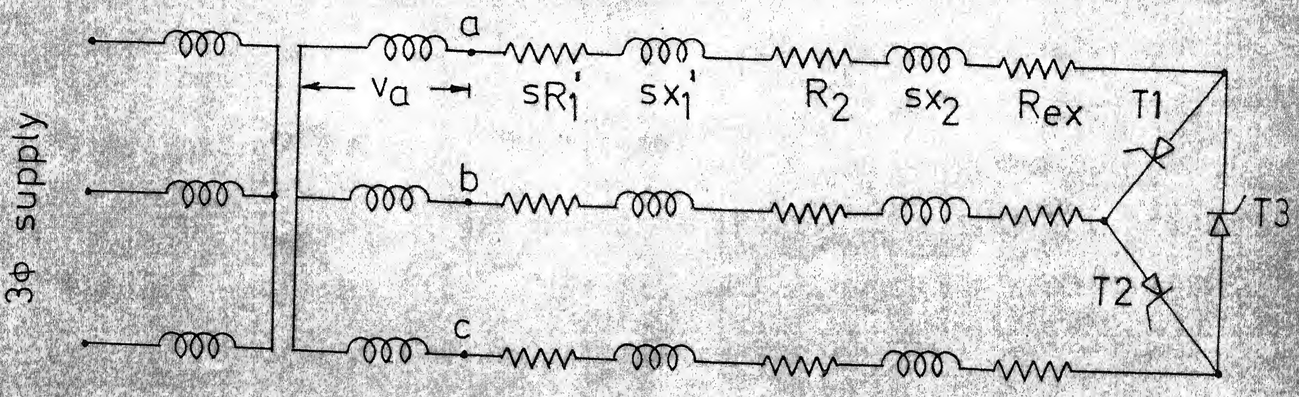
3Φ supply
a
b
c
V_a
sR_1'
sx_1'
R_2
sx_2
Rex
T1
T2
T3

FIG.7·2 EQUIVALENT CIRCUIT WITH PARAMETERS REFERRED TO SECONDARY the following chapter. The speed control of the system is achieved by varying the firing angle of the phase controlled SCRs. The thyristors are triggered symmetrically at interval of $2\pi/3$ electrical radians apart. Therefore the rotor current waveforms do have three phase symmetry. The sequence in which the thyristors are turned ON is T1, T2, T3, T1 and so on. At any instant of time more than two SCRs can not conduct because the third one experiences reverse bias when the other two are already conducting. The conduction period of the SCRs varies with the operating condition. The conducting SCR goes off at natural current zero. The various modes of operation of the system are discussed in the following section. The steady state equivalent circuit of the machine [29, 30, 31] with parameters referred to secondary is used for the analysis of the present system. The equivalent circuit is shown in Fig. 7.2.

7.3 Various Modes of Operation

The thyristors are fired at interval of $2\pi/3$ electrical radians apart in time. The firing angle α is measured with respect to the rotor induced emf. The rotor line-to-line induced emfs are shown in Fig. 7.3. The conduction period β of each thyristor is decided by the firing angle and speed. If each thyristor conducts for $4\pi/3$ electrical radians, then full conduction occurs and the system is in normal three phase operation. Under this condition two of the three SCRs conduct at any instant of time. If the value of β lies between $2\pi/3$ and $4\pi/3$ radians, then two SCR conduction and one SCR conduction alternates. When any two SCRs conduct the system is in three phase operation and is single phasing when one of the three alone conducts. As two device conduction and one device conduction alternates when β lies between $2\pi/3$ and $4\pi/3$ radians, this mode of operation is denoted as 2/1 mode of operation. Referring to Fig. 7.3(b), thyristor T1 is turned ON at θ_0. Since the value of β is greater than $2\pi/3$, thyristor T3 which is fired at $\theta = \theta_0 - 2\pi/3$ is still ON when T1 is turned ON at θ_0. Therefore both T3 and T1 are ON from θ_0 to θ_1 when T3 turns off. After θ_1, the system is single phasing with T1 alone conducting in the rotor circuit. The system is once again brought into three phase operation when T2 is turned ON at θ_2 $(\theta_0 + 2\pi/3)$ and 2/1 mode of operation repeats.

During the interval when T1 alone conducts, the phase a current is positive and when T2 alone conducts the rotor current is negative. The rotor current builds up from a negative level to the positive half when T3 and T1 are ON together in the circuit. Thus the rotor phase current is bidirectional. Fig. 7.3(b) shows an approximate current waveform. Phase a of the rotor is disconnected when T1 and T3 are off. The duration of this off period is equal to $(2\pi/3 - \mu)$ radians, where μ is the two SCR conduction period.

It can also be called as overlapping interval.

1/o mode of operation occurs when the value of β is less than 2π/3 radians. In this case every conducting SCR turns off before the next one is fired. Every time one of the three devi devices conducts the system is single phasing and it is put into off state from the instant when the conducting SCR turns off to the instant when the next one is turned ON. Since the system alternates between one device conduction and off state, this mode of operation is named as 1/o mode of operation. The positive portion of the current waveform of i_a occurs when T1 conducts and the negative portion occurs when T2 conducts. As the conduction period of each SCR is β radians, the total off period in the rotor current waveform over a slip cycle is (2π - 2β) radians. Fig. 7.3(c) shows an approximate rotor current waveform when the system is in 1/o mode.

The solution for 1/o mode of operation can be obtained easily knowing the rotor induced emfs and the machine parameters. The solution for 2/1 mode of operation is complicated because of the unknown instant at which the conducting SCR turns off. In the following sections the solution procedures for these two modes of operation are discussed.

7.4 Solution for 1/o Mode

The solution for 1/o mode is simple and can be obtained as follows : As there is no overlapping period, the rotor current can be easily obtained considering the induced emfs and equivalent machine parameters. When T1 is ON T2 and T3 are off and therefore, referring to Fig. 7.2, the differential equation of the system can be written as

$$v_{ab} = R\, i_a + X \frac{di_a}{d\theta} - R\, i_b - X \frac{di_b}{d\theta} \tag{7.1}$$

Since T2 and T3 are off, $i_a = - i_b$ and $i_c = 0$

Substituting these conditions in equation (7.1),

$$v_{ab} = 2R\, i_a + 2X \frac{di_a}{d\theta} \tag{7.2}$$

where

$R = sR_1' + R_2 + R_{ex}$

$X = sX_1' + sX_2$

$v_{ab} = \sqrt{3}\, V_m \sin \theta$

V_m = maximum per phase induced emf

and $\theta = s2\pi ft$

The solution to equation (7.2) is given by

$$i_a(\theta) = \frac{\sqrt{3}\, V_m}{2\sqrt{R^2+X^2}} \left\{ e^{-\frac{R}{X}(\theta-\alpha)} \sin(\nu - \alpha) - \sin(\nu - \theta) \right\} \tag{7.3}$$

where $\nu = \tan^{-1}(X/R)$

The firing angle α is measured with respect to line-to-line rotor induced emfs. Referring to Fig. 7.3(c), SCR T1 goes off at $\theta = (\alpha + \beta)$

Therefore $i_a'(\alpha + \beta) = 0$

Substituting the above condition in equation (7.3), we have

$$e^{-\frac{R}{X}\beta} \sin(\nu - \alpha) - \sin(\nu - \alpha - \beta) = 0 \tag{7.5}$$

Equation (7.5) can be solved for β using Newton - Raphson's method. The solution of equation (7.3) from $\theta = \alpha$ to $\alpha+\beta$ gives the positive portion of the phase a current waveform. The negative portion appears when T3 conducts from $\theta = (\alpha + \frac{4\pi}{3})$ to $\theta = (\alpha + \beta + 4\pi/3)$. The total off period in the current waveform is $2(\pi - \beta)$ radians. The resultant current waveform is resolved into harmonic components and the developed torque is calculated using the following equations.

$$T_d = [\sqrt{3}\, V_{ab}\, I_a \cos\phi - 3\, I_{rms}^2\, sR_1']/s \quad \text{watts}$$

$$= [\sqrt{3}\, V_{ab}\, I_a \cos\phi - 3\, I_{rms}^2\, sR_1']/(s2\pi n_s) \quad \text{Nm} \tag{7.6}$$

where

I_a is the rms value of the fundamental rotor frequency current

I_{rms} is the rms value of the rotor current waveform

V_{ab} is the rms value of the line-to-line rotor induced emf s is the slip of the rotor

ϕ is the phase angle between rotor phase a induced emf and $\bar{I}_a$

n_s is the synduronous speed of the motor in r.p.s.

I_a and I_{rms} can be obtained using the following equations.

$$I_{ac} = \frac{1}{N}\left[\sum_{K=1,2,..}^{2N} f_k \cos\left(K\frac{\pi}{N}\right)\right] \tag{7.7}$$

$$I_{as} = \frac{1}{N}\left[\sum_{K=1,2,..}^{2N} f_k \sin\left(K\frac{\pi}{N}\right)\right] \tag{7.8}$$

$$I_a = \sqrt{I_{ac}^2 + I_{as}^2} \tag{7.9}$$

$$\phi = \frac{\pi}{6} + \tan^{-1}\left(\frac{I_{ac}}{I_{as}}\right) \tag{7.10}$$

$$I_{rms} = \sqrt{\frac{1}{2N}\sum_{K=1,2}^{2N} f_k^2} \tag{7.11}$$

However, the solution for 2/1 mode spof operation is not straight forward and therefore state space and harmonic analysis methods are developed in the following sections for this mode of operation.

7.5 State Space Solution for 2/1 Mode of Operation

In 2/1 mode of operation, the system is subject to three phase and single phase state alternatively. Referring to Fig. 7.3, T1 is turned ON at θ_o and T3 and T1 conduct together from $\theta = \theta_o$ to $\theta_o + \mu$, where μ is the overlapping angle or angle of two SCR conduction. This is interval I in Fig. 7.3(b). During interval II T1 alone conducts and phase c of the rotor gets open circuited. During interval I, the equivalent circuit reduces to the form shown in Fig. 7.4. The voltage drops due to the devices are neglected

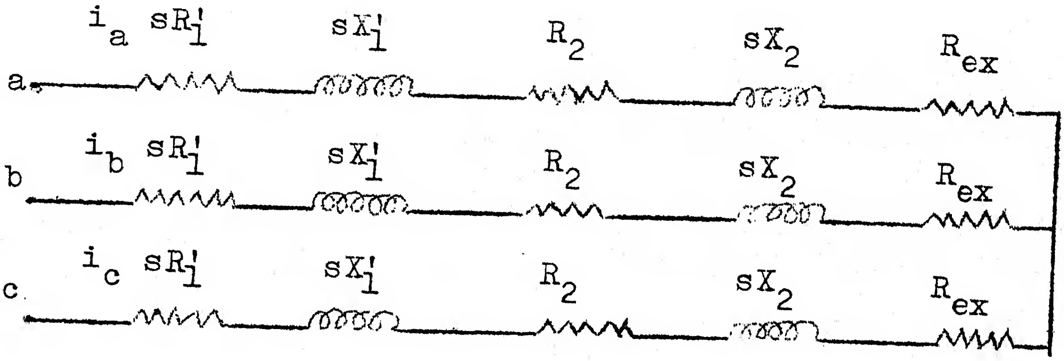

Fig. 7.4 The equivalent circuit when T3 and T1 are ON

The differential equations of the system are

$$v_{ab} = (sR_1' + R_2 + R_{ex})\, i_a + (sX_1' + sX_2)\frac{di_a}{d\theta} - (sR_1' + R_2 + R_{ex})\, i$$

$$- (sX_1' + sX_2)\frac{di_b}{d\theta} \qquad (7.12)$$

$$v_{bc} = (sR_1' + R_2 + R_{ex})\, i_b + (sX_1' + sX_2)\frac{di_b}{d\theta} - (sR_1' + R_2 + R_{ex})\, i$$

$$- (sX' + sX_2)\frac{di_c}{d\theta} \qquad (7.13)$$

$$v_{ca} = (sR_1' + R_2 + R_{ex})\, i_c + (sX_1' + sX_2)\frac{di_c}{d\theta} - (sR_1' + R_2 + R_{ex})\, i$$

$$- (sX_1' + sX_2)\frac{di_a}{d\theta} \qquad (7.14)$$

Putting $v_{ab} = V_1(\theta)$ and $v_{ca} - v_{bc} = V_2(\theta)$ and applying the condition $i_a + i_b + i_c = 0$,

$$V_1(\theta) = (sR_1' + R_2 + R_{ex})\, i_a + (sX_1' + sX_2)\frac{di_a}{d\theta}$$

$$-(sR_1' + R_2 + R_{ex})\, i_b - (sX_1' + sX_2)\frac{di_b}{d\theta} \qquad (7.15)$$

$$V_2(\theta) = -3(sR_1' + R_2 + R_{ex})\, i_a - 3(sX_1' + sX_2)\frac{di_a}{d\theta}$$

$$-3(sR_1' + R_2 + R_{ex})\, i_b - 3(sX_1' + sX_2)\frac{di_b}{d\theta} \qquad (7.16)$$

$$V_1(\theta) = \sqrt{3}\, V_m \sin\theta \qquad (7.17)$$

$$V_2(\theta) = 3\, V_m \cos\theta \qquad (7.18)$$

The forcing functions $V_1(\theta)$ and $V_2(\theta)$ can also be written in differential equation form.

Differentiating equation (7.17),

$$\frac{dV_1(\theta)}{d\theta} = \sqrt{3}\, V_m \cos\theta \qquad (7.19)$$

Differentiating equation (7.18),

$$\frac{dV_2(\theta)}{d\theta} = -3\, V_m \sin\theta \qquad (7.20)$$

Substituting equation (7.18) in (7.19) and (7.17) in (7.20),

$$\frac{dV_1(\theta)}{d\theta} = \frac{1}{\sqrt{3}}\, V_2(\theta) \qquad (7.21)$$

$$\frac{dV_2(\theta)}{d\theta} = -\sqrt{3}\ V_1(\theta) \tag{7.22}$$

Equations (7.15), (7.16), (7.21) and (7.22) are arranged in matrix form as follows :

$$\begin{bmatrix} (sX_1' + sX_2) & -(sX_1' + sX_2) & 0 & 0 \\ -3(sX_1' + sX_2) & -3(sX_1' + sX_2) & 0 & 0 \\ 0 & 0 & 1 & 0 \\ 0 & 0 & 0 & 1 \end{bmatrix} \begin{bmatrix} \frac{di_a}{d\theta} \\ \frac{di_b}{d\theta} \\ \frac{dV_1}{d\theta} \\ \frac{dV_2}{d\theta} \end{bmatrix} =$$

$$\begin{bmatrix} -(sR_1' + R_2 + R_{ex}) & (sR_1' + R_2 + R_{ex}) & 1 & 0 \\ 3(sR_1' + R_2 + R_{ex}) & 3(sR_1' + R_2 + R_{ex}) & 0 & 1 \\ 0 & 0 & 0 & \frac{1}{\sqrt{3}} \\ 0 & 0 & -\sqrt{3} & 0 \end{bmatrix} \begin{bmatrix} i_a \\ i_b \\ V_1 \\ V_2 \end{bmatrix} \tag{7.23}$$

Symbolically,

$$\underline{A}\ \underline{\dot{x}} = \underline{B}\ \underline{x} \tag{7.24}$$

$$\underline{\dot{x}} = \underline{A}^{-1}\ \underline{B}\ \underline{x} \tag{7.25}$$

$$\underline{\dot{x}} = \underline{\mathcal{C}}\ \underline{x} \tag{7.26}$$

Equation (7.26) represents the system when it is in three phase operation. During interval II, SCR T1 alone conducts and therefore phase c gets open circuited. The equivalent circuit reduces to the form shown in Fig. 7.5.

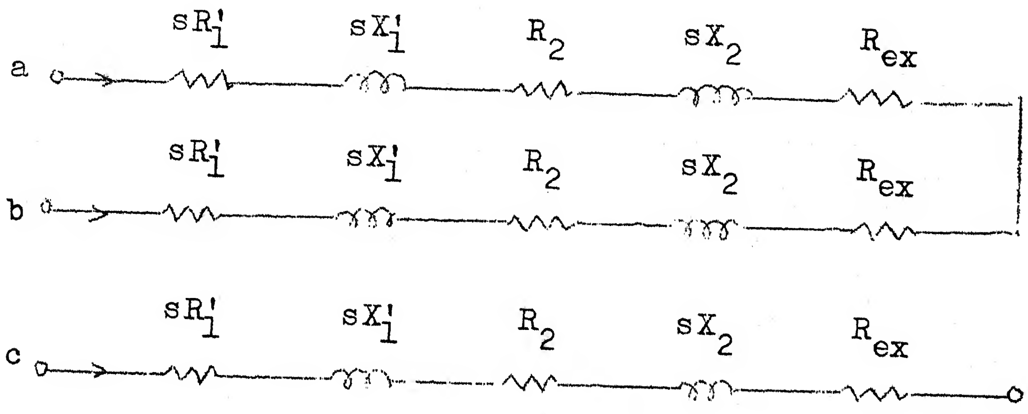

Fig. 7.5 Equivalent circuit when T1 alone conducts

The differential equation of the system is as follows ,

$$v_{ab} = V_1(\theta) = 2(sR_1' + R_2 + R_{ex})\, i_a + 2(sX_1' + sX_2)\frac{di_a}{d\theta} \tag{7.27}$$

Since phase c is disconnected, i_c becomes zero. The other two phase currents and their derivatives are equal and opposite to each other. Therefore, the differential equation which impose the current zero in the mathematical model is

$$\frac{di_a}{d\theta} = -\frac{di_b}{d\theta} \tag{7.28}$$

Equations (7.17), (7.18), (7.27) and (7.28) are arranged in matrix form

$$\begin{bmatrix} 2(sX_1' + sX_2) & 0 & 0 & 0 \\ 1 & 1 & 0 & 0 \\ 0 & 0 & 1 & 0 \\ 0 & 0 & 0 & 1 \end{bmatrix} \begin{bmatrix} \frac{di_a}{d\theta} \\ \frac{di_b}{d\theta} \\ \frac{dV_1}{d\theta} \\ \frac{dV_2}{d\theta} \end{bmatrix} =$$

$$\begin{bmatrix} -2(sR_1' + R_2 + R_{ex}) & 0 & 1 & 0 \\ 0 & 0 & 0 & 0 \\ 0 & 0 & 0 & \frac{1}{\sqrt{3}} \\ 0 & 0 & -\sqrt{3} & 0 \end{bmatrix} \begin{bmatrix} i_a \\ i_b \\ V_1 \\ V_2 \end{bmatrix} \tag{7.29}$$

Symbolically,

$$\underline{D}\,\underline{\dot{x}} = \underline{E}\,\underline{x} \tag{7.30}$$

$$\underline{\dot{x}} = \underline{D}^{-1}\,\underline{E}\,\underline{x} \tag{7.31}$$

$$\underline{\dot{x}} = F\,\underline{x} \tag{7.32}$$

The problem can be defined as, given the slip and two SCR conduction period, the firing angle α and the rotor current waveform are to be obtained. Once the rotor current waveform is known, the other performance characteristics can be obtained easily. The first step in the solution procedure is to solve for the initial state vector. As the thyristors are symmetrically fired at interval of 2π/3 rad apart, the system current waveforms have three phase symmetry. The three phase symmetry can be represented mathematically as follows :

Considering phase currents,

$$i_a(\theta + 2\pi/3) = i_c(\theta) \qquad (7.33)$$

but $$i_c(\theta) = -(i_a(\theta) + i_b(\theta)) \qquad (7.34)$$

therefore $$i_a(\theta + 2\pi/3) = -i_a(\theta) - i_b(\theta) \qquad (7.35)$$

$$i_b(\theta + 2\pi/3) = i_a(\theta) \qquad (7.36)$$

Considering the variables $V_1(\theta))$ and $V_2(\theta)$,

$$V_1(\theta + 2\pi/3) = v_{ab}(\theta + 2\pi/3) \qquad (7.37)$$

Applying three phase symmetry, $v_{ab}(\theta + 2\pi/3) = v_{ca}(\theta)$ (7.38)

but $$V_2(\theta) - V_1(\theta) = v_{ca}(\theta) - v_{bc}(\theta) - v_{ab}(\theta) \qquad (7.39)$$

$$= 2\, v_{ca}(\theta)$$

Therefore $$v_{ca}(\theta) = -\tfrac{1}{2} V_1(\theta) + \tfrac{1}{2} V_2(\theta) \qquad (7.40)$$

That is,

$$V_1(\theta + 2\pi/3) = -\tfrac{1}{2} V_1(\theta) + \tfrac{1}{2} V_2(\theta) \tag{7.41}$$

$$V_2(\theta + 2\pi/3) = v_{ca}(\theta + 2\pi/3) - v_{bc}(\theta + 2\pi/3) \tag{7.42}$$

$$= v_{bc}(\theta) - v_{ab}(\theta) \tag{7.43}$$

but

$$v_{ab}(\theta) = V_1(\theta) \tag{7.44}$$

and

$$v_{bc}(\theta) = -\tfrac{1}{2}[V_1(\theta) + V_2(\theta)] \tag{7.45}$$

Substituting (7.44) and (7.45) in (7.43),

$$V_2(\theta + 2\pi/3) = -3/2\ V_1(\theta) - \tfrac{1}{2} V_2(\theta) \tag{7.46}$$

Equations (7.35), (7.36), (7.41) and (7.46) can be arranged in matrix form as follows :

$$\begin{bmatrix} i_a \\ i_b \\ V_1 \\ V_2 \end{bmatrix}_{\theta = \theta_1 + \frac{2\pi}{3}} = \begin{bmatrix} -1 & -1 & 0 & 0 \\ 1 & 0 & 0 & 0 \\ 0 & 0 & -\frac{1}{2} & \frac{1}{2} \\ 0 & 0 & -\frac{3}{2} & -\frac{1}{2} \end{bmatrix} \begin{bmatrix} i_a \\ i_b \\ V_1 \\ V_2 \end{bmatrix}_{\theta = \theta_1} \tag{7.47}$$

Symbolically,

$$x(\theta + \frac{2\pi}{3}) = T\, x(\theta) \tag{7.48}$$

Equation (7.48) shows that any two state vector separated by $2\pi/3$ electrical radians can be related by a connection matrix $\underline{T}$. Therefore it is sufficient if the rotor current waveforms is obtained for any 120° interval. The initial state vector $\underline{x}(\theta_o)$ is obtained following the similar procedure explained in Chapter 6.

Referring to Fig. 7.3(b), if $\underline{x}(\theta_o)$ is the state of the system at θ_o, then state of the system at $(\theta_o + \mu)$ is given by

$$\underline{x}(\theta_o + \mu) = e^{\underline{C}\mu}\, \underline{x}(\theta_o) \tag{7.49}$$

The state of the system at $(\theta_o + 2\pi/3)$ is

$$\begin{aligned}\underline{x}(\theta_o + 2\pi/3) &= e^{\underline{F}\left(\frac{2\pi}{3} + \theta_o - \theta_o - \mu\right)}\, \underline{x}(\theta_o + \mu) \\ &= e^{\underline{F}\left(\frac{2\pi}{3} - \mu\right)}\, \underline{x}(\theta_o + \mu)\end{aligned} \tag{7.50}$$

Substituting equation (7.49) in (7.50),

$$\underline{x}(\theta_o + 2\pi/3) = e^{\underline{F}\left(\frac{2\pi}{3} - \mu\right)}\, e^{\underline{C}\mu}\, \underline{x}(\theta_o) \tag{7.51}$$

$$\underline{x}(\theta_o + 2\pi/3) = \underline{G}\, \underline{x}\, (\theta_o) \tag{7.52}$$

From equations (7.48) and (7.52),

$$\underline{G}\, \underline{x}(\theta_o) = \underline{T}\, \underline{x}(\theta_o) \tag{7.53}$$

The initial state vector $X(\theta_o)$ is solved for the given slip and two SCR conduction period μ. Equation (7.53) is rearranged as follows

$$\begin{bmatrix} \underline{H}_1 & \underline{H}_2 \\ \underline{H}_3 & \underline{H}_4 \end{bmatrix} \begin{bmatrix} \underline{i}(\theta_o) \\ V(\theta_o) \end{bmatrix} = \underline{0} \tag{7.54}$$

$$\underline{H}_1\ \underline{i}(\theta_o) + \underline{H}_2\ \underline{V}(\theta_o) = 0 \tag{7.55}$$

$$\underline{i}(\theta_o) = -\ \underline{H}_1^{-1}\ \underline{H}_2\ \underline{V}(\theta_o) \tag{7.56}$$

$$\underline{i}(\theta_o) = \underline{U}\ \underline{V}(\theta_o) \tag{7.57}$$

SCR T1 is turned ON at θ_o. Before firing T1, T3 alone was ON. Therefore $i_b = 0$ at θ_o.

From equation (7.57),

$$i_b(\theta_o) = U_{21}\ V_1(\theta_o) + U_{22}\ V_2(\theta_o) \tag{7.58}$$

Equating the right hand side of the above equation to zero,

$$\frac{V_1(\theta_o)}{V_2(\theta_o)} = -\ \frac{U_{22}}{U_{21}} \tag{7.59}$$

Referring to Fig. 7.3, $V_1(\theta_o) = \sqrt{3}\ V_m \sin\alpha$ (7.60)

$$V_2(\theta_o) = 3\ V_m \cos\alpha \tag{7.61}$$

Therefore
$$\frac{V_1(\theta_o)}{V_2(\theta_o)} = \frac{1}{\sqrt{3}} \tan \alpha \tag{7.62}$$

From equations (7.59) and (7.62),

$$\tan \alpha = - \frac{\sqrt{3}\, U_{22}}{U_{21}} \tag{7.63}$$

Equation (7.63) gives the triggering angle α for a given slip s and two SCR conduction period μ. The initial state vector $\underline{x}(\theta_o)$ can be obtained from equations (7.57), (7.60), (7.61) and (7.63). The solution for an interval of $2\pi/3$ electrical radians from $\theta = \theta_o$ to $\theta = (\theta_o + 2\pi/3)$ radians is obtained using equations (7.26) and (7.32). The repetitive application of equation (7.48) gives the solution for one complete cycle.

This procedure is first applied to a passive load with R/X ratio of 0.5 where R is the total per phase resistance and X is the total per phase reactance. The current waveform thus obtained using the state space procedure discussed above is shown in Fig. 7.6. This agrees closely with the experimental result given in [35]. The same problem is also solved by the harmonic analysis method and the results are compared. The method of analysis is explained in the following section.

7.6 Harmonic Method of Solution for 2/1 Mode

It is not possible to avoid iterations in the harmonic analysis method. The commutating instant of the conducting SCR

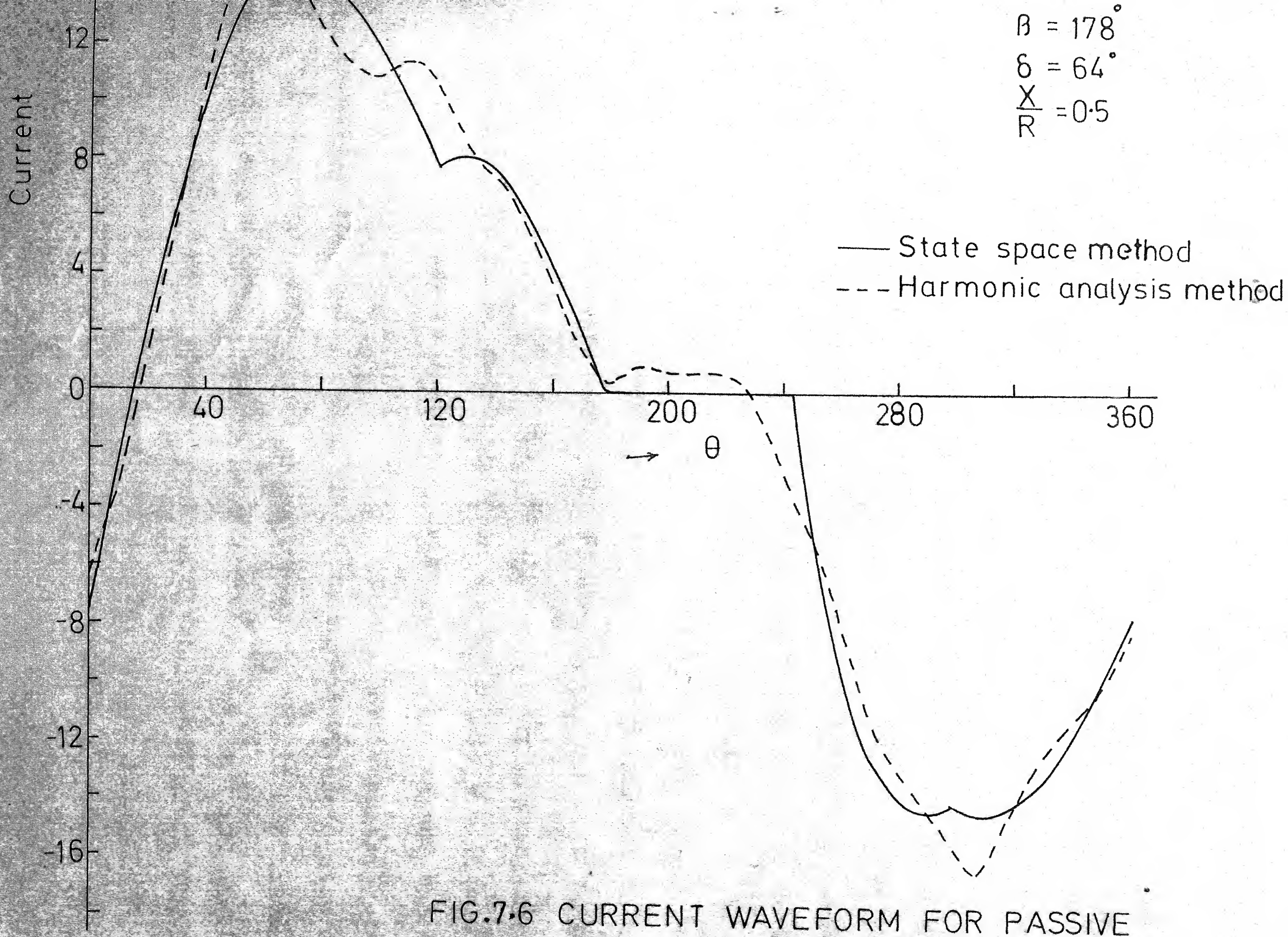

FIG.7·6 CURRENT WAVEFORM FOR PASSIVE LOAD is obtained using an iterative procedure. The problem may be redefined as follows : Given the firing angle α and slip s, the two SCR conduction period μ is to be obtained. The value of μ is first assumed and from the system operational characteristics the voltage waveform e_a that appears across phase a of the steady state equivalent circuit is obtained. Referring to Fig. 7.3(b), SCR T1 is turned ON at θ_o. From $\theta = 0$ to $\theta = \theta_o$ SCR T3 alone is conducting. Since the rotor circuit is single phasing during this interval with phase b disconnected, the voltage that appears across phase a of the equivalent circuit is one half of v_{ac}. The rotor circuit is in three phase operation from $\theta = \theta_o$ to $\theta_o + \mu$. Therefore the voltage that appears across the phase a of the equivalent circuit is v_a, the phase a induced emf. SCR T3 commutates out at $\theta_1 (= \theta_o + \mu)$. SCR T2 is turned ON at θ_2. The system is once again experiencing single phase operation from $\theta = \theta_o + \mu$ to $\theta = \theta_2 (= \theta_o + 2\pi/3)$. During this interval phase c gets open circuited and one half of the line a-b induced emf v_{ab} appears across phase a of the equivalent circuit. When SCR T2 is turned ON the system is again brought into three phase operation and it continues until $\theta = \theta_2 + \mu$. SCR T1 goes off at $\theta = \theta_2 + \mu$ and phase a is disconnected. Phase a remains disconnected until SCR T3 is turned ON at θ_3 $(= \theta_o + 4\pi/3)$. The system is again in three phase operation from $\theta = \theta_3$ to $\theta = \theta_3 + \mu$. SCR T2 gets commutated out at $\theta = \theta_3 + \mu$. Now SCR T3 alone conducts bringing $v_{ac}/2$ across phase a of the equivalent circuit and this continues until SCR T1 is fired again at θ $(=\theta_o + 2\pi)$ and the cycle of operation repeats. Therefore voltage e_a, that comes across the phase a of the equivalent circuit can be defined as follows :

$$
\begin{aligned}
e_a &= \frac{v_{ac}}{2} && 0 \leq \theta \leq \theta_o \\
&= v_a && \theta_o \leq \theta \leq \theta_o + \mu \\
&= \frac{v_{ab}}{2} && \theta_o + \mu \leq \theta \leq \theta_o + 2\pi/3 \\
&= v_a && (\tfrac{2\pi}{3} + \theta_o) \leq \theta \leq (\tfrac{2\pi}{3} + \theta_o + \mu) \\
&= 0 && (\tfrac{2\pi}{3} + \theta_o + \mu) \leq \theta \leq \tfrac{4\pi}{3} + \theta_o \\
&= v_a && (\tfrac{4\pi}{3} + \theta_o) \leq \theta \leq \tfrac{4\pi}{3} + \theta_o + \mu \\
&= \frac{v_{ac}}{2} && (\tfrac{4\pi}{3} + \theta_o + \mu) \leq \theta \leq 2\pi
\end{aligned}
\tag{7.64}
$$

The voltage waveform e_a is resolved into its harmonic components. The triplen harmonic currents are absent in the system. All other odd and even harmonics are present. The following equations are used for the harmonic analysis.

$$e_{nc} = \frac{1}{\pi} \int_0^{2\pi} e_a \cos n\theta \, d\theta \tag{7.65}$$

$$e_{ns} = \frac{1}{\pi} \int_{0}^{2\pi} e_a \sin n\theta \, d\theta \tag{7.66}$$

$$e_n = \sqrt{e_{nc}^2 + e_{ns}^2} \tag{7.67}$$

$$\phi_n = \tan^{-1} (e_{nc}/e_{ns}) \tag{7.68}$$

The harmonic currents are obtained using the harmonic equivalent circuits. The nth harmonic equivalent circuit is given in Fig. 7.7. e_n is the nth harmonic phase voltage obtained using equation (7.67). The following equation gives nth harmonic rotor current.

$$\bar{I}_n = \frac{e_n \underline{/\phi_n}}{(sR_1' + R_2 + R_{ex}) + j\ (sX_1' + sX_2)} \tag{7.69}$$

The resultant phase a current is obtained by adding the harmonic components. For the chosen value of μ, the rms value of current during the off period is calculated and checked whether it is less than a pre-assigned value. If not, the value of μ is adjusted until the off period current is reasonably low. The validity of this procedure is first tested with the passive load as done before for the state space method. The current waveform obtained by this method is shown in Fig. 7.6. It agrees closely with the state space results.

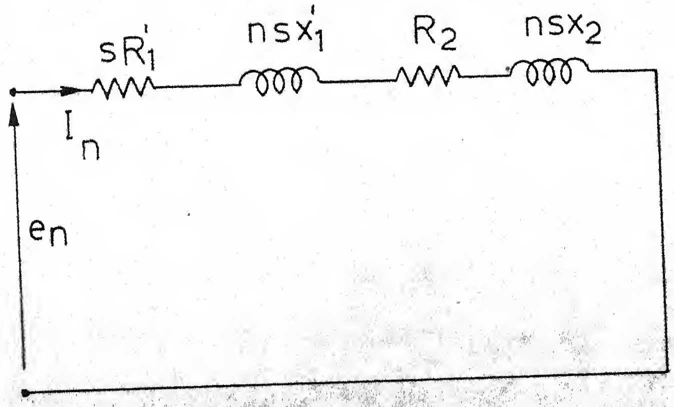
sR_1'
nsx_1'
R_2
nsx_2
I_n
e_n

FIG. 7·7 n th HARMONIC EQUIVALENT CIRCUIT

7.7 Application to Steady State Analysis of Induction Motor

Both the above procedures are now applied to the equivalent circuit of the test machine. The test machine used for the study is the same slipring machine used for the study of three thyristors - three diodes system discussed in Chapter 3. The parameters of the test machine referred to the secondary circuit are given below.

$R_1' = .232$ ohm $R_2 = .592$ ohm

$X_1' = .395$ ohm $X_2 = .395$ ohm

$R_{ex} = 5$ ohm

For a given slip s and two SCR conduction period μ, the developed torque is calculated using equation (7.6). The speed-torque characteristic of the system for various values of the off period δ is shown in Fig. 7.8. The total off period in the phase current waveform for 2/1 mode of operation is $(\frac{2\pi}{3} - \mu)$ radians. In the case of 1/o mode of operation the total off period is $2(\pi-\beta)$. The experimental results are also marked in the figure. The rotor current waveforms demonstrating the two different modes of operation are shown in Fig. (7.9). At high speed operations the rotor current is superimposed with slot ripples. It is clear from the oscillogram shown in the figure. The firing and control schemes used for this system

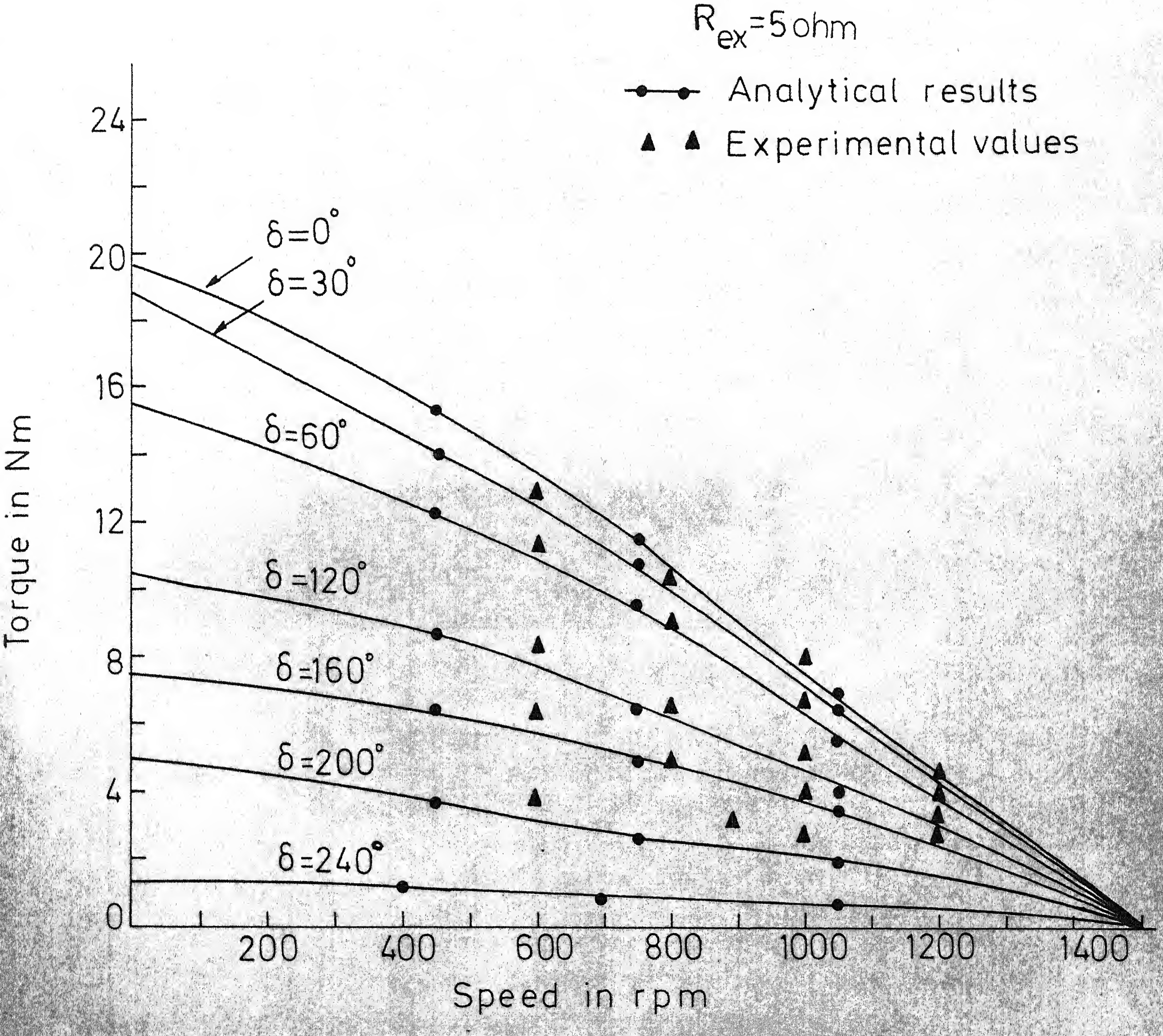

FIG·7·8 SPEED–TORQUE CHARACTERISTIC

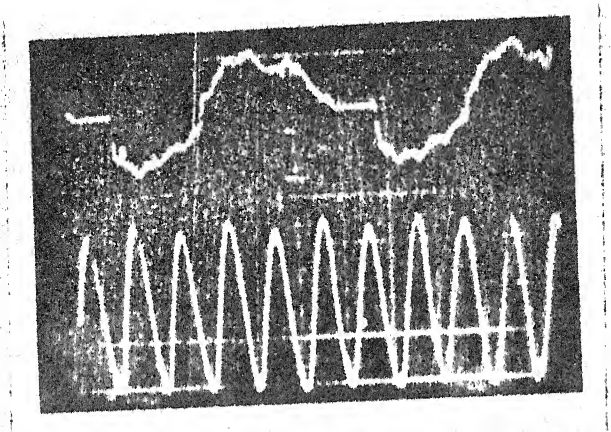

(a) 2/1 mode

Upper trace : rotor current, 4A/division

Lower trace : Stator current, 1A/division

Speed = 1200 rpm, Rex = 1.5 ohm

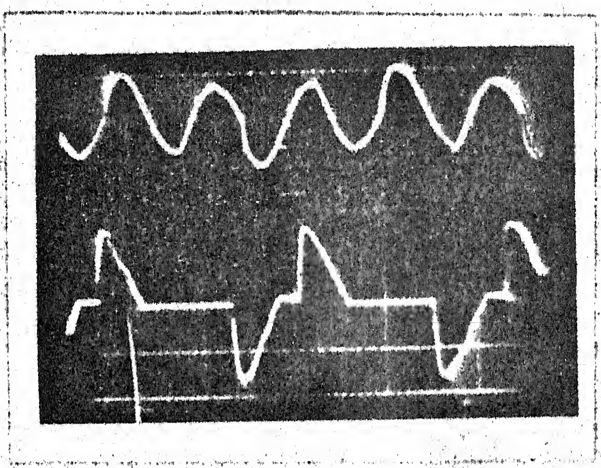

(b) 1/0 mode

Upper trace : Stator current, 5A/division

Lower trace : rotor current, 4A/division

Speed = 800 rpm, Rex = 5 ohms

Fig. 7.9 Oscillograms of current waveforms

are explained in the following chapter. The speed-torque characteristic obtained using harmonic analysis method is found to be very close to the results obtained by the state space procedure shown in Fig. 7.8. Hence no separate performance characteristics are given for the harmonic analysis method.

7.8 Conclusion

A rotor impedance control scheme which uses only three phase-controlled SCRs in the rotor circuit has been studied in this chapter. The scheme is simple and it provides a wide speed variation. State space procedure and harmonic analysis method have been developed to obtain the speed-torque characteristic of the system. The state space procedure used for the present study is similar to that discussed in Chapter 6 for phase controlled resistance scheme. The analytical results agree closely with the experimental values. The oscillograms of the rotor current demonstrating the various modes of operation of the system are given. Even for a highly distorted rotor current the stator current waveform is fairly sinusoidal as shown in Fig. 7.9. Therefore, the amount of harmonic currents injected into the three phase supply terminals is negligibly small. In the case of stator voltage control schemes considerable amount of harmonic currents are drawn from the supply.

Though the delta configuration is simple and involves less control circuitry, it is not used to a large extent today because of the following reasons [35].

i) It needs thyristors of large current rating (rms value) compared to six thyristor delta configuration (approximately twice)

ii) The rotor phase currents have large harmonic current compared to conventional circuits.

As the cost of large current rating thyristors are falling and the harmonic currents demanded from the supply is considerably low with rotor side control, the present scheme may find wide applications in the field of speed control of small and medium capacity motors in future. A firing scheme suitable for the present scheme and the closed loop speed control of the system are discussed in the following chapter.

CHAPTER 8

FIRING SCHEME AND FEED-BACK CONTROL FOR ROTOR PHASE CONTROL SYSTEM WITH DELTA CONNECTED SCRs

8.1 Introduction

A simple and economical control scheme suitable for the variable speed operation of wound rotor induction motor has been discussed in the last chapter. The importance of the scheme is that with only three phase controlled SCRs it achieves wide speed variation for all types of loads. The speed control is obtained by adjusting the firing angle of the SCRs. The steady state analysis of the system has been already discussed using state space and harmonic analysis methods.

In the present chapter a triggering scheme suitable for this delta connected configuration is developed. Quite a good number of triggering schemes are available in the literature, but most of them work with constant voltage and constant frequency anode supply. In the present system, as the voltage and frequency of the rotor circuit vary with speed of the machine, existing triggering schemes are to be modified suitably. A scheme which gives firing angle α proportional to the control voltage is discussed. The firing angle α remains same for a given control voltage over a wide range of speed.

The closed loop performance of the system with speed feed back is studied. The various functional blocks of the feed back system are developed and the performance of the system for sudden change in load torque and reference voltage are obtained. Both P (proportional) and PI (proportional plus integral) controllers are considered for the study. The experimental observations are compared with the analytical results.

8.2 Review of Triggering Schemes Used for Rotor Phase Control

A few triggering schemes have been discussed in the literature for rotor phase control circuits. Most of them use an auxiliary machine or a synchro similar in construction to the main motor to provide the firing circuit with ac sine wave of slip frequency. From this voltage a constant amplitude ac signal is derived over the entire speed range and this is compared with a dc control signal. The firing pulse is given to the respective SCR at the instant when the ac signal crosses the dc level of the control voltage. The firing angle α remains constant for a given control voltage over a wide range of slip frequency so long as the amplitude of the sine wave given by the controller remains constant over the operating speed range. The firing angle α is measured from the zero crossing instant of the input sine wave. If this sine wave is in phase with the secondary induced emf of the main machine, then by varying the control voltage level the value of α can be changed from 0 to 90 electrical degrees. If the sine wave is phase advanced by 90 electrical degrees with respect to the induced emf of the rotor, then a variation of 0 to 180° can be obtained by varying the control voltage.

A special commutator type frequency changer has been used in [25] to give the required ac signal to the control circuit. In this scheme, the commutator type auxiliary machine gives six phase output for a given three phase input voltage. The commutator machine is called as Pilot Generator and it is coupled with the main motor. The output of this commutator machine is of slip frequency and the amplitude of the output remains however constant over the entire speed range.

A synchro similar in construction to the main machine is used in [28] to provide the control circuit with the required ac signal. The rotor of the synchro is properly aligned with the rotor of the main motor so that there is no mechanical phase difference between the synchro and the main motor secondary fluxes. As the amplitude and frequency of the rotor induced emf change with speed, the constant amplitude ac signals have been obtained by feeding the slip frequency synchro emf through a simple RC integrating circuit. The integrating circuit also provides the necessary phase shift.

In the schemes discussed above, auxiliary machines and integrating circuits have been used to obtain constant amplitude ac sinusoidal signal of slip frequency. This ac signal and the control voltage are fed to the comparator to detect the cross over point. In this case the firing angle α is not linear with the control voltage. The ac signal which is fed to the comparator should be free from ripples. It is difficult to eliminate completely the ripples which is present in the controller output. It is also difficult to keep the amplitude of the ac signal constant over a wide speed range. In [32], a triggering scheme which avoids auxiliary machines and uses analog circuits to obtain the synchronized signals has been discussed. The limitation of the scheme is that the firing angle is not constant for a given control voltage as the machine speed changes. In this chapter, an alternative scheme which gives constant firing angle for the given control voltage over a wide speed range is discussed. The triggering scheme discussed here is different from the analog and digital adaptive circuits discussed in [36].

8.3 Proposed Firing Scheme

The circuit diagram of the proposed scheme is given in Fig. 8.1. The scheme does not use auxiliary machine to obtain the slip frequency ac signal. It uses the signals which are available across the sliprings of the machine. These signals are not sinusoidal because of the switching action of the SCRs.

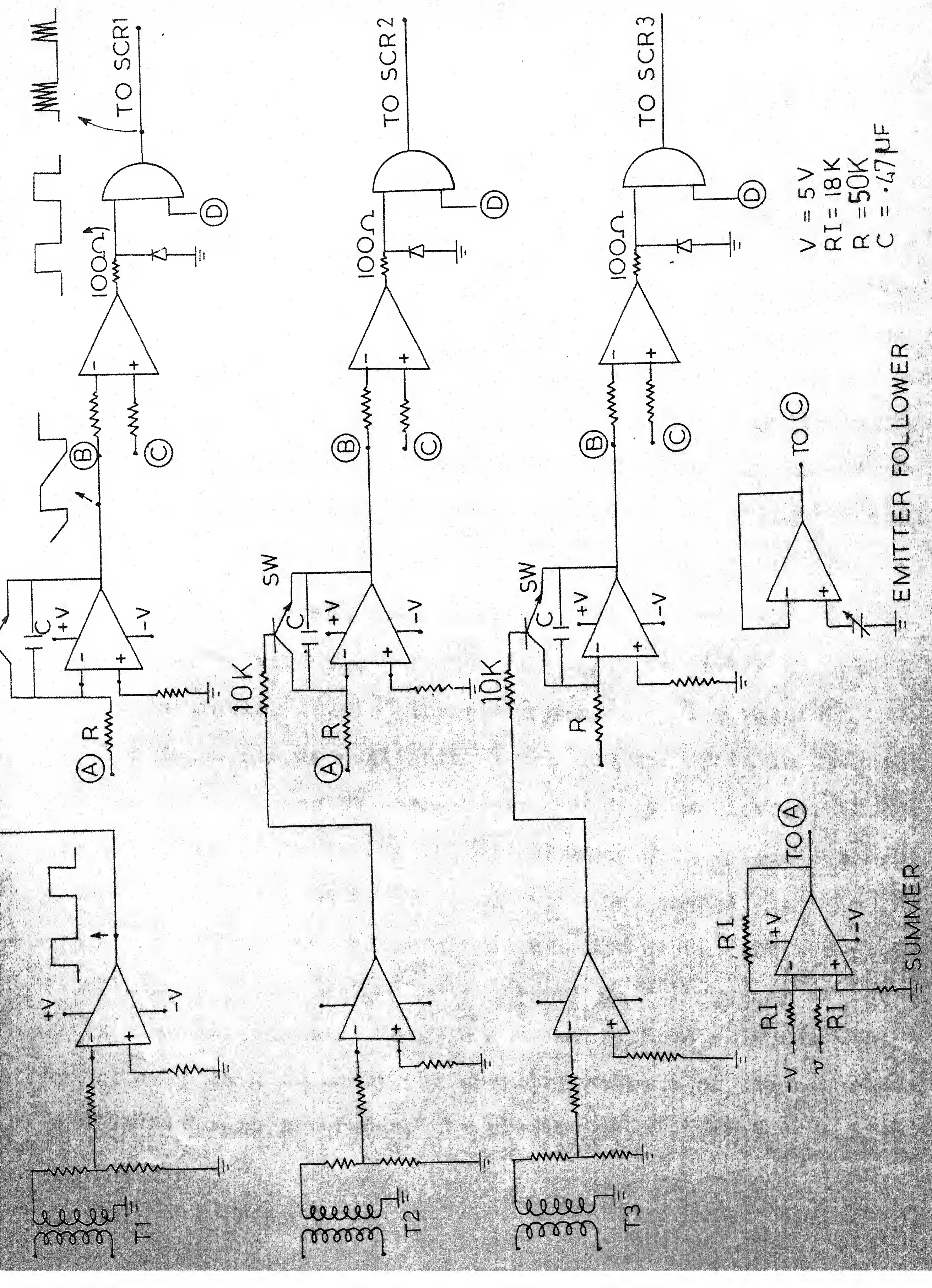
T1
T2
T3
+V
-V
A
R
10K
SW
C
B
C
D
100Ω
TO SCR1
TO SCR2
TO SCR3
R1
RI
-V
v
TO A
SUMMER
TO C
EMITTER FOLLOWER
V = 5 V
RI = 18 K
R = 50K
C = ·47 µF

They are fed to the control circuit through isolating transformers as shown in Fig. 8.1. In the delta configuration, there are three SCRs and they are triggered one at a time at interval of $\frac{2\pi}{3}$ electrical radians apart in time. To have this required phase displacement of $2\pi/3$ electrical radians, three separate isolating transformers are used. The output of this transformer is given to zero crossing detectors. OP-AMP µA 741 is used as zero crossing detector. The noninverting terminal of the OP-AMP is grounded through a resistance and the output of the isolating transformer is given to the inverting terminal through a potential divider.

The output of the zero crossing detector will be a rectangular waveform with the positive and negative levels clipped to its saturating level. Therefore a rectangular waveform of slip frequency is available at the output. This is used to actuate the switches SW which reset the ramp generators. Since the frequency of the rotor voltage changes with speed, a ramp of constant amplitude syndronized with the signal which is available between the sliprings is needed. Therefore the slope of this ramp should get adjusted as the slip frequency of the rotor circuit changes. This is done as follows : As the slope of the ramp is decided by the charging current of the capacitor used in the ramp generator, the present problem will be solved if the ramp generator is fed with voltage proportional to slip frequency. For this, a dc voltage proportional to the rotor speed is subtracted from a fixed dc proportional to the synchronous speed. This is done using a summer as shown in Fig. 8.1. The output of this summer is given to the ramp generators. As the speed of the machine changes, the output voltage of the summer charges in proportion to the slip speed and therefore the changing current of the ramp generators gets adjusted automatically. As the charging current of the ramp generator is proportional to the slip speed, a ramp of constant amplitude synchronized with the signals available at the slip-rings is obtained. The parameters of the ramp generators are adjusted so that the ramp will reach saturation level approximately at the end of the half period at all slip frequencies. The ramp is reset by the switch SW which is actuated by the output of the zero crossing detector.

The output of the ramp generator is given to the comparator at (B). The control voltage is fed to the comparator at (C) through the OP-AMP which is in emitter follower configuration. The comparator switches to high state at the instant when the ramp crosses the dc level of the control voltage. The output of the comparator is ANDED with a carrier frequency signal. The AND gate output is connected to the SCR gate through pulse transformer. The firing angle α of the SCR is controlled by adjusting dc level of the control voltage, manually in the case of open loop operation. In the case of closed loop operation, the tacho generator output voltage is compared with the set value and the error voltage is given to the controller which may have P or PI configuration. The output of the controller is given to the comparator at (C) through the emitter follower to adjust the firing angle to the required value automatically. In the present system three separate firing circuits are used one for each SCR.

The scheme explained above is simple and it gives satisfactory performance. The experimental results obtained using this firing scheme are given in the previous chapter for the purpose of comparision with the analytical values. In the following section the closed loop operation of the above system has been analysed.

8.4 Performance of Closed Loop System with Delta Connected SCRs in the Rotor

8.4.1 System description

In the previous section a simple and reliable firing scheme suitable for delta connected SCRs in the rotor circuit has been discussed. A closed loop control scheme which uses this firing scheme and feed back controlling elements is discussed in this section. The block diagram of the closed loop control scheme is given in Fig. 8.2. The stator of the test machine is fed with constant voltage constant frequency supply. The delta connected SCRs and external rotor resistances are connected in the rotor circuit as discussed in the previous chapter. For the purpose of speed feed back, a permanent magnet tachogenerator is mounted in the rotor shaft of the main motor. The same generator output is also used for the generation of ramp in the control circuit. The tacho generator output voltage is proportional to the rotor speed and is compared with a fixed dc level V_R which represents the set speed. The error voltage is given to the controller. The set speed is changed by varying V_R. The controller may be P (proportional) or PI (Proportional plus Integral) or PID (Proportional plus Integral plus Derivative). In the present study, P and PI controllers are considered. The function of the controller is to give the required control voltage which will adjust the firing angle α to the suitable value.

8.4.2 Transfer functions of the functional blocks

The aim of the present study is to obtain the performance of the feed back system for small perturbations in load torque and reference voltage analytically and compare it with the experimental values. For this, the transfer functions of the various functional blocks which are valid for small variations about the given operating point is derived in the following subsections.

8.4.2.1 Tachogenerator and filter

The tachogenerator and the associated filter are shown in Fig. 8.3. This is represented as Block B_1 in the functional block diagram given in Fig. 8.4. A RC filter is used to remove the ripples present in the tachogenerator output. The tachogenerator output is also attenuated. The transfer function of this block is represented by

$$G_1(S) = \frac{K_1}{1 + ST_1} \tag{8.1}$$

where K_1 is the combined gain of the tachogenerator and the filter and T_1 is the effective time constant of the filter.

8.4.2.2 Controller

Referring to Fig. 8.4, the change in output voltage of block B_1 is compared with ΔV_R, the change in the reference voltage and the resultant change in voltage is fed to the controller. The controller output voltage is corrected in accordance with the input change in voltage. The change in the controller output voltage is denoted as ΔV_C. The controller is represented as block B_2 in Fig. 8.4. In the present study, P and PI controllers are considered. The circuit configurations of these two controllers are given in Fig. 8.5. The transfer functions of the controllers are as follows :

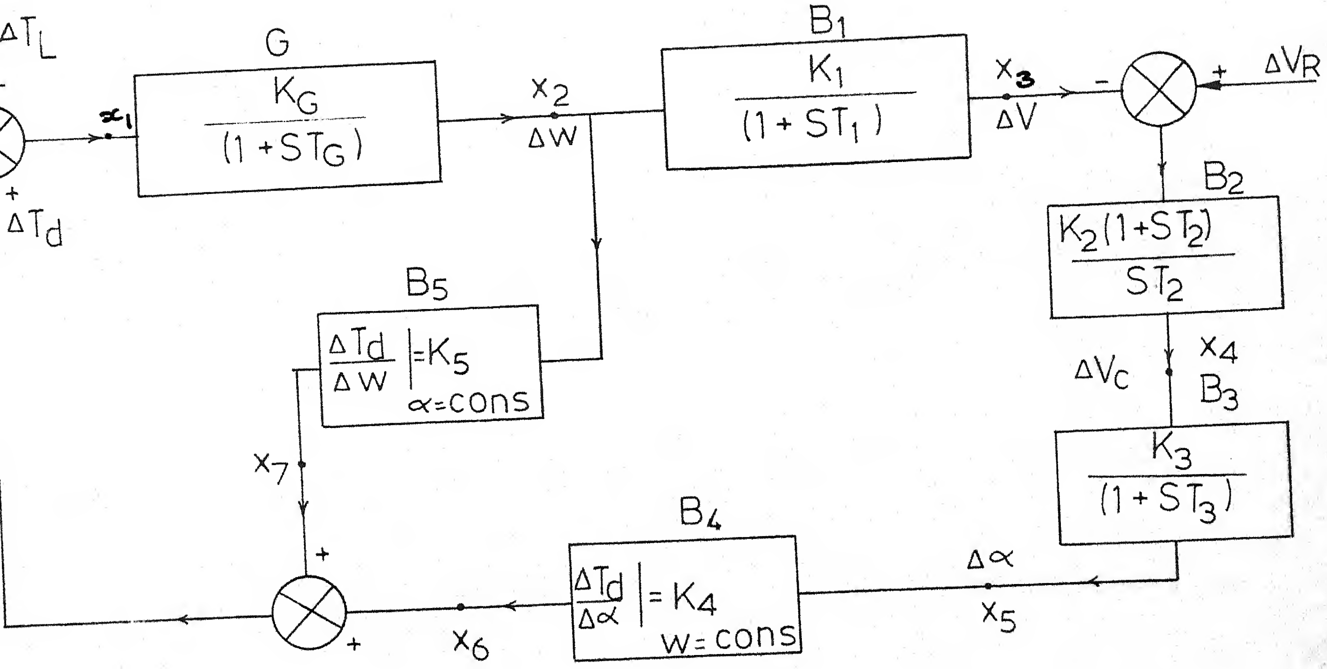
ΔT_L
G
K_G / (1 + ST_G)
x_1
+
ΔT_d
x_2
ΔW
B_1
K_1 / (1 + ST_1)
x_3
ΔV
-
+
ΔV_R
B_2
K_2(1+ST_2) / ST_2
ΔV_C
x_4
B_3
K_3 / (1 + ST_3)
B_5
ΔT_d / ΔW |=K_5
α=cons
x_7
+
B_4
ΔT_d / Δα | = K_4
W= cons
Δα
x_5
x_6
+

FIG.8.4 FUNCTIONAL BLOCKS OF THE CLOSED LOOP SYSTEM

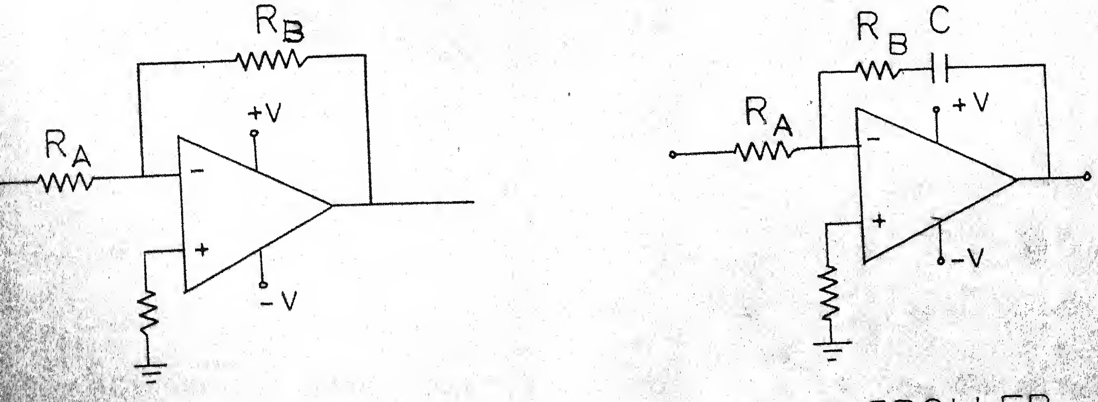
R_B
+V
R_A
-
+
-V
R_B
C
+V
R_A
-
+
-V

P CONTROLLER

PI CONTROLLER

FIG.8.5 CIRCUIT CONFIGURATION OF THE CONTROLLERS

i) Proportional controller (P)

$$G_C(S) = K_2 \tag{8.2}$$

ii) Proportional plus Integral controller (PI)

$$G_C(S) = \frac{K_2(1 + S\,T_2)}{S\,T_2} \tag{8.3}$$

8.4.2.3 Firing circuit

Block B_3 decides the change in firing angle α in accordance with the change in control voltage V_c. Block B_3 consists of ramp generator and a comparator. The ramp is synchronized with the signal available across the sliprings of the machine. For a given change in V_c, the change in firing angle is given by

$$\Delta\alpha = \frac{1}{m}\,\Delta V_c \tag{8.4}$$

where m is the slope of the ramp. The comparator switches to the high state and firing pulses are given to the thyristors when the ramp crosses the control voltage. Although the comparator adjusts the firing angle to the new value as soon as there is change in V_c, the thyristors may not respond immediately. The thyristors are triggered in sequence at the interval of 120 electrical degrees. If the change is control voltage has occured just after one firing instant, then the new firing angle will have effect only at the next firing instant which will occur after 120 electrical degrees. If the change in firing angle occurs just at the moment of a firing instant, then the new firing angle will have immediate effect and no delay is involved. Therefore in the actual system this delay may vary from 0 to 120 electrical degrees and this is to be viewed as a sampled data system[37,38]. However, for the present study, it is assumed that block B_3 is a first order system with gain K_3 equal to 1/m and time constant equal to one half of the maximum expected delay. In the present system the maximum expected delay is 120 electrical degrees. If the slip of the rotor at the operating point is s, then the time constant of block B_3 is given by

$$T_3 = \frac{1}{\cancel{s \times f \times 2 \times 3}\ 6sf} \text{ secs} \qquad (8.4)$$

The transfer function of block B_3 can now be written as

$$G_3(S) = \frac{K_3}{1 + S\,T_3} \qquad (8.5)$$

8.4.2.4 Induction motor

The torque developed by the machine at the given operating point is a function of speed of the machine and the firing angle of the thyristors. The difference between the developed torque and the load torque is given to the rotating system. The torque developed by the machine can be represented as

$$T_d = F(w, \alpha) \qquad (8.6)$$

The present study is about the dynamic behaviour of the system about the operating point for a given perturbation. Therefore, the small change in developed torque can be expressed in terms of the small changes in speed and firing angle as follows :

$$\Delta T_d = \frac{\Delta T_d}{\Delta \alpha}\Bigg|_{\omega=\mathrm{const}} \Delta\alpha + \frac{\Delta T_d}{\Delta \omega}\Bigg|_{\alpha\,=\,\mathrm{const}} \Delta\omega \qquad (8.7)$$

$$\Delta T_d = K_4 \;\Delta\alpha \;+\; K_5\Delta\omega \qquad (8.8)$$

The constants K_4 and K_5 depend upon the operating point and are to be obtained from the steady state characteristics of the system. In the previous chapter, the speed torque characteristic of the system has been obtained using steady state and harmonic analysis methods. The variation of torque with firing angle at different rotor speeds obtained using the above procedures is given in Fig. 8.6. As it is difficult to measure the firing angle α with respect to the voltage zero of the rotor induced emf, in the present study, the off period δ_o of the rotor phase current at the operating point is noted and the corresponding α_o is obtained from the δ V_s α graph given in Fig. 8.7. This graph is also obtained from the results of the steady state analysis. This value of α_o is used for the perturbation study. The constant K_4 is the slope of

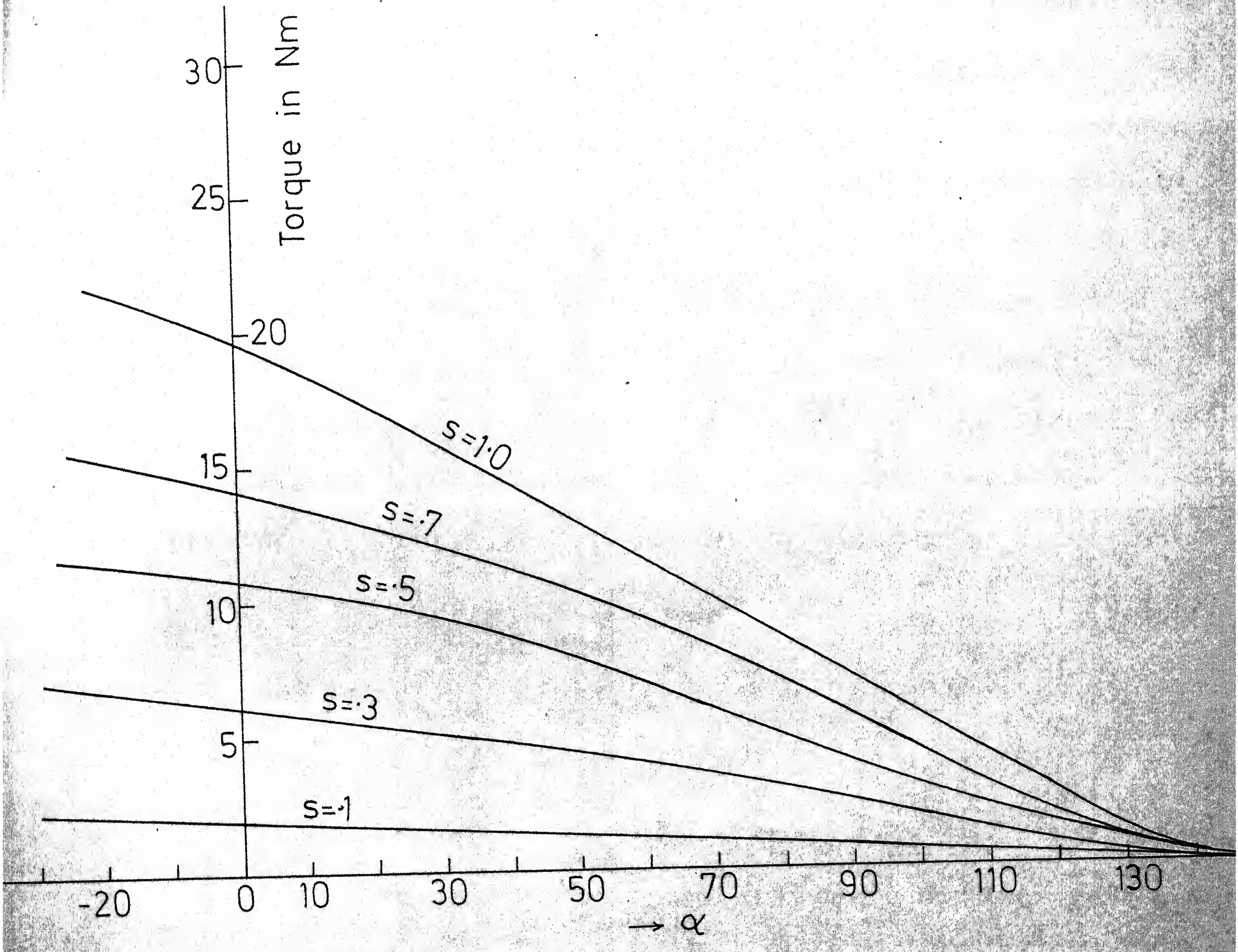

FIG·8·6 VARIATION OF TORQUE WITH α

torque V_s firing angle graph at the given operating point (ω_o, α_o). This is obtained from Fig. 8.6. The constant K_5 is the slope of torque V_s ω (speed of the machine in electrical radians per sec.) graph at the given operating point (ω_o, α_o). This graph is also obtainable from Fig. 8.6. For example, the torque V_3 ω graph for $\alpha_o = 25^\circ$ is given in Fig. 8.8.

Thus the value of K_4 and K_5 are obtained from the results of the steady state analysis and are used for the present perturbation study. In Fig. 8.4 the resultant change in developed torque is represented as the summation of the outputs of the two blocks B_4 and B_5. The change in developed torque is compared with the change in load torque and the resultant value is given to the mechanical system. The transfer-function of the mechanical system can be written as

$$G_m(S) = \frac{K_G}{1 + S\,T_G} \tag{8.9}$$

where $K_G = \frac{1}{F}$ and

$T_G = \frac{J}{F}$

F is the frictional constant in Nm/rad/sec and

J is the moment of inertia of the rotating system in $Kg\text{-}m^2$.

Fig. 8.4 shows the various functional blocks which are to be considered for the perturbation study.

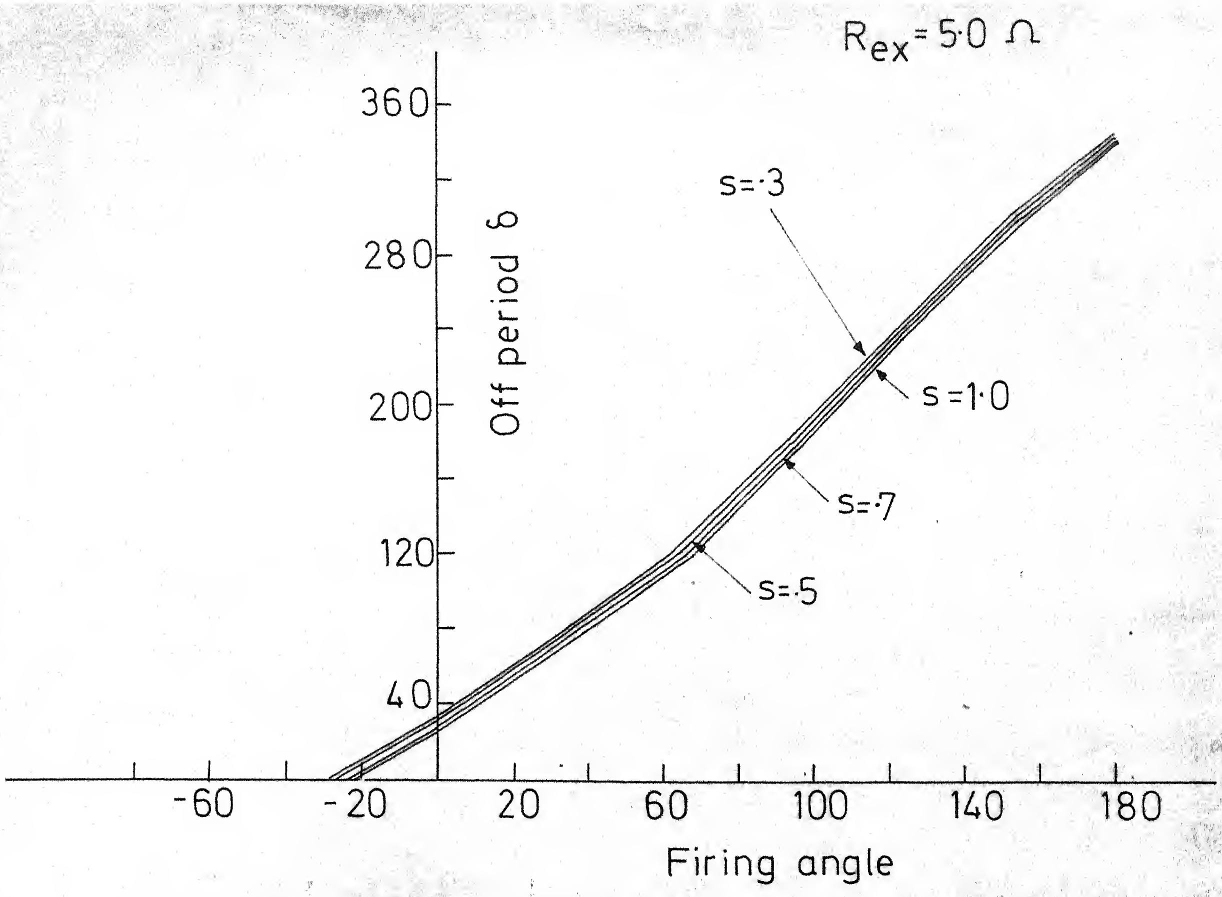

FIG. 8·7 δ Vs GRAPH

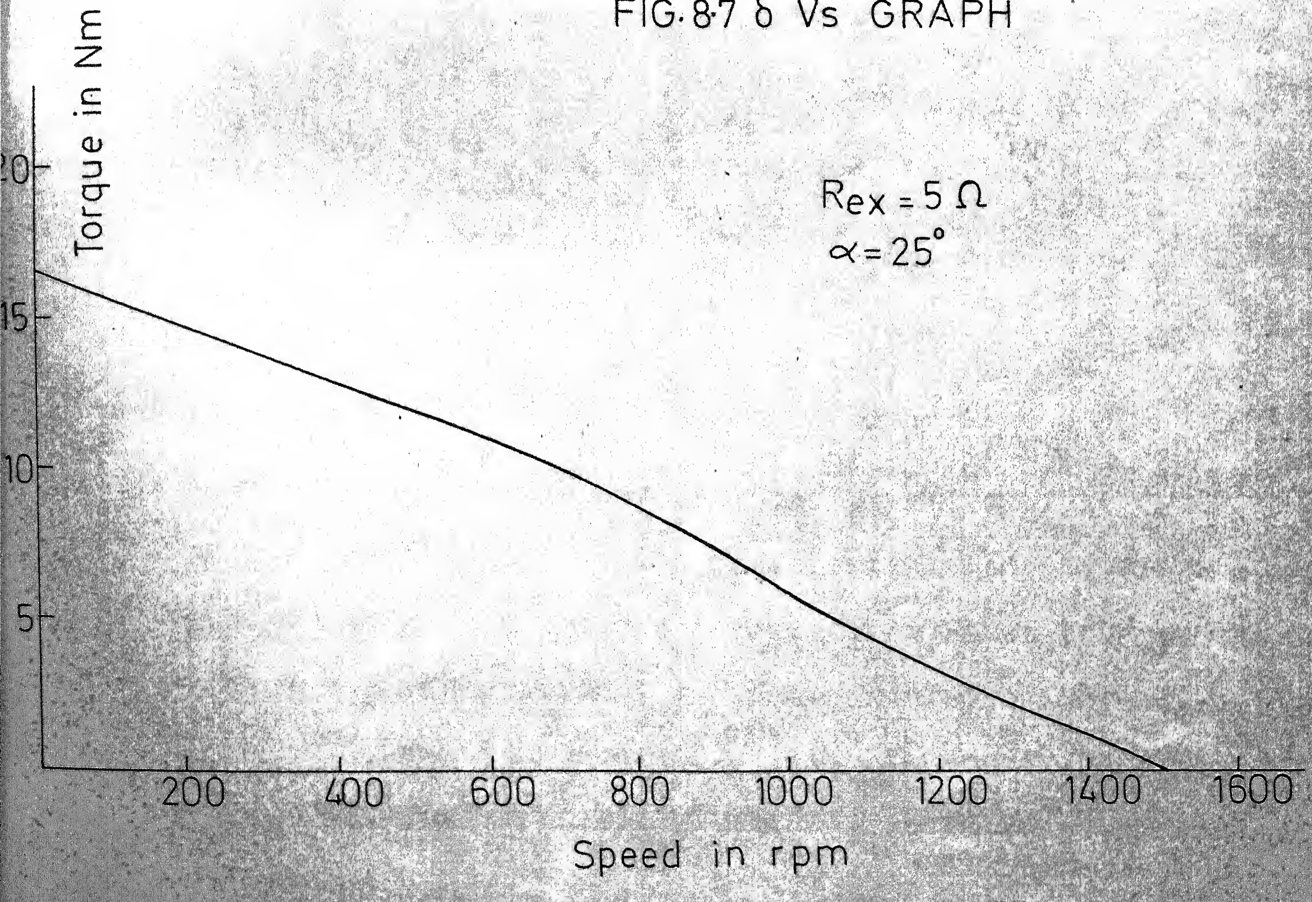

FIG. 8·8 TORQUE Vs SPEED GRAPH

8.4.3 System performance

The present interest is to study how the rotor speed changes with reference voltage (set speed) and load torque perturbations. The analytical results are obtained considerin the various functional blocks given in Fig. 8.4. The differen input and output variables of the various blocks are denoted a x_1, x_2, x_3, x_4, x_5, x_6 and x_7. These variables are defined as follows :

$$x_1 = \Delta T_d - \Delta T_L \qquad (8.10)$$

$$x_2 = \Delta\omega \qquad (8.11)$$

$$x_3 = \Delta V \qquad (8.12)$$

$$x_4 = \Delta V_c \qquad (8.13)$$

$$x_5 = \Delta\alpha \qquad (8.14)$$

$$x_6 = K_4 \, \Delta\alpha \qquad (8.15)$$

$$x_7 = K_5 \, \Delta\omega \qquad (8.16)$$

$$\Delta T_d = x_6 + x_7 \qquad (8.17)$$

These variable names are also marked in Fig. 8.4. For the perturbation study, the differential and algebraic equations which govern the small variations about the operating point are first written down in terms of the above variables. Then these equations are solved simultaneously using Runge-kutta fourth order numerical method. Both P and PI controllers are considered for the study. The following are the equation when PI controller is used.

$$x_1 = x_6 + x_7 - \Delta T_L \tag{8.18}$$

$$\frac{dx_2}{dt} = \frac{K_G}{T_G} x_1 - \frac{x_2}{T_G} \tag{8.19}$$

$$\frac{dx_3}{dt} = \frac{K_1}{T_1} x_2 - \frac{x_3}{T_1} \tag{8.20}$$

$$\frac{dx_4}{dt} = \frac{K_2}{T_2} (\Delta V_R - x_3) - K_2 \frac{dx_3}{dt} \tag{8.21}$$

$$\frac{dx_5}{dt} = \frac{K_3}{T_3} x_4 - \frac{x_5}{T_3} \tag{8.22}$$

$$x_6 = K_4 x_5 \tag{8.23}$$

$$x_7 = K_5 x_2 \tag{8.24}$$

When P controller is used, equation (8.21) is replaced by the following equations.

$$x_4 = K_2(\Delta V_R - x_3) \tag{8.25}$$

$$\frac{dx_4}{dt} = -K_2 \frac{dx_3}{dt} \tag{8.26}$$

The initial values of the above system variables are zero as the system is in steady state before the disturbance. When the study is made for perturbation in load torque keeping the reference voltage constant, ΔT_L assumes a small finite value and ΔV_R is zero. In the case of perturbation in reference voltage, ΔV_R assumes a small finite value and ΔT_L is zero.

The perturbation studies are carried out at two operating points, one at $N_o = 1050$ rpm, $\alpha_o = 25^\circ$ and another one at $N_o = 750$ rpm, $\alpha_o = 70^\circ$. The various system parameters (gains and time constants) used for the study are given in Appendix `E. The test is carried out on the same slipring machine used for the steady state analysis discussed in the previous chapters. The analytical results of the present perturbation study are given in Figs. 8.9-8.14 . Figs.8.9-8.10 show the responses when the P controller is used and Figs. 8.11-8.14 show the responses when PI controller is considered. The respective experimental observations are given in Figs. 8.15-8.20 Comparision of these figures validate the small signal model developed here. It is observed that the system comes to steady state faster with P controller than with PI controller, but the P controller introduces steady state error. The steady state error is negligible with PI controller. This is clear from the oscillograms shown in Figs. 8.17 and 8.19 It is also observed that there is close agreement between the analytical and experimental results.

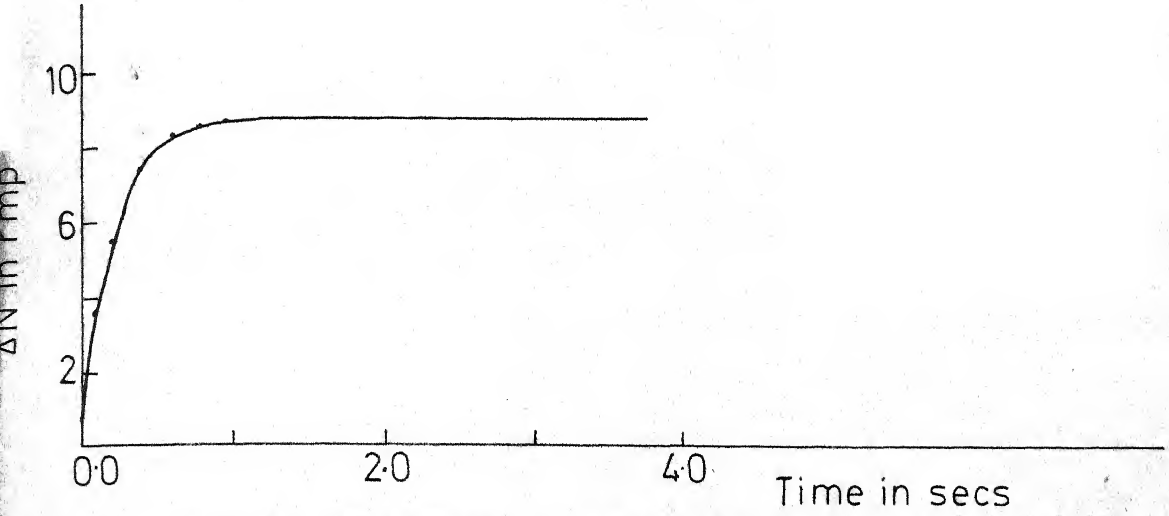

FIG.8·9 RESPONSE CURVE FOR LOAD PERTURBATION WITH P CONTROLLER (N_o=1050 rpm)

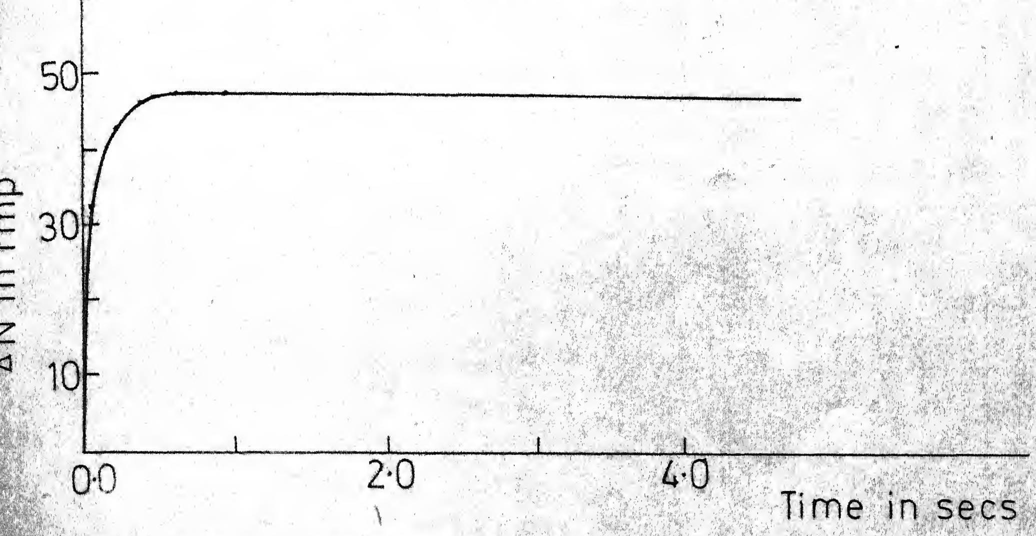

FIG.8·10 RESPONSE CURVE FOR REFERENCE SPEED PERTURBATION WITH P CONTROLLER (N_o=750 rpm)

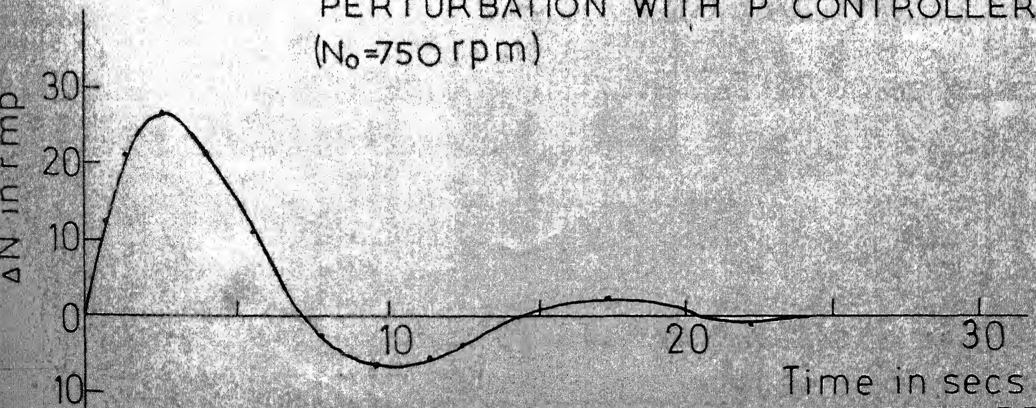

FIG.8·11 RESPONSE CURVE FOR LOAD PERTURBATION WITH PI CONTROLLER (N_o=1050 rpm)

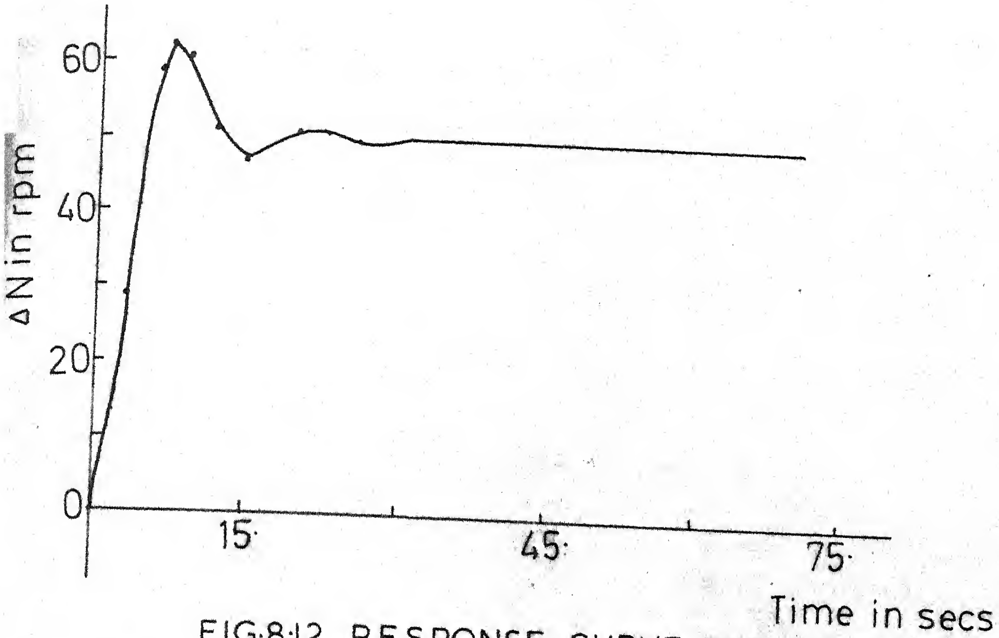

FIG·8·12 RESPONSE CURVE FOR SPEED PERTURBATION WITH PI CONTROLLER (N_o =1050 rpm)

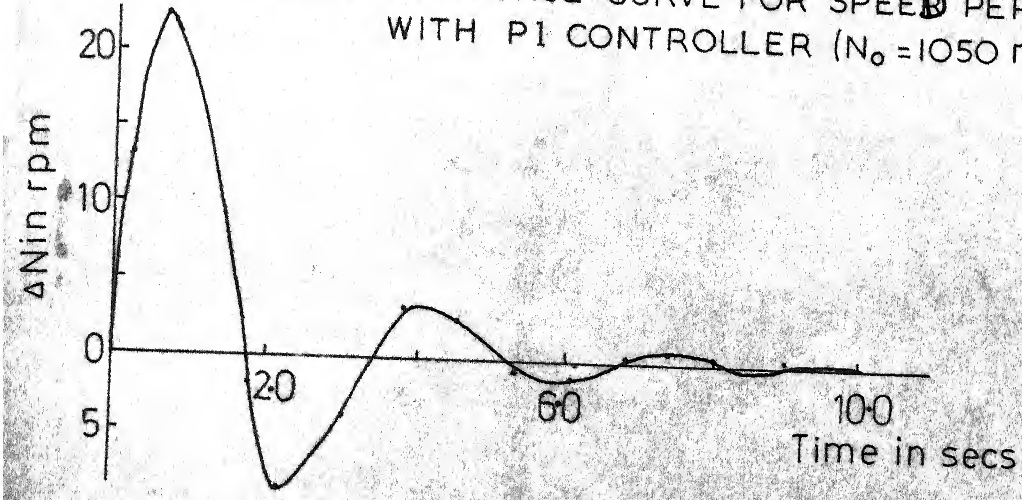

FIG·8·13 RESPONSE CURVE FOR LOAD PERTURBATION WITH PI CONTROLLER (N_o=750 rpm)

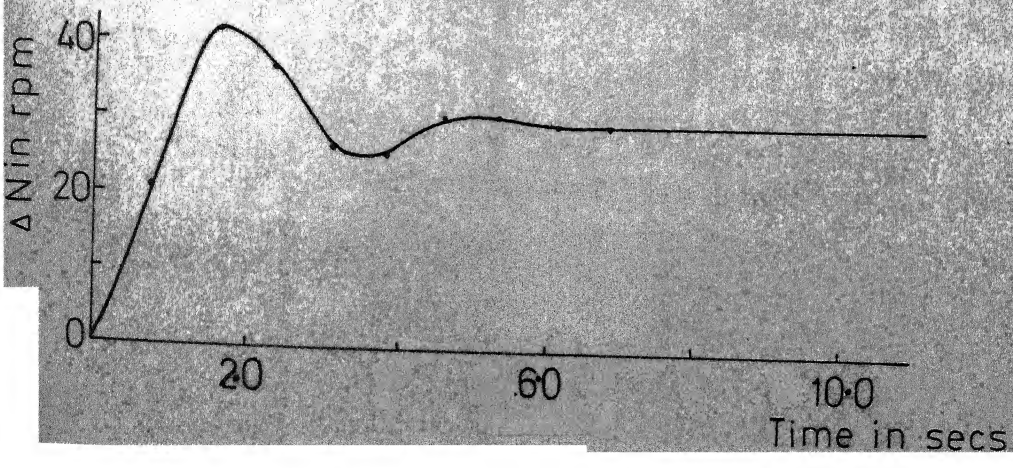

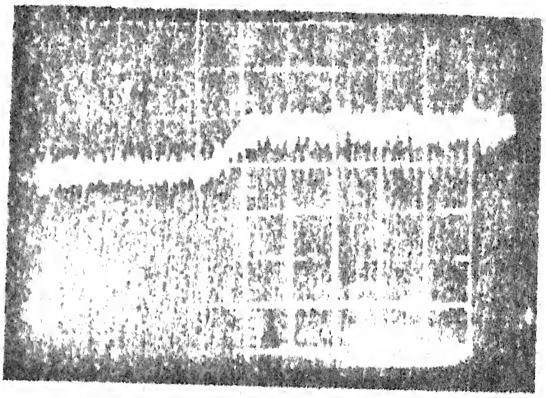

Fig. 8.15 Response to load perturbation
(N$_o$ = 1050 rpm, I controller)
10 rpm/division, .2 sec/division

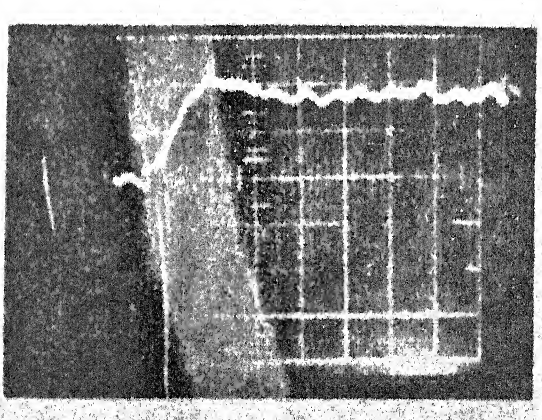

Fig. 8.16 Response to reference speed perturbati
(N$_o$ = 750 rpm, I controller)
25 rpm/division, .2 sec/division

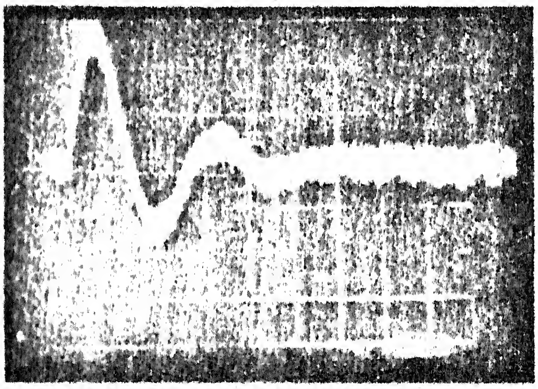

Fig. 8.17 Response to load perturbation
(N_o = 1050 rpm, PI controller)
20 rpm/division, 5 sec/division

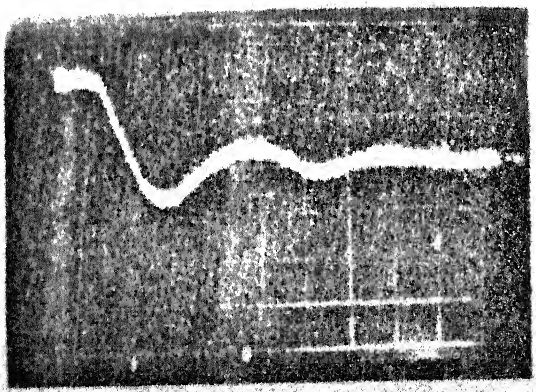

Fig. 8.18 Response to reference speed perturbation
(N_o = 1050 rpm, PI controller)
(trace is inverted)

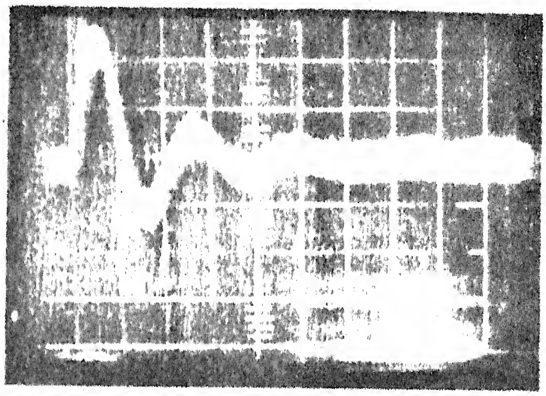

Fig. 8.19 Response to load perturbation
(N$_o$ = 750 rpm, PI controller)
10 rpm/division, 2 sec/division

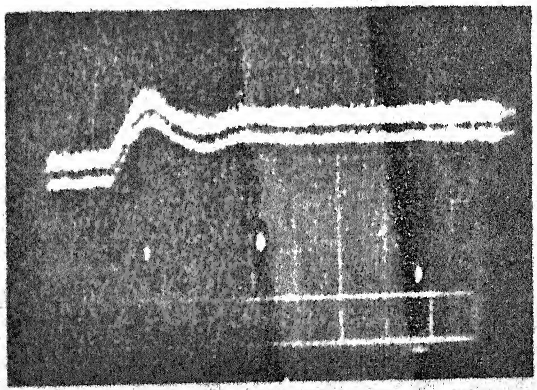

Fig. 8.20 Response to reference speed perturbation
(N$_o$ = 750 rpm, PI controller)

8.5 Conclusion

In this chapter, a simple and reliable firing scheme is developed for the rotor phase control system which uses three phase-controlled SCRs in delta configuration. The importance of the firing scheme is that it does not use any auxiliary machine to get the synchronized control signal and the firing angle α for a given control voltage is constant over a wide speed range.

The closed loop operation of the present system has been studied in this chapter. The dynamic response of the system for load and reference speed perturbations is also investigated. Transfer functions for the functional blocks of the system are derived and the analytical study has been carried out considering the differential and algebraic equations which govern the small variations of the system variables about the operating point. The theoretical response for the change in speed with time for the given load torque and reference speed perturbations are plotted and are compared with experimental results.

CHAPTER 9

CONCLUSION

9.1 General

In this thesis, the different speed control schemes which are simple and economical and provide reasonably wide speed variations have been discussed. The summary of the work done is given in this concluding chapter. The scope for future work in this field is also outlined.

9.2 Review of the Work Done

As stated in the introductory chapter, the main aims of the investigations are to develop proper control schemes suitable for variable speed operations and methods for the steady state and dynamic analysis of SCR controlled induction motors. In this thesis, the major part of the work has been devoted to the study of speed control systems which use phase controlled circuits either to control the stator voltage or to control the effective rotor impedance. The reasons for giving attention to the phase controlled circuits are that they are simple, ~~does~~ do not need additional commutating components, and are economical for low and medium power applications. However, the analysis of these phase controlled systems are complicated due to reasons stated in the introductory chapter, and therefore attempt has been made in this thesis to develop suitable

nt economical
r high power
pplications?

methods for obtaining the steady state and dynamic performance of some of the economical speed control systems.

Two methods of analysis, namely, (i) state space, and (ii) harmonic analysis have been used in this thesis. The various speed control systems considered for the study are :

i) phase controlled single phase machine
ii) three thyristors - three diodes voltage control scheme for three phase induction motors
iii) the voltage and current fed induction motors
iv) the phase controlled resistance method of speed control of three phase induction motor
v) rotor phase control system which use delta connected SCRs in the rotor and
vi) a ~~feed-back~~ feedback control scheme for the system considered in (v).

The results of the investigations are summarised below to highlight the contributions made in the thesis.

1. For the phase controlled single phase machine, an improved harmonic analysis method which iterates only on the conduction period of the stator current waveform and avoids simultaneous iteration on the stator induced emf has been developed. The results obtained by this procedure are compared with the state space and experimental values. ~~A~~ what is the result ?

2. A three thyristors - three diodes voltage control scheme suitable for three phase induction motor has been investigated. The state space and harmonic analysis methods suitable for the study of steady state performance of the above scheme have been developed. The state space procedure is the extension of the one suggested in the literature for the study of six thyristors voltage control scheme. The harmonic analysis method makes use of the harmonic equivalent circuits of the machine. This procedure is named as the modified harmonic analysis method and it makes use of the advantage of both state space technique and steady state harmonic equivalent circuits. An attempt has been made to consider the frequency dependency of the machine parameters with the help of harmonic analysis method. The major advantage of the harmonic analysis method, is that it can conveniently take into account the frequency dependent machine parameters. In this thesis, a slipring machine of 3 HP capacity has been considered for the study and it has been observed that the harmonic components do not have much effect on the performance characteristic of the machine. In the case of large squirrel cage machines with deep bar rotors the harmonics may affect the performance characteristics and the present method can be conveniently used for the study.

Why go
r harmonic
ethod?

better
one
than

3. The applicability of the harmonic analysis method to steady state performance study of inverter driven systems has als

been investigated in this thesis. An iterative technique which estimates the amount of sixth harmonic components present in the dc link has been developed. The procedure uses the steady state harmonic equivalent circuits for the calculation of various system variables.

4. A phase controlled resistance method of speed control has been investigated. The method uses controlled rectifier in the rotor circuit to control the amount of rotor power fed to the external resistance. The effective rotor impedance and hence the speed of the machine is controlled by varying the firing angle of the thyristor bridge. The system uses line commutation and provides a wide speed variation. The steady state analysis of the system has been done using state space procedure. The steady state equivalent circuit of the machine with parameters referred to the secondary circuit is considered for the analysis and the state variables used are the actual rotor voltages and currents. The procedure does not involve iterations. The equivalent circuit is simplified further replacing the thyristor bridge and external resistance by an equivalent impedance. This simplified equivalent circuit is convenient for hand calculations. The results of the analytical procedures have been compared with the experimental results which were already available. This system is simple and provides a wide speed variation.

5. A rotor phase control system which uses only three SCRs connected in delta and placed at the open star point of the rotor circuit of the machine has been investigated. The various modes of operation of the system have been discussed. A state space analysis similar to that developed for the phase controlled resistance method of speed control has been discussed. A harmonic analysis procedure suitable for this system has also been developed. The results of the analytical procedures have been compared with experimental values. The oscillograms demonstrating the various modes of operation have been shown to validate the assumptions made in the analytical procedures.

6. A firing scheme suitable for the above system has been discussed. The scheme does not use auxiliary machines and uses analog circuits to achieve the firing angle control. For a given control voltage the firing angle remains constant over a wide speed range.

one wo

7. A feed-back control system which uses the above phase controlled circuit has been studied. The various functional blocks which govern the small variations of the system variables about the steady state operating point have been developed and the dynamic performance of the system has been obtained using the differential and algebraic equations of the system. Two types of controllers, namely, (i) Proportional (P), and (ii) Proportional plus Integral (PI) have been

considered for the study. The analytical results have been compared with experimental oscillograms.

9.3 Scope for Future Research Work

1. The modified harmonic analysis method reported in Chapter 3 can be easily extended to other SCR controlled squirrel cage machines of larger capacity whose rotor bar resistance may vary considerably with the amount of distortion present in the stator excitation.

2. A six stepped voltage waveform is assumed for the analysis of voltage fed system discussed in Chapter 5. Here each of the SCRs conducts for 180°. If the conduction angle is restricted to 120°, then the analysis becomes complicated because of the unknown stator induced phase voltages during the open circuit conditions. The modified harmonic analysis method discussed in Chapter 3 can be conveniently extended to the study of the above system.

3. A half controlled bridge can be used instead of a fully controlled one in the speed control system discussed in Chapter 6. The analysis developed for the fully controlled bridge circuit can be easily extended to the system which uses half controlled circuit.

4. The state space procedure developed for the rotor phase control systems can be extended to the prediction of exact line and dc link current waveforms of phase controlled dc drives. The system equations will be similar to that developed for rotor phase controlled resistance method of speed control system with the external resistance replaced by the internal resistance, inductance and back emf of the machine.

5. The dynamic analysis developed in Chapter 8 can be extended to other speed control systems which use chopper controlled external resistance or slip power recovery arrangement in the rotor circuit.

LIST OF REFERENCES

1. B. Ilango, 'Analysis of thyristor controlled DC and AC motors', Ph.D. thesis, August 1971, I.I.T. Kanpur.

2. D. Novotny and A.F. Fath, 'The analysis of induction machines controlled by series connected semiconductor switches', IEEE Transactions on Power Apparatus and Systems, Vol. PAS-87, pp 597-605, Feb. 1968.

3. T.A. Lipo, 'The analysis of induction motors with voltage control by symmetrically triggered thyristors', IEEE Transactions on Power Apparatus and Systems, Vol. PAS-90, No.2, March/April, 1971.

4. T.J. Takenchi, 'Theory of SCR circuit and application to Motor control Tokyo: Tokyo Electrical Engineering College Press, 1968.

5. D.A. Paice, 'Induction motor speed control by stator voltage control', IEEE Transactions on Power Apparatus and Systems, Vol. PAS-87, pp 585-590, Feb. 1968.

6. W. Shepherd, 'On the analysis of the three-phase induction motor with voltage control by thyristor switching', IEEE Transactions on Industry and General Applications, Vol. IGA-4, No.3, May/June, 1968.

7. M. Ramamoorty and M.F. Samek, 'Steady-state analysis of phase controlled induction motor with isolated neutral', IEEE Transactions on Industrial Electronics and Control Instrumentation, Vol. IECI-23, No.2, pp 178-184, May 1976.

8. B. Ilango and M. Ramamoorty, 'Steady state analysis of thyristor controlled three phase induction motors using state space techniques', IEEE Transactions on Power Apparatus and Systems, Vol. PAS-98, No.4, pp 1165-1172, July/August, 1974.

9. N. Hayashi, 'Analysis of Induction motors controlled by symmetrically triggered delta-connected thyristors', Electrical Engineering in Japan, Vol. 92, pp 105-115, Sep/Oct, 1972.

10. William Mc Murray, 'A comparative study of symmetrical three-phase circuits for phase controlled AC motor drives', IEEE Transactions on Industry Applications, Vol. IA-10, No.3, pp 403-411, May/June 1974.

11. Linos, J. Jacovides, 'Analysis of induction motor drives with a nonsinusoidal supply voltage using fourier analysis', IEEE Transactions on Industry Applications, Vol. IA-9, No.6, pp 741-747, Nov/Dec. 1973.

12. A. Klingshirn and H.E. Jordan, 'Polyphase induction motor performance and losses on nonsinusoidal voltage sources', IEEE Transactions on Power Apparatus and Systems, Vol. PAS-87, pp 624-631, March 1968.

13. T.A. Lipo and P.C. Krause, 'Stability analysis of a rectifier inverter induction motor drive', IEEE Transactions on Power Apparatus and Systems, Vol. PAS-88, pp 55-56, January 1969.

14. G.C. Jain, 'The effect of voltage waveform on the performance of a three phase induction motor', IEEE Transactions on Power Apparatus and Systems, Vol. PAS-83, pp 561-566, June, 1964.

15. T.A. Lipo, P.C. Krause and H.E. Jordan, 'Harmonic torque and speed fluctuations in a rectifier-inverter induction motor drive', IEEE Transactions on Power Apparatus and Systems, Vol. PAS-88, pp 579-587, May 1969.

16. Stuart, D.T. Robertson and K.M. Hebbar, 'Torque pulsations in induction motor with inverter drives', IEEE Transactions on Industry and General Applications, Vol. IGA-7, No.2, pp 318-322, March/April 1971.

17. M. Ramamoorty and M. Arunachalam, 'Steady state analysis of inverter driven induction motor using iterative technique', 1977 All India Seminar on Design, Development and Standardization of Electrical Equipment (Institution of Engineers, India).

18. M. Ramamoorty, 'Steady state analysis of inverter driven induction motor using harmonic equivalent circuits', Proceedings of Industry Applications Annual Meeting 1973, pp. 437-440.

19. E.E. Ward, 'Inverter suitable for operation over a range of frequency', Proceedings. Institutions of Electrical Engineering, Vol. 111, pp 1423-1434, August 1964.

20. K.P. Phillips, 'Current source inverter for ac motor drives', IEEE Transactions on Industry Applications, Vol. IA-8, pp 679-683, Nov/Dec. 1972.

21. G.R. Slemon, S.B. Dewan, and J.W.A. Wilson,'''Synchronous motor drive with current source inverter', IEEE Transactions on Industry Applications, Vol. IA-10, No.4, pp 412-416 , May/June, 1974.

22. Thomas, A. Lipo and Edward P. Cornell, 'State variable steady state analysis of a controlled current induction motor drive', IEEE Transactions on Industry Applications, Vol. IA-11, pp 704-712, Nov/Dec 1975.

23. R.H. Nelson and T.A. Radomshi, 'Design methods for current source inverter induction motor drive systems', IEEE Transactions on Industrial Electronics and Control Instrumentations, Vol. IECI-22, No.2, pp 141-145, May 1975.

24. K. Ranganatha Rao and V.V. Sastry, 'Current-fed induction motor analysis using boundary-value approach', IEEE Transactions on Industrial Electronics and Control Instrumentation, Vol. IECI-24, No.2, pp 178-182, May 1977.

25. H. Kazuno, 'A wide range of speed control of an induction motor with static Scherbius and Kramer Systems, Electrical Engineering in Japan, Vol. 89, No.2, pp 10-19, 1969.

26. Willian Shepherd and Jack Stanway, 'Slip power recovery in an induction motor by the use of a thyristor inverter, IEEE Transactions on Industry and General Applications, Vol. IGA-5, No.1, pp 74-82, Jan/Feb. 1969.

27. Shepherd, W. and Slemon, G.R., 'Rotor impedance control and wound rotor induction motors', AIEE Transactions (Power Apparatus and Systems), Vol. PAS-78, pp 814, Oct. 1959.

28. P.R. Basu, 'Variable speed induction motor using thyristors in the secondary circuit', IEEE Transaction on Power Apparatus and Systems', Vol. PAS-90, pp 509-514, March/April 1971.

29. P.C. Sen and K.H.J. MA, Rotor chopper control for induction motor drive: TRC strategy', IEEE Transaction on Industry Applications, Vol. IA-11, pp 43-49, Jan/ Feb. 1975.

30. M. Ramamoorty and N.S. Wani, 'Chopper controlled slipring induction motor with closed loop control', IEEE Transactions on Industrial Electronics and Control Instrumentation, Vol. IECI-24, No.2, pp 153-161, May 1977.

31. M. Ramamoorty and M. Arunachalam, 'A solid state controller for slipring induction motors', 1977 IEEE Annual Meeting on Industry Applications.

32. S. Doraipandy, 'A solid state controller for slipring induction motors', Ph.D. thesis, I.I.T. Delhi, July 1976.

33. E.W. Kimbark, 'Direct current transmission', Vol. 1, Wiley-Inter Science Publication.

34. M. Ramamoorty, 'Thyristors and their applications', East West Press, 1977.

35. Edward D. Spooner, 'Three-phase three-thyristor voltage control scheme', IEEE Transactions on Industry Applications, Vol. IA-11, No.5, pp 478-482, Sep/Oct 1975.

36. S. Murugesan and C. Kameswara Rao, 'Simple adaptive analog and digital trigger circuits for thyristors working under wide range of supply frequencies', IEEE Transactions on Industrial Electronics and Control Instrumentation, Vol. IECI-24, No.1, pp 46-49, Feb. 1977.

37. E.A. Parrish, Jr., and E.S. Mc Vey, 'A theoretical model for single phase silicon controlled rectifier systems', IEEE Transactions on Automatic Control, pp. 577-579, Oct. 1967.

38. Thadiappan Krishnan and Bellamkonda Ramaswami, 'A Fast-Response DC motor speed control systems', IEEE Transactions on Industry Applications, Vol. IA-10, No.5, Sep/Oct. 1974.

APPENDIX A

TO OBTAIN THE INITIAL GUESS FOR β THE CONDUCTION ANGLE USED IN THE HARMONIC ANALYSIS METHOD OF SINGLE PHASE MACHINE

Considering the machine as a passive element, the net impedance of the machine looking from the stator terminals is

$$Z = R + j\omega L \tag{A.1}$$

If a sinusoidal voltage $v_s = V_m \sin(\omega t + \alpha)$ is applied at $t = 0$ to the machine, the line current is obtained by solving the differential equation

$$v_s = R\, i_s + L \frac{di_s}{dt} \tag{A.2}$$

The solution is given by

$$i_s(t) = \frac{V_m}{Z}\left[\sin(\omega t+\alpha-\alpha_c) - e^{-Rt/L} \sin(\alpha-\alpha_c)\right] \tag{A.3}$$

where $\alpha_c = \tan^{-1}(X/R)$

The stator current is zero at $t = 0$ and at $t = \beta/\omega$

therefore $i_s(\beta/\omega) = 0$

That is,

$$e^{-R\beta/\omega L} \cdot \frac{V_m}{Z} \sin(\alpha_c-\alpha) + \frac{V_m}{Z} \sin(\beta+\alpha-\alpha_c) = 0 \tag{A.4}$$

The left hand side is denoted by $F(\beta)$. This transcedental equation can be solved using Newton-Raphson technique. An initial guess of $\beta = \pi + \alpha - \alpha_c$ is used and every new value of β is obtained from the old value using the following equation

$$\beta_{new} = \beta_{old} - \frac{F(\beta_{old})}{F'(\beta_{old})} \tag{A.5}$$

The solution can be obtained in two or three iterations. The value of β thus obtained is used as the initial guess value for the harmonic analysis method.

APPENDIX B

HARMONIC ANALYSIS ON THE VOLTAGE WAVEFORM APPLIED TO THE STATOR OF THE SINGLE PHASE INDUCTION MACHINE

For the harmonic analysis, the instant where SCR1 is fired is chosen as the origin. Referring to Fig. 2.3, the voltage waveform applied to the machine is defined as

$$\begin{aligned} v_s(\theta) &= V_m \sin(\theta + \alpha) & 0 \leqslant \theta \leqslant \beta \\ &= e & \beta \leqslant \theta \leqslant \pi \end{aligned} \qquad (B.1)$$

where e is the induced emf of the machine during the off period. It is assumed to be a sinusoidal waveform in phase with the supply voltage. The expression for e can be written as

$$e = EN \sin(\theta + \alpha)$$

Since this voltage waveform is having half wave symmetry, it is sufficient if we consider only one-half of the voltage waveform. The coefficients of the harmonic components can be obtained using the following equations.

$$A_n = \frac{2}{\pi}\int_0^{\pi} v_s(\theta) \cos n\theta \cdot d\theta \qquad (B.2)$$

$$B_n = \frac{2}{\pi}\int_0^{\pi} v_s(\theta) \sin n\theta \cdot d\theta \qquad (B.3)$$

The integration yields,

$$A_1 = A + B$$

where

$$A = \frac{V_n}{2\pi}\left[2\beta \sin\alpha + \cos\alpha - \cos(2\beta + \alpha)\right] \qquad (B.4)$$

$$B = \frac{EN}{\pi}\left[.5 \cos(2\beta + \alpha) - .5 \cos\alpha + (\pi-\beta)\sin\alpha\right] \qquad (B.5)$$

$A_n = E_n + F_n$, n takes values 3,5,....M

where

$$E_n = \frac{V_m}{\pi}\left\{\frac{\cos[(n-1)\beta-\alpha]}{(n-1)} - \frac{\cos[(n+1)\beta+\alpha]}{(n+1)} - \frac{2\cos\alpha}{(n^2-1)}\right\} \qquad (B.6)$$

$$F_n = \frac{EN}{\pi}\left\{-\frac{\cos\alpha}{(n+1)} + \frac{\cos[(n+1)\beta+\alpha]}{(n+1)} + \frac{\cos\alpha}{(n-1)} - \frac{\cos[(n-1)\beta-\alpha]}{(n-1)}\right\} \qquad (B.7)$$

$$B_1 = C + D$$

where

$$C = \frac{V_m}{2\pi}(2\beta \cos\alpha - \sin(2\beta+\alpha) + \sin\alpha) \qquad (B.8)$$

$$D = \frac{EN}{\pi}\left[(\pi-\beta)\cos\alpha - .5 \sin\alpha + .5 \sin(2\beta+\alpha)\right] \qquad (B.9)$$

$B_n = G_n + H_n$, n takes values 3,5, ...M

where

$$G_n = \frac{V_m}{\pi}\left[\frac{\sin[(n-1)\beta-\alpha]}{(n-1)} + \frac{2n \sin\alpha}{(n^2-1)} - \frac{\sin[(n+1)\beta+\alpha]}{(n+1)}\right] \qquad (B.10)$$

$$H_n = \frac{EN}{\pi}\left[-\frac{\sin\alpha}{(n-1)} - \frac{\sin[(n-1)\beta-\alpha]}{(n-1)} - \frac{\sin\alpha}{(n+1)} + \frac{\sin[(n+1)\beta+\alpha]}{(n+1)}\right] \qquad (B.11)$$

$$v_s(\theta) = \sum_{n=1,3,..}^{M} \sqrt{A_n{}^2 + B_n{}^2}\,\sin(n\theta + \varphi_n), \qquad (B.12)$$

where $\varphi_n = \tan^{-1}\frac{A_n}{B_n}$

APPENDIX C

HARMONIC ANALYSIS ON MACHINE VOLTAGE WAVEFORM

The harmonic analysis is made on the waveform shown in Fig. 5.4(b) in this section. The waveform contains only odd harmonics. The coefficients of the cosine terms are given by

$$a_n = \frac{2}{\pi} \int_0^{\pi} f(\theta) \cos n\theta \, d\theta$$

$$= \frac{2}{\pi} \{\int_0^{\pi/3} [\frac{E_d}{3} \sin(6\theta + \beta')] \cos n\theta \, d\theta +$$

$$\int_{\pi/3}^{2\pi/3} \frac{2E_6}{3} . \sin(6\theta + \beta')] \cos n\theta +$$

$$\int_{2\pi/3}^{\pi} [\frac{E_d}{3} + \frac{E_6}{3} \sin(6\theta + \beta')] \cdot \cos n\theta \, d\theta] \} \qquad (C.1)$$

Upto 13th order harmonic is considered for the analysis. The coefficients of the sine terms are given by

$$b_n = \frac{2}{\pi} \int_0^{\pi} f(\theta) \cdot \sin n\theta \, d\theta \qquad (C.2)$$

where f(θ) is same as given in the evaluation of cosine terms.

The resultant nth harmonic phase voltage is given by

$$v_n(\theta) = \sqrt{a_n^2 + b_n^2} \quad \sin(n\theta + \psi_n) \qquad (C.3)$$

where $\psi_n = \tan^{-1} a_n/b_n$.

APPENDIX D

HARMONIC ANALYSIS ON THE MACHINE CURRENT WAVEFORM

The harmonic analysis on the machine current waveform is done using the following expression. The coefficients of the cosine terms are given by

$$a_n = \frac{2}{\pi}\int_0^{\pi} f(\theta)\cdot\cos n\theta\cdot d\theta \qquad (D.1)$$

where

$$f(\theta) = 0 \qquad 0 \leq \theta \leq \pi/6$$

$$= I_d + I_6\cos(6\theta + \gamma) \qquad \pi/6 \leq \theta \leq 5\pi/6$$

$$= 0 \qquad 5\pi/6 \leq 0 \leq \pi$$

$$a_n = \frac{2}{\pi}\int_{\pi/6}^{5\pi/6} \{I_d + I_6\cos(6\theta + \gamma)\}\ \cos n\theta\ d\theta \qquad (D.2)$$

The coefficients of the sine terms :

$$b_n = \frac{2}{\pi}\int_0^{\pi} f(\theta)\cdot d\theta \qquad (D.3)$$

The nth harmonic line current is given by

$$i_n(\theta) = \sqrt{a_n^2 + b_n^2}\ \sin(n\theta + \psi_n) \qquad (D.4)$$

when $\tan\ \psi_n = a_n/b_n$.

APPENDIX B

THE VARIOUS GAINS AND TIME CONSTANTS USED FOR THE PERTURBATION STUDY

$R_{ex} = 5$ ohms

Speed	1050 rpm	750 rpm
K_1	.032	.032
T_1	.009	.009
K_2	.25 (For PI controller)	1.832 (For PI controller)
	25.0 (For P controller)	25.0 (For P controller)
T_2	.22 (For PI controller)	.22 (For PI controller)
K_3	-60.0	-60.0
T_3	.01111	.00667
K_4	-.0363	-.09375
K_5	-.095	-.075
K_G	40.0	34.5
T_G	15.6	13.5

CURRICULUM VITAE

a. Name : M. ARUNACHALAM

b. Academic Background :

Degree	Specilization	University	Year
B.E.	Electrical Engineering	Madras	1970
M.Sc. (Engg)	Power System Engineering	Madras	1972

c. Publications :

1. 'A Solid State Controller for Slip-Ring Induction Motors', (with Dr. M. Ramamoorty), Presented at the 1977 Industry Application Society Annual Meeting.

2. 'Solid-State Speed Control of Slip-Ring Induction Motors', (with Dr. M. Ramamoorty and Dr. S.S. Venkata), - 1977 Mid West Power Symposium.

3. 'Steady State Analysis of Inverter Driven Induction Motor', (with Dr. M. Ramamoorty), Presented at the 1977 All India Conference on Design, Development and Standardization of Electrical Equipment (Institution of Engineers, India).

4.*'Solid State Voltage Control of Resistive Load', (with Dr. M. Ramamoorty), Journal of the Institution of Electronics and Telecommunication Engineers (India), January, 1977.

* not pertaining to thesis.

A 55482

Date Slip A 55482

This book is to be returned on the date last stamped.

CD 6.72.9

EE-1977-D-ARU-SOL